

Independent finite approximations for Bayesian nonparametric inference

Tin D. Nguyen¹, Jonathan Huggins², Lorenzo Masoero¹, Lester Mackey³,
Tamara Broderick¹

¹*LIDS, MIT, e-mail: tdn@mit.edu; lom@mit.edu; tamarab@mit.edu*

²*Department of Mathematics & Statistics, Boston University, e-mail: huggins@bu.edu*

³*Microsoft Research New England, e-mail: lmackey@microsoft.com*

Abstract:

Completely random measures (CRMs) and their normalizations (NCRMs) offer flexible models in Bayesian nonparametrics. But their infinite dimensionality presents challenges for inference. Two popular finite approximations are truncated finite approximations (TFAs) and independent finite approximations (IFAs). While the former have been well-studied, IFAs lack similarly general bounds on approximation error, and there has been no systematic comparison between the two options. In the present work, we propose a general recipe to construct practical finite-dimensional approximations for homogeneous CRMs and NCRMs, in the presence or absence of power laws. We call our construction the *automated independent finite approximation* (AIFA). Relative to TFAs, we show that AIFAs facilitate more straightforward derivations and use of parallel computing in approximate inference. We upper bound the approximation error of AIFAs for a wide class of common CRMs and NCRMs — and thereby develop guidelines for choosing the approximation level. Our lower bounds in key cases suggest that our upper bounds are tight. We prove that, for worst-case choices of observation likelihoods, TFAs are more efficient than AIFAs. Conversely, we find that in real-data experiments with standard likelihoods, AIFAs and TFAs perform similarly. Moreover, we demonstrate that AIFAs can be used for hyperparameter estimation even when other potential IFA options struggle or do not apply.

1. Introduction

Many data analysis problems can be seen as discovering a latent set of traits in a population — for example, recovering topics or themes from scientific papers, ancestral populations from genetic data, interest groups from social network data, or unique speakers across audio recordings of many meetings (Palla, Knowles and Ghahramani, 2012; Blei, Griffiths and Jordan, 2010; Fox et al., 2010). In all of these cases, we might reasonably expect the number of latent traits present in a data set to grow with the number of observations. One might choose a prior for different data set sizes, but then model construction potentially becomes inconvenient and unwieldy. A simpler approach is to choose a single prior that naturally yields different expected numbers of traits for different numbers of data points. In theory, Bayesian nonparametric (BNP) priors have exactly this desirable property due to a countable infinity of traits, so that there are always more traits to reveal through the accumulation of more data.

However, the infinite-dimensional parameter presents a practical challenge; namely, it is impossible to store an infinity of random variables in memory or learn the distribution over an infinite number of variables in finite time. Some authors have developed conjugate priors and likelihoods (Orbanz, 2010; James, 2017; Broderick, Wilson and Jordan, 2018) to

circumvent the infinite representation; in particular, these models allow marginalization of the infinite collection of latent traits. These models will typically be part of a more complex generative model where the remaining components are all finite. Therefore, users can apply approximate inference schemes such as Gibbs sampling. However, these marginal forms typically limit the user to a constrained family of models; are not amenable to parallelization; would require substantial new development to use with modern inference engines like NIMBLE (de Valpine et al., 2017); and are not straightforward to use with variational Bayes.

An alternative approach is to approximate the infinite-dimensional prior with a finite-dimensional prior that essentially replaces the infinite collection of random traits by a finite subset of “likely” traits. Unlike a fixed finite-dimensional prior across all data set sizes, this finite-dimensional prior is an approximation to the BNP prior. Therefore, its cardinality can be informed directly by the BNP prior and the size of the observed data. Any moderately complex model will necessitate approximate inference, such as Markov chain Monte Carlo (MCMC) or variational Bayes (VB). Therefore, as long as the error due to the finite-dimensional prior approximation is small compared to the error due to using approximate inference, inferential quality is not affected. Unlike marginal representations, probabilistic programming languages like NIMBLE (de Valpine et al., 2017) natively support such finite approximations.

Much of the previous work on finite approximations developed and analyzed truncations of series representations of the random measures underlying the nonparametric prior; we call these *truncated finite approximations* (TFAs) and refer to Campbell et al. (2019) for a thorough study. TFAs start from a sequential ordering of population traits in a random measure. The TFA retains a finite set of approximating traits; these match the population traits until a finite point and do not include terms beyond that (Doshi-Velez et al., 2009; Paisley, Blei and Jordan, 2012; Roychowdhury and Kulis, 2015; Arbel and Prünster, 2017; Campbell et al., 2019). However, we show in Section 5 that the sequential nature of TFAs makes it difficult to derive update steps in an approximate inference algorithm (either MCMC or VB) and is not amenable to parallelization.

Here, we instead develop and analyze a general-purpose finite approximation consisting of independent and identically distributed (i.i.d.) representations of the traits together with their rates within the population; we call these *independent finite approximations* (IFAs). At the time of writing, we are aware of two alternative lines of work on generic constructions of finite approximations using i.i.d. random variables, namely Lijoi, Prünster and Rigon (2023) and Lee, Miscouridou and Caron (2022); Lee, James and Choi (2016). Lijoi, Prünster and Rigon (2023) design approximations for clustering models, characterize the posterior predictive distribution, and derive tractable inference schemes. However, the authors have not developed their method for trait allocations, where data points can potentially belong to multiple traits and can potentially exhibit traits in different amounts. And in particular it would require additional development to perform inference in trait allocation models using their approximations.¹ Lee, Miscouridou and Caron (2022); Lee, James and Choi (2016) construct finite approximations through a novel augmentation scheme. However, Lee, Miscouridou and Caron (2022); Lee, James and Choi (2016) lack explicit constructions in important situations, such as exponential-family rate measures, because the functions involved in the augmentation are, in general, only implicitly defined. When the augmentation

¹We also note that, without modification, their approximation is not suitable for use in statistical models where the unnormalized atom sizes of the CRM are bounded, as arise when modeling the frequencies (in $[0, 1]$) of traits. While model reparameterization may help, it requires (at least) additional steps.

is implicit, there is not currently a way to evaluate (up to proportionality constant) the probability density of the finite-dimensional distribution; therefore standard Markov chain Monte Carlo and variational approaches for approximate inference are unavailable.

Our contributions. We propose a general-purpose construction for IFAs that subsumes a number of special cases that have already been successfully used in applications (Section 3.1). We call our construction the *automated independent finite approximation*, or AIFA. We show that AIFAs can handle a wide variety of models — including homogeneous completely random measures (CRMs) and normalized CRMs (NCRMs) (Section 3.3).² Our construction can handle (N)CRMs exhibiting power laws and has an especially convenient form for exponential family CRMs (Section 3.2). We show that our construction works for useful CRMs not previously seen in the BNP literature (Example 3.4). Unlike marginal representations, AIFAs do not require conditional conjugacy and can be used with VB. We show that, unlike TFAs, AIFAs facilitate straightforward derivations within approximate inference schemes such as MCMC or VB and are amenable to parallelization during inference (Section 5). In existing special cases, practitioners report similar predictive performance between AIFAs and TFAs (Kurihara, Welling and Teh, 2007) and that AIFAs are also simpler to use compared to TFAs (Fox et al., 2010; Johnson and Willsky, 2013). In contrast to the methods of Lee, Miscouridou and Caron (2022); Lee, James and Choi (2016), one can always evaluate the probability density (up to a proportionality constant) of AIFAs; furthermore, in Section 6.4, AIFAs accurately learn model hyperparameters by maximizing the marginal likelihood where the methods of Lee, Miscouridou and Caron (2022); Lee, James and Choi (2016) struggle.

In Section 4, we bound the error induced by approximating an exact infinite-dimensional prior with an AIFA. Our analysis provides interpretable error bounds with explicit dependence on the size of the approximation and the data cardinality; our bounds can be used to set the size of the approximation in practice. Our error bounds reveal that for the worst-case choice of observation likelihood, to approximate the target to a desired accuracy, it is necessary to use a large IFA model while a small TFA model would suffice. However, in practical experiments with standard observations likelihoods, we find that AIFAs and TFAs of equal sizes have similar performance. Likewise, we find that, when both apply, AIFAs and alternative IFAs (Lee, Miscouridou and Caron, 2022; Lee, James and Choi, 2016) exhibit similar predictive performance (Section 6.3). But AIFAs apply more broadly and are amenable to hyperparameter learning via optimizing the marginal likelihood, unlike Lee, Miscouridou and Caron (2022); Lee, James and Choi (2016) (Section 6.4). As a further illustration, we show that we are able to learn whether a model is over- or underdispersed, and by how much, using an AIFA approximating a novel BNP prior in Section 6.5.

2. Background

Our work will approximate nonparametric priors, so we first review construction of these priors from completely random measures (CRMs). Then we cover existing work on the construction of truncated and independent finite approximations for these CRM priors. For some space Ψ , let $\psi_i \in \Psi$ represent the i -th trait of interest, and let $\theta_i > 0$ represent the corresponding rate or frequency of this trait in the population. If the set of traits is finite, we let I equal its cardinality; if the set of traits is countably infinite, we let $I = \infty$.

²NCRMs are also called *normalized random measures with independent increments* (NRMIs) (Regazzini, Lijoi and Prünster, 2003; James, Lijoi and Prünster, 2009).

Collect the pairs of traits and frequencies in a measure Θ that places non-negative mass θ_i at location ψ_i : $\Theta := \sum_{i=1}^I \theta_i \delta_{\psi_i}$, where δ_{ψ_i} is a Dirac measure placing mass 1 at location ψ_i . To perform Bayesian inference, we need to choose a prior distribution on Θ and a likelihood for the observed data $Y_{1:N} := \{Y_n\}_{n=1}^N$ given Θ . Then, applying a disintegration, we can obtain the posterior on Θ given the observed data.

Homogeneous completely random measures. Many common BNP priors can be formulated as completely random measures (Kingman, 1967; Lijoi and Prünster, 2010).³ CRMs are constructed from Poisson point processes,⁴ which are straightforward to manipulate analytically (Kingman, 1992). Consider a Poisson point process on $\mathbb{R}_+ := [0, \infty)$ with rate measure $\nu(d\theta)$ such that $\nu(\mathbb{R}_+) = \infty$ and $\int \min(1, \theta) \nu(d\theta) < \infty$. Such a process generates a countably infinite set of rates $(\theta_i)_{i=1}^\infty$ with $\theta_i \in \mathbb{R}_+$ and $0 < \sum_{i=1}^\infty \theta_i < \infty$ almost surely. We assume throughout that $\psi_i \stackrel{\text{i.i.d.}}{\sim} H$ for some diffuse distribution H . The distribution H , called the ground measure, serves as a prior on the traits in the space Ψ . For example, consider a common topic model. Each trait ψ_i represents a latent topic, modeled as a probability vector in the simplex of vocabulary words. And θ_i represents the frequency with which the topic ψ_i appears across documents in a corpus. H is a Dirichlet distribution over the probability simplex, with dimension given by the number of words in the vocabulary.

By pairing the rates from the Poisson process with traits drawn from the ground measure, we obtain a completely random measure and use the shorthand $\text{CRM}(H, \nu)$ for its law: $\Theta = \sum_i \theta_i \delta_{\psi_i} \sim \text{CRM}(H, \nu)$. Since the traits ψ_i and the rates θ_i are independent, the CRM is *homogeneous*. When the total mass $\Theta(\Psi)$ is strictly positive and finite, the corresponding *normalized CRM* (NCRM) is $\Xi := \Theta/\Theta(\Psi)$, which is a discrete probability measure: $\Xi = \sum_i \xi_i \delta_{\psi_i}$, where $\xi_i = \theta_i/(\sum_j \theta_j)$ (Regazzini, Lijoi and Prünster, 2003; James, Lijoi and Prünster, 2009).

The CRM prior on Θ is typically combined with a likelihood that generates trait counts for each data point. Let $\ell(\cdot | \theta)$ be a proper probability mass function on $\mathbb{N} \cup \{0\}$ for all θ in the support of ν . The process $X_n := \sum_i x_{ni} \delta_{\psi_i}$ collects the trait counts, where $x_{ni} | \Theta \sim \ell(\cdot | \theta_i)$ independently across atom index i and i.i.d. across data index n . We denote the distribution of X_n as $\text{LP}(\ell, \Theta)$, which we call the *likelihood process*. Together, the prior on Θ and likelihood on X given Θ form a generative model for allocation of data points to traits; hence, this generative model is a special case of a *trait allocation model* (Campbell, Cai and Broderick, 2018). Analogously, when the trait counts are restricted to $\{0, 1\}$, this generative model represents a special case of a *feature allocation model*.

Since the trait counts are typically just a latent component in a full generative model specification, we define the observed data to be $Y_n | X_n \stackrel{\text{indep}}{\sim} f(\cdot | X_n)$ for a probability kernel $f(dY | X)$. Consider the topic modeling example: θ_i represents the rate of topic ψ_i in a document corpus; Θ captures the rates of all topics; X_n captures how many words in document n are generated from each topic; and Y_n gives the observed collection of words for that document.

Finite approximations. Since the set $\{\theta_i\}_{i=1}^\infty$ is countably infinite, it is not possible to simulate or perform posterior inference for every θ_i . One approximation scheme uses a *finite approximation* $\Theta_K := \sum_{i=1}^K \rho_i \delta_{\psi_i}$. The atom sizes $\{\rho_i\}_{i=1}^K$ are designed so that Θ_K is a good approximation of Θ in a suitable sense. Since it involves a finite number of parameters

³Conversely, some important priors, such as Pitman-Yor processes, are not CRMs or their normalizations and are outside the scope of the present paper (Pitman and Yor, 1997; Arbel, De Blasi and Prünster, 2019; Lijoi, Prünster and Rigon, 2020a).

⁴For brevity, we do not consider the fixed-location and deterministic components of a CRM (Kingman, 1967). When these are purely atomic, they can be added to our analysis without undue effort.

unlike Θ , Θ_K can be used directly in standard posterior approximation schemes such as Markov chain Monte Carlo or variational Bayes. But not using the full CRM Θ introduces approximation error.

A *truncated finite approximation* (TFA; Doshi-Velez et al., 2009; Paisley, Blei and Jordan, 2012; Roychowdhury and Kulis, 2015; Arbel and Prünster, 2017; Campbell et al., 2019) requires constructing an ordering on the set of rates from the Poisson process; let $(\theta_i)_{i=1}^\infty$ be the corresponding *sequence* of rates. The approximation uses $\rho_i = \theta_i$ for i up to some K ; i.e. one keeps the first K rates in the sequence and ignores the remaining ones. We refer to the number of instantiated atoms K as the *approximation level*. Campbell et al. (2019) categorizes and analyzes TFAs. TFAs offer an attractive nested structure: to refine an existing truncation, it suffices to generate the additional terms in the sequence. However, the complex dependencies between the rates $(\theta_i)_{i=1}^K$ potentially make inference more challenging.

We instead develop a family of *independent finite approximations* (IFAs). An IFA is defined by a sequence of probability measures ν_1, ν_2, \dots such that at approximation level K , there are K atoms whose weights are given by $\rho_1, \dots, \rho_K \stackrel{\text{i.i.d.}}{\sim} \nu_K$. The probability measures are chosen so that the sequence of approximations converges in distribution to the target CRM: $\Theta_K \xrightarrow{D} \Theta$ as $K \rightarrow \infty$. For random measures, convergence in distribution can also be characterized by convergence of integrals under the measures (Kallenberg, 2002, Lemma 12.1 and Theorem 16.16). The advantages and disadvantages of IFAs reverse those of TFAs: the atoms are now i.i.d., potentially making inference easier, but a completely new approximation must be constructed if K changes.

Next consider approximating an NCRM $\Xi = \sum_i \xi_i \delta_{\psi_i}$, where $\xi_i = \theta_i / (\sum_j \theta_j)$, with a finite approximation. A normalized TFA might be defined in one of two ways. In the first approach, the rates $\{\rho_i\}_{i=1}^K$ that target the CRM rates $\{\theta_i\}_{i=1}^\infty$ are normalized to form the NCRM approximation; i.e. the approximation has atom sizes $\rho_i / \sum_{j=1}^K \rho_j$ (Campbell et al., 2019). The second approach directly constructs an ordering over the sequence of normalized rates ξ_i and truncates this representation.⁵ We construct normalized IFAs in a similar manner to the first TFA approach: the NCRM approximation has atom sizes $\rho_i / \sum_{j=1}^K \rho_j$ where $\{\rho_i\}_{i=1}^K$ are the IFA rates.

In the past, independent finite approximations have largely been developed on a case-by-case basis (Paisley and Carin, 2009; Broderick et al., 2015; Acharya, Ghosh and Zhou, 2015; Lee, James and Choi, 2016). Our goal is to provide a general-purpose mechanism. Lijoi, Prünster and Rigon (2023) and Lee, Miscouridou and Caron (2022) have also recently pursued a more general construction, but we believe there remains room for improvement. Lijoi, Prünster and Rigon (2023) focus on NCRMs for clustering; it is not immediately clear how to adapt this work for inference in trait allocation models. Also, Lijoi, Prünster and Rigon (2023, Theorem 1) employ infinitely divisible random variables. Since infinitely divisible distributions that are not Dirac measures cannot have bounded support, the approximate rates $\{\rho_i\}_{i=1}^K$ are not naturally compatible with the trait likelihood $\ell(\cdot | \theta)$ if the support of the rate measure ν is bounded. But the support of ν is often bounded in applications to trait allocation models; e.g., θ_i may represent a feature frequency, taking values in $[0, 1]$, and $\ell(\cdot | \theta)$ may take the form of a Bernoulli, binomial, or negative binomial distribution. Therefore, applications of the finite approximations of Lijoi, Prünster and Rigon (2023, Theorem 1) to these models may require some additional work. The construction in Lee, Miscouridou and Caron (2022, Proposition 3.2) yields $\{\rho_i\}_{i=1}^K$ that are compatible with $\ell(\cdot | \theta)$ and recovers

⁵In this case, $\sum_{i=1}^K \xi_i < 1$. Therefore, setting the final atom size in the NCRM approximation to be $1 - \sum_{i=1}^K \xi_i$ ensures the approximation is a probability measure.

important cases in the literature. However, outside these special cases, it is unknown if the i.i.d. distributions are tractable because the densities ν_K are not explicitly defined; see the discussion around Eq. (3) for more details.

Example 2.1 (Running example: beta process). For concreteness, we consider the (*three-parameter*) *beta process*⁶ (Teh and Görür, 2009; Broderick, Jordan and Pitman, 2012) as a running example of a CRM. The process $\text{BP}(\gamma, \alpha, d)$ is defined by a mass parameter $\gamma > 0$, discount parameter $d \in [0, 1)$, and concentration parameter $\alpha > -d$. It has rate measure

$$\nu(d\theta) = \gamma \frac{\Gamma(\alpha + 1)}{\Gamma(1 - d)\Gamma(\alpha + d)} \mathbf{1}\{0 \leq \theta \leq 1\} \theta^{-d-1} (1 - \theta)^{\alpha+d-1} d\theta. \quad (1)$$

The $d = 0$ case yields the standard beta process (Hjort, 1990; Thibaux and Jordan, 2007). The beta process is typically paired with the Bernoulli likelihood process with conditional distribution $\ell(x | \theta) = \theta^x (1 - \theta)^{1-x} \mathbf{1}\{x \in \{0, 1\}\}$. The resulting *beta-Bernoulli process* has been used in factor analysis models (Doshi-Velez et al., 2009; Paisley, Blei and Jordan, 2012) and for dictionary learning (Zhou et al., 2009).

3. Automated independent finite approximations

In this section we introduce *automated independent finite approximations*, a practical construction of independent finite approximations (IFAs) for a broad class of CRMs. We highlight a useful special case of our construction for exponential family CRMs (Broderick, Wilson and Jordan, 2018) without power laws and apply our construction to approximate NCRMs. In all of these cases, we prove that as the approximation size increases, the distribution of the approximation converges (in some relevant sense) to that of the exact infinite-dimensional model.

3.1. Applying our approximation to CRMs

Formally, we define IFAs in terms of a fixed, diffuse probability measure H and a sequence of probability measures ν_1, ν_2, \dots . The K -atom IFA Θ_K is

$$\Theta_K := \sum_{i=1}^K \rho_i \delta_{\psi_i}, \quad \rho_i \stackrel{\text{i.i.d.}}{\sim} \nu_K, \quad \psi_i \stackrel{\text{i.i.d.}}{\sim} H,$$

which we write as $\Theta_K \sim \text{IFA}_K(H, \nu_K)$. We consider CRM rate measures ν with densities that, near zero, are (roughly) proportional to θ^{-1-d} , where $d \in [0, 1)$ is the *discount* parameter. We will propose a general construction for IFAs given a target random measure and prove that it converges to the target (Theorem 3.1). We first summarize our requirements for which CRMs we approximate in Assumption 1. We show in Appendix A that popular BNP priors satisfy Assumption 1; specifically, we check the beta, gamma (Ferguson and Klass, 1972; Kingman, 1975; Titsias, 2008), generalized gamma (Brix, 1999), beta prime (Broderick et al., 2015), and PG(α, ζ)-generalized gamma (James, 2013) processes.

Assumption 1. For $d \in [0, 1)$ and $\eta \in V \subseteq \mathbb{R}^d$, we take $\Theta \sim \text{CRM}(H, \nu(\cdot; \gamma, d, \eta))$ for

$$\nu(d\theta; \gamma, d, \eta) := \gamma \theta^{-1-d} g(\theta)^{-d} \frac{h(\theta; \eta)}{Z(1-d, \eta)} d\theta$$

such that

⁶Also known as the *stable beta process* (Teh and Görür, 2009)

1. for $\xi > 0$ and $\eta \in V$, $Z(\xi, \eta) := \int \theta^{\xi-1} g(\theta)^\xi h(\theta; \eta) d\theta < \infty$;
2. g is continuous, $g(0) = 1$, and there exist constants $0 < c_* \leq c^* < \infty$ such that $c_* \leq g(\theta)^{-1} \leq c^*(1 + \theta)$;
3. there exists $\epsilon > 0$ such that for all $\eta \in V$, the map $\theta \mapsto h(\theta; \eta)$ is continuous and bounded on $[0, \epsilon]$.

Other than the discount d and mass γ , the rate measure ν potentially depends on additional hyperparameters η . The finiteness of the normalizer Z is necessary in defining finite-dimensional distributions whose densities are similar in form to ν . The conditions on the behaviors of $g(\theta)$ and $h(\theta; \eta)$ ensure that the overall rate measure's behavior near $\theta = 0$ is dominated by the θ^{-1-d} term. The support of the rate measure is implicitly determined by $h(\theta; \eta)$.

Given a CRM satisfying Assumption 1, we can construct a sequence of IFAs that converge in distribution to that CRM.

Theorem 3.1. *Suppose Assumption 1 holds. Let*

$$S_b(\theta) = \begin{cases} \exp\left(\frac{-1}{1-(\theta-b)^2/b^2} + 1\right) & \text{if } \theta \in (0, b) \\ \mathbf{1}\{\theta > 0\} & \text{otherwise.} \end{cases} \quad (2)$$

For $c := \gamma h(0; \eta)/Z(1-d, \eta)$, let

$$\nu_K(d\theta) := \theta^{-1+cK^{-1}-dS_{1/K}(\theta-1/K)} g(\theta)^{cK^{-1}-d} h(\theta; \eta) Z_K^{-1} d\theta$$

be a family of probability densities, where Z_K is chosen such that $\int \nu_K(d\theta) = 1$. If $\Theta_K \sim \text{IFA}_K(H, \nu_K)$, then $\Theta_K \xrightarrow{\mathcal{D}} \Theta$ as $K \rightarrow \infty$.

See Appendix B.1 for a proof of Theorem 3.1. We choose the particular form of $S_b(\theta)$ in Eq. (2) for concreteness and convenience. But our theory still holds for a more general class of S_b forms, as we describe in more detail in the proof of Theorem 3.1.

Definition 3.2. We call the K -atom IFA resulting from Theorem 3.1 the *automated IFA* (AIFA_K).

Although the normalization constant Z_K is not always available analytically, numerical implementation remains straightforward. When Z_K is a quantity of interest, such as in Section 6.4, we estimate it using standard numerical integration schemes for a one-dimensional integral (Piessens et al., 2012; Virtanen et al., 2020). For other tasks, we need not access Z_K directly. In our experiments, we show that we can use either Markov chain Monte Carlo (Sections 6.1 and 6.5) or variational Bayes (Sections 6.2 and 6.3) with the unnormalized density.

To illustrate our construction, we next apply Theorem 3.1 to $\text{BP}(\gamma, \alpha, d)$ from Example 2.1. In Appendix A, we show how to construct AIFAs for the beta prime, gamma, generalized gamma, and $\text{PG}(\alpha, \zeta)$ -generalized gamma processes.

Example 3.1 (Beta process AIFA). To apply Assumption 1, let $\eta = \alpha + d$, $V = \mathbb{R}_+$, $g(\theta) = 1$, $h(\theta; \eta) = (1-\theta)^{\eta-1} \mathbf{1}[\theta \leq 1]$, and $Z(\xi, \eta)$ equal the beta function $B(\xi, \eta)$. Then the CRM rate measure ν in Assumption 1 corresponds to that of $\text{BP}(\gamma, \alpha, d)$ from Example 2.1. Note that we make no additional restrictions on the hyperparameters γ, α, d beyond those in the original CRM (Example 2.1). Observe that h is continuous and bounded on $[0, 1/2]$, and

the normalization function $B(\xi, \eta)$ is finite for $\xi > 0, \eta \in V$; it follows that Assumption 1 holds. By Theorem 3.1, then, the AIFA density is

$$\frac{1}{Z_K} \theta^{-1+c/K-dS_{1/K}(\theta-1/K)} (1-\theta)^{\alpha+d-1} \mathbf{1}\{0 \leq \theta \leq 1\} d\theta,$$

where $c := \gamma/B(\alpha + d, 1 - d)$ and Z_K is the normalization constant. The density does not in general reduce to a beta distribution in θ due to the θ in the exponent.

Comparison to an alternative IFA construction. Lee, Miscouridou and Caron (2022, Proposition 3.2) verify the validity of a different IFA construction. Their construction requires two functions: (1) a bivariate function $\Lambda(\theta, t)$ such that for any $t > 0$, $\Delta(t) := \int \Lambda(\theta, t) \nu(d\theta) < \infty$ and (2) a univariate function $f(n)$ such that $\Delta(f(n))$ is bounded from both above and below by n as $n \rightarrow \infty$. If these functions exist and

$$\tilde{\nu}_K(d\theta) := \frac{\Lambda(\theta, f(K)) \nu(d\theta)}{\Delta(f(K))}, \quad (3)$$

Lee, Miscouridou and Caron (2022, Proposition 3.2) show that $\text{IFA}_K(H, \tilde{\nu}_K)$ converges in distribution to $\text{CRM}(H, \nu)$ as $K \rightarrow \infty$. The usability of Eq. (3) in practice depends on the tractability of Λ and f . There are typically many tractable $\Lambda(\theta, t)$ (Lee, Miscouridou and Caron, 2022, Section 4). Proposition B.2 of Lee, Miscouridou and Caron (2022) lists tractable f for the important cases of the beta process and generalized gamma process with $d > 0$. However, the choice of f provided there for general power-law processes is not tractable because its evaluation requires computing complicated inverses in the asymptotic regime. Furthermore, for processes without power laws, no general recipe for f is known. In contrast, the AIFA construction in Theorem 3.1 always yields densities that can be evaluated up to proportionality constants.

Example 3.2 (Beta process: an IFA comparison). We next compare our beta process AIFA to the two separate IFAs proposed by Lee, Miscouridou and Caron (2022) and Lee, James and Choi (2016) for disjoint subcases within the case $d > 0$. First consider the subcase where $\alpha = 0, d > 0$. Lee, James and Choi (2016) derive⁷ what we call⁸ the *BFRY IFA*. The IFA density, denoted $\nu_{\text{BFRY}}(d\theta)$, is equal to

$$\frac{\gamma}{K} \frac{\theta^{-d-1}(1-\theta)^{d-1}}{B(d, 1-d)} \left[1 - \exp\left(-\left(\frac{K\Gamma(d)d}{\gamma}\right)^{1/d} \frac{\theta}{1-\theta}\right) \right] \mathbf{1}\{0 \leq \theta \leq 1\} d\theta. \quad (4)$$

Second, consider the subcase where $\alpha > 0, d > 0$, Lee, Miscouridou and Caron (2022, Section 4.5) derive another K -atom IFA, which we call⁹ the *generalized Pareto IFA* (GenPar IFA). The IFA density, denoted $\nu_{\text{GenPar}}(d\theta)$, is equal to

$$\frac{\gamma}{K} \frac{\theta^{-d-1}(1-\theta)^{\alpha+d-1}}{B(1-d, \alpha+d)} \left(1 - \frac{1}{\left(\theta \left[\left(1 + \frac{Kd}{\gamma\alpha}\right)^{\frac{1}{d}} - 1\right] + 1\right)^\alpha} \right) \mathbf{1}\{0 \leq \theta \leq 1\} d\theta. \quad (5)$$

⁷There is a typo in Lee, James and Choi (2016, Theorem 2, item (iii)): θ/K should be $(\theta/\Gamma(\alpha))/K$.

⁸Devroye and James (2014) introduce the acronym BFRY to denote a distribution named for the authors Bertoin et al. (2006). We here use “BFRY IFA” to denote what Lee, James and Choi (2016) call the “BFRY process” and thereby emphasize that this process forms an IFA.

⁹We use the term “generalized Pareto” because Lee, Miscouridou and Caron (2022, Section 4.5) use generalized Pareto variates to define $\Lambda(\theta, t)$ from Eq. (3).

Since the BFRY IFA and GenPar IFA apply to disjoint hyperparameter regimes, they are not directly comparable. Since our AIFA applies to the whole domain $\alpha \geq -d$, we can separately compare it to each of these alternative IFAs; we also highlight that the AIFA still applies when $\alpha \in (-d, 0)$, a case not covered by either the BFRY IFA or GenPar IFA.

We find in Section 6.3 that the AIFA and BFRY IFA have comparable predictive performance; the AIFA and GenPar IFA also have comparable predictive performance. But in Section 6.4, we show that the AIFA is much more reliable than the BFRY IFA or the GenPar IFA for estimating the discount (d) hyperparameter by maximizing the marginal likelihood. Conversely, sampling from a BFRY IFA or GenPar IFA prior is easier than sampling from an AIFA prior since the BFRY and GenPar IFA priors are formed from standard distributions.

3.2. Applying our approximation to exponential family CRMs

Exponential family CRMs with $d = 0$ comprise a widely used special case of CRMs. In what follows, we show how Theorem 3.1 simplifies in this special case.

In common BNP models, the relationship between the likelihood $\ell(\cdot | \theta)$ and the CRM prior is closely related to finite-dimensional exponential family conjugacy (Broderick, Wilson and Jordan, 2018, Section 4). In particular, the likelihood has an exponential family form,

$$\ell(x | \theta) := \kappa(x) \theta^{\phi(x)} \exp(\langle \mu(\theta), t(x) \rangle - A(\theta)). \quad (6)$$

Here $x \in \mathbb{N} \cup \{0\}$, $\kappa(x) \in \mathbb{R}$ is the base density, $\phi(x) \in \mathbb{R}$ and $t(x) \in \mathbb{R}^{D'}$ (for some D') form the vector of sufficient statistics $(t(x), \phi(x))^T$, $A(\theta) \in \mathbb{R}$ is the log partition function, $\mu(\theta) \in \mathbb{R}^{D'}$ and $\ln \theta$ form the vector of natural parameters $(\mu(\theta), \ln \theta)^T$, and $\langle \mu(\theta), t(x) \rangle$ denotes the standard Euclidean inner product. The rate measure nearly matches the form of the conjugate prior, but behaves like θ^{-1} near 0:

$$\nu(d\theta) := \gamma' \theta^{-1} \exp \left\{ \left\langle \left(\begin{array}{c} \psi \\ \lambda \end{array} \right), \left(\begin{array}{c} \mu(\theta) \\ -A(\theta) \end{array} \right) \right\rangle \right\} \mathbf{1}\{\theta \in U\} d\theta, \quad (7)$$

where $\gamma' > 0$, $\lambda > 0$, $\psi \in \mathbb{R}^{D'}$ and $U \subseteq \mathbb{R}_+$ is the support of ν . Eq. (7) leads to the suggestive terminology of *exponential family* CRMs. The θ^{-1} dependence near 0 means that these models lack power-law behavior. Models that can be cast in this form include the standard beta process with Bernoulli or negative binomial likelihood (Zhou et al., 2012; Broderick et al., 2015) and the gamma process with Poisson likelihood (Acharya, Ghosh and Zhou, 2015; Roychowdhury and Kulis, 2015). We refer to these models as, respectively, the beta–Bernoulli, beta–negative binomial, and gamma–Poisson processes.

We now specialize Assumption 1 and Theorem 3.1 to exponential family CRMs in Assumption 2 and Corollary 3.3, respectively.

Assumption 2. Let ν be of the form in Eq. (7) and assume that

1. For any $\xi > -1$, for any $\eta = (\psi, \lambda)^T$ where $\lambda > 0$, the normalizer defined as

$$Z(\xi, \eta) := \int_U \theta^\xi \exp \left\{ \left\langle \eta, \left(\begin{array}{c} \mu(\theta) \\ -A(\theta) \end{array} \right) \right\rangle \right\} d\theta \quad (8)$$

is finite, and

2. there exists $\epsilon > 0$ such that, for any $\eta = (\psi, \lambda)^T$ where $\lambda > 0$, the map

$$\varsigma : \theta \mapsto \exp \left\{ \left\langle \eta, \begin{pmatrix} \mu(\theta) \\ -A(\theta) \end{pmatrix} \right\rangle \right\} \mathbf{1}\{\theta \in U\}$$

is a continuous and bounded function of θ on $[0, \epsilon]$.

Corollary 3.3. *Suppose Assumption 2 holds. For $c := \gamma' \varsigma(0)$, let*

$$\nu_K(\theta) := \frac{\theta^{c/K-1} \varsigma(\theta)}{Z(c/K-1, \eta)}. \quad (9)$$

If $\Theta_K \sim \text{IFA}_K(H, \nu_K)$, then $\Theta_K \xrightarrow{\mathcal{D}} \Theta$.

The density in Eq. (9) is almost the same as the rate measure of Eq. (7), except the θ^{-1} term has become $\theta^{c/K-1}$. As a result, Eq. (9) is a proper exponential-family distribution. In Appendix A, we detail the corresponding $d = 0$ special cases of the AIFA for beta prime, gamma, generalized gamma, and $\text{PG}(\alpha, \zeta)$ -generalized gamma processes. We cover the beta process case next.

Example 3.3 (Beta process AIFA for $d = 0$). Corollary 3.3 is sufficient to recover known IFA results for $\text{BP}(\gamma, \alpha, 0)$; when $d = 0$, the AIFA from Example 3.1 simplifies to $\nu_K = \text{Beta}(\gamma\alpha/K, \alpha)$. Doshi-Velez et al. (2009) approximates $\text{BP}(\gamma, 1, 0)$ with $\nu_K = \text{Beta}(\gamma/K, 1)$. For $\text{BP}(\gamma, \alpha, 0)$, Griffiths and Ghahramani (2011) set $\nu_K = \text{Beta}(\gamma\alpha/K, \alpha)$, and Paisley and Carin (2009) use $\nu_K = \text{Beta}(\gamma\alpha/K, \alpha(1 - 1/K))$. The difference between $\text{Beta}(\gamma\alpha/K, \alpha)$ and $\text{Beta}(\gamma\alpha/K, \alpha(1 - 1/K))$ is negligible for moderately large K .

We can also use Corollary 3.3 to create a new finite approximation for a nonparametric process so far not explored in the Bayesian nonparametric literature.

Example 3.4 (CMP likelihood and extended gamma process). The *CMP likelihood*¹⁰ (Shmueli et al., 2005) is given by

$$\ell(x | \theta) = \frac{\theta^x}{(x!)^\tau} \frac{1}{Z_\tau(\theta)}, \quad \text{where } Z_\tau(\theta) := \sum_{y=0}^{\infty} \frac{\theta^y}{(y!)^\tau}. \quad (10)$$

The conjugate CRM prior, which we call an *extended gamma* (or *Xgamma*) *process*, has four hyperparameters: mass γ , concentration c , maximum T , and shape τ :

$$\nu(d\theta) = \gamma \theta^{-1} Z_\tau^{-c}(\theta) \mathbf{1}\{0 \leq \theta \leq T\} d\theta. \quad (11)$$

Unlike existing BNP models, the model in Eqs. (10) and (11), which we call *Xgamma-CMP process*, is able to capture different dispersion regimes. For $\tau < 1$, the variance of the counts from $\ell(x | \theta)$ is larger than the mean of the counts, corresponding to overdispersion. For $\tau > 1$, the variance of the counts from $\ell(x | \theta)$ is smaller than the mean of the counts, corresponding to underdispersion. As we show in Section 6.5, the latent shape τ can be inferred using observed data. Zhou et al. (2012); Broderick et al. (2015) provide BNP trait allocation models that handle overdispersion. Canale and Dunson (2011) provide a BNP model that handles both underdispersion and overdispersion, but for clustering rather than traits. We are not aware of trait allocation models that handle underdispersion, or any

¹⁰CMP stands for Conway-Maxwell-Poisson.

trait allocation models that handle both underdispersion and overdispersion. Following the approach of Broderick, Wilson and Jordan (2018), in Appendix D we show that as long as $\gamma > 0$, $c > 0$, $T \geq 1$, and $\tau > 0$, the total mass of the rate measure is infinite and the number of active traits is almost surely finite. Under these conditions, we show in Appendix A that Corollary 3.3 applies to the CRM in Eq. (11), and we construct the resulting AIFA.

3.3. Normalized independent finite approximations

Given that AIFAs are approximations that converge to the corresponding target CRM, it is natural to ask if normalizations of AIFAs converge to the corresponding normalization of the target CRM, i.e., the corresponding NCRM. Our next result shows that normalized AIFAs indeed converge, in the sense that the exchangeable partition probability functions, or EPPFs (Pitman, 1995), converge. Given a random sample of size N from an NCRM Ξ , the EPPF gives the probability of the induced partition from such a sample. In particular, consider the model $\Xi \sim \text{NCRM}$, $X_n \mid \Xi \stackrel{\text{i.i.d.}}{\sim} \Xi$ for $1 \leq n \leq N$.¹¹ Grouping the indices n with the same value of X_n induces a partition over the set $\{1, 2, \dots, N\}$. Let b represent the number of distinct values in the set $\{X_n\}_{n=1}^N$, so $b \leq N$. Let n_i be the number of indices n with X_n equal to the i -th distinct value of X_n , for some ordering of the values. So $\sum_{i=1}^b n_i = N$ and $\forall i, n_i \geq 1$. With this notation in hand, we can write the EPPF, which gives the probability of the induced partition under the model, as a symmetric function $p(n_1, n_2, \dots, n_b)$ that depends only on the counts n_i . Similarly, we let $p_K(n_1, n_2, \dots, n_b)$ be the EPPF for the normalized AIFA $_K$. Note that $p_K(n_1, n_2, \dots, n_b) = 0$ when $K < b$ since the normalized AIFA $_K$ at approximation level K generates at most K blocks.

Theorem 3.4. *Suppose Assumption 1 holds. Take any positive integers $N, b, \{n_i\}_{i=1}^b$ such that $b \leq N$, $n_i \geq 1$, and $\sum_{i=1}^b n_i = N$. Let p be the EPPF of the NCRM $\Xi := \Theta/\Theta(\Psi)$. If Θ_K is the AIFA for Θ at approximation level K , and p_K is the EPPF for the corresponding NCRM approximation $\Theta_K/\Theta_K(\Psi)$, then*

$$\lim_{K \rightarrow \infty} p_K(n_1, n_2, \dots, n_b) = p(n_1, n_2, \dots, n_b).$$

See Appendix B.3 for the proof. Since the EPPF gives the probability of each partition, the point-wise convergence in Theorem 3.4 certifies that the distribution over partitions induced by sampling from the normalized AIFA $_K$ converges to that induced by sampling from the target NCRM, for any finite sample size N .

4. Non-asymptotic error bounds

Theorems 3.1 and 3.4 justify the use of our proposed AIFA construction in the limit $K \rightarrow \infty$ but do not provide guidance on how to choose the approximation level K when N observations are available. In Section 4.1, we quantify the error introduced by replacing an exponential family CRM with the AIFA. In Section 4.2, we quantify the error introduced by replacing a Dirichlet process (DP) (Ferguson, 1973; Sethuraman, 1994) with the corresponding normalized AIFA. We derive error bounds that are simple to manipulate and yield recommendations for the appropriate K for a given N and a desired accuracy level.

¹¹We reuse the X_n notation from the CRM description, even though X_n now is a scalar, because the role of the draws from Ξ is the same as that of the draws from Θ .

4.1. Bounds when approximating an exponential family CRM

Recall from Section 2 that the CRM prior Θ is typically paired with a likelihood process LP, which manifests features X_n , and a probability kernel f relating active features to observations Y_n . The target nonparametric model can be summarized as

$$\begin{aligned}\Theta &\sim \text{CRM}(H, \nu), \\ X_n | \Theta &\stackrel{\text{i.i.d.}}{\sim} \text{LP}(\ell, \Theta), \quad n = 1, 2, \dots, N, \\ Y_n | X_n &\stackrel{\text{indep}}{\sim} f(\cdot | X_n), \quad n = 1, 2, \dots, N.\end{aligned}\tag{12}$$

The approximating model, with ν_K as in Theorem 3.1 (or Corollary 3.3), is

$$\begin{aligned}\Theta_K &\sim \text{AIFA}_K(H, \nu_K), \\ Z_n | \Theta_K &\stackrel{\text{i.i.d.}}{\sim} \text{LP}(\ell, \Theta_K), \quad n = 1, 2, \dots, N, \\ W_n | Z_n &\stackrel{\text{indep}}{\sim} f(\cdot | Z_n), \quad n = 1, 2, \dots, N.\end{aligned}\tag{13}$$

Active traits in the approximate model are collected in Z_n and observations are W_n . Let $P_{N,\infty}$ be the marginal distribution of the observations $Y_{1:N}$ and $P_{N,K}$ be the marginal distribution of the observations $W_{1:N}$. The *approximation error* we analyze is the total variation distance $d_{\text{TV}}(P_{N,K}, P_{N,\infty}) := \sup_{0 \leq g \leq 1} |\int g dP_{N,K} - \int g dP_{N,\infty}|$ between the two observational processes, one using the CRM and the other one using the approximate AIFA $_K$ as the prior. Total variation is a standard choice of error when analyzing CRM approximations (Ishwaran and Zarepour, 2002; Doshi-Velez et al., 2009; Paisley, Blei and Jordan, 2012; Campbell et al., 2019). Small total variation distance implies small differences in expectations of bounded functions.

Conditions. In our analysis, we focus on exponential family CRMs and conjugate likelihood processes. We will suppose Assumption 2 holds. Our analysis guarantees that $d_{\text{TV}}(P_{N,K}, P_{N,\infty})$ is small whenever a conjugate exponential family CRM–likelihood pair and the corresponding AIFA model satisfy certain conditions, beyond those already stated in Assumption 2. In the proof of the error bound, these conditions serve as intermediate results that ultimately lead to small approximation error. Because we can verify the conditions for common models, we have error bounds in the most prevalent use cases of CRMs. To express these conditions, we use the *marginal process* representation of the target and the approximate model, i.e., the series of conditional distributions of $X_n | X_{1:(n-1)}$ (or $Z_n | Z_{1:(n-1)}$) with Θ (or Θ_K) integrated out. Corollary 6.2 of Broderick, Wilson and Jordan (2018) guarantees that the marginal $X_n | X_{1:(n-1)}$ is a random measure with finite support and with a convenient form. Since we will use this form to write our conditions (Condition 1 below), we first review the requisite notation — and establish analogous notation for $Z_n | Z_{1:(n-1)}$.

We start by defining h and M to describe the conditional distribution $X_n | X_{1:(n-1)}$. Let K_{n-1} be the number of unique atom locations in X_1, X_2, \dots, X_{n-1} , and let $\{\zeta_i\}_{i=1}^{K_{n-1}}$ be the collection of unique atom locations in X_1, X_2, \dots, X_{n-1} . Fix an atom location ζ_j (the choice of j does not matter). For m with $1 \leq m \leq n$, let x_m be the atom size of X_m at atom location ζ_j ; x_m may be zero if there is no atom at ζ_j in X_m . The distribution of x_n depends *only* on the $x_{1:(n-1)}$ values, which are the atom sizes of previous measures X_m at ζ_j . We use $h(x | x_{1:(n-1)})$ to denote the probability mass function (p.m.f.) of x_n at value x . Furthermore, X_n has a finite number of new atoms, which can be grouped together by atom size. Consider any potential atom size $x \in \mathbb{N}$. Define $p_{n,x}$ to be the number of atoms of size

x . Regardless of atom size, each atom location is a fresh draw from the ground measure H and $p_{n,x}$ is Poisson-distributed; we use $M_{n,x}$ to denote the mean of $p_{n,x}$.

Next, we define \tilde{h} , which governs the conditional distribution of $Z_n | Z_{1:(n-1)}$. Let 0_{n-1} be the zero vector with $n-1$ components. Although $h(x | x_{1:(n-1)})$ is defined only for count vectors $x_{1:(n-1)}$ that are not identically zero, we will see that $\tilde{h}(x | 0_{n-1})$ is well-defined. In particular, let $\{\zeta_i\}_{i=1}^{K_{n-1}}$ be the union of atom locations in Z_1, Z_2, \dots, Z_{n-1} . Fix an atom location ζ_j . For $1 \leq m \leq n$, let x_m be the atom size of Z_m at atom location ζ_j . We write the p.m.f. of x_n at x as $\tilde{h}(x | x_{1:(n-1)})$. In addition, Z_n also has a maximum of $K - K_{n-1}$ new atoms with locations disjoint from $\{\zeta_i\}_{i=1}^{K_{n-1}}$, and the distribution of atom sizes is governed by $\tilde{h}(x | 0_{n-1})$. Note that we reuse the x_n and ζ_j notation from $X_n | X_{1:(n-1)}$ without risk of confusion, since x_n and ζ_j are dummy variables whose meanings are clear given the context of h or \tilde{h} .

In Appendix C, we describe the marginal processes in more detail and give formulas for h , \tilde{h} , and $M_{n,x}$ in terms of the functions that parametrize Eqs. (6) and (7) and the normalizer Eq. (8). For the beta-Bernoulli process with $d = 0$, the functions have particularly convenient forms.

Example 4.1. For the beta-Bernoulli model with $d = 0$, we have

$$\begin{aligned} h(x | x_{1:(n-1)}) &= \frac{\sum_{i=1}^{n-1} x_i}{\alpha - 1 + n} \mathbf{1}\{x = 1\} + \frac{\alpha + \sum_{i=1}^{n-1} (1 - x_i)}{\alpha - 1 + n} \mathbf{1}\{x = 0\}. \\ \tilde{h}(x | x_{1:(n-1)}) &= \frac{\sum_{i=1}^{n-1} x_i + \gamma\alpha/K}{\alpha - 1 + n + \gamma\alpha/K} \mathbf{1}\{x = 1\} + \frac{\alpha + \sum_{i=1}^{n-1} (1 - x_i)}{\alpha - 1 + n + \gamma\alpha/K} \mathbf{1}\{x = 0\}, \\ M_{n,1} &= \frac{\gamma\alpha}{\alpha - 1 + n}, \quad M_{n,x} = 0 \text{ for } x > 1. \end{aligned}$$

We now formulate conditions on h , \tilde{h} , and $M_{n,x}$ that will yield small $d_{\text{TV}}(P_{N,K}, P_{N,\infty})$.

Condition 1. There exist constants $\{C_i\}_{i=1}^5$ such that

1. for all $n \in \mathbb{N}$,

$$\sum_{x=1}^{\infty} M_{n,x} \leq \frac{C_1}{n - 1 + C_1}; \quad (14)$$

2. for all $n \in \mathbb{N}$,

$$\sum_{x=1}^{\infty} \tilde{h}(x | x_{1:(n-1)} = 0_{n-1}) \leq \frac{1}{K} \frac{C_1}{n - 1 + C_1}; \quad (15)$$

3. for any $n \in \mathbb{N}$, for any $\{x_i\}_{i=1}^{n-1} \neq 0_{n-1}$,

$$\sum_{x=0}^{\infty} \left| h(x | x_{1:(n-1)}) - \tilde{h}(x | x_{1:(n-1)}) \right| \leq \frac{1}{K} \frac{C_1}{n - 1 + C_1}; \text{ and} \quad (16)$$

4. for all $n \in \mathbb{N}$, for any $K \geq C_2(\ln n + C_3)$,

$$\sum_{x=1}^{\infty} \left| M_{n,x} - K \tilde{h}(x | x_{1:(n-1)} = 0_{n-1}) \right| \leq \frac{1}{K} \frac{C_4 \ln n + C_5}{n - 1 + C_1}. \quad (17)$$

Note that the conditions depend only on the functions governing the exponential family CRM prior and its conjugate likelihood process — and not on the observation likelihood f . Eq. (14) constrains the growth rate of the target model since $\sum_{n=1}^N \sum_{x=1}^{\infty} M_{n,x}$ is the expected number of components for data cardinality N . Because each $\sum_{x=1}^{\infty} M_{n,x}$ is at most $O(1/n)$, the total number of components after N samples is $O(\ln N)$. Similarly, Eq. (15) constrains the growth rate of the approximate model. The third condition (Eq. (16)) ensures that \tilde{h} is a good approximation of h in total variation distance and that there is also a reduction in the error as n increases. Finally, Eq. (17) implies that $K\tilde{h}(x|0_{n-1})$ is an accurate approximation of $M_{n,x}$, and there is also a reduction in the error as n increases.

We show that Condition 1 holds for the most commonly used non-power-law CRM models; see Example 4.2 for the case of the beta–Bernoulli model with discount $d = 0$ and Appendix F for the beta–negative binomial and gamma–Poisson models with $d = 0$. As we detail next, we believe Condition 1 is also reasonable beyond these common models. The $O(1/n)$ quantity in Eq. (14) is the typical expected number of new features after observing n observations in non-power-law BNP models. Eqs. (15), (16) and (17) are likely to hold when \tilde{h} is a small perturbation of h and $K\tilde{h}$ is a small perturbation of $M_{n,x}$. For instance, in Example 4.1, the functional form of \tilde{h} is very similar to that of h , except that \tilde{h} has the additional $\gamma\alpha/K$ factor in both numerator and denominator. The functional form of $K\tilde{h}$ is very similar to that of $M_{n,x}$, except that $K\tilde{h}$ has an additional $\gamma\alpha/K$ factor in the denominator.

Example 4.2 (Beta–Bernoulli with $d = 0$, continued). The growth rate of the target model is

$$\sum_{x=1}^{\infty} M_{n,x} = M_{n,1} = \frac{\gamma\alpha}{n-1+\alpha}.$$

Since \tilde{h} is supported on $\{0, 1\}$, the growth rate of the approximate model is

$$\tilde{h}(1 | x_{1:(n-1)} = 0_{n-1}) = \frac{\gamma\alpha/K}{\alpha-1+n+\gamma\alpha/K} \leq \frac{1}{K} \frac{\gamma\alpha}{n-1+\alpha}.$$

Since both h and \tilde{h} are supported on $\{0, 1\}$, Eq. (16) becomes

$$\left| h(1 | x_{1:(n-1)}) - \tilde{h}(1 | x_{1:(n-1)}) \right| = \left| \frac{\sum_{i=1}^{n-1} x_i + \gamma\alpha/K}{\alpha-1+n+\gamma\alpha/K} - \frac{\sum_{i=1}^{n-1} x_i}{\alpha-1+n} \right| \leq \frac{\gamma\alpha}{K} \frac{1}{n-1+\alpha}.$$

And because $M_{n,x} = 0 = \tilde{h}(x | \cdot)$ for $x > 1$, Eq. (17) becomes

$$\left| M_{n,1} - K\tilde{h}(1 | x_{1:(n-1)} = 0_{n-1}) \right| = \left| \frac{\gamma\alpha}{\alpha-1+n} - \frac{\gamma\alpha}{\alpha-1+n+\frac{\gamma\alpha}{K}} \right| \leq \frac{\gamma^2\alpha}{K} \frac{1}{n-1+\alpha}.$$

Calibrating $\{C_i\}$ based on these inequalities is straightforward.

Upper bound. We now make use of Condition 1 to derive an upper bound on the approximation error induced by AIFAs.

Theorem 4.1 (Upper bound for exponential family CRMs). *Recall that $P_{N,\infty}$ is the distribution of $Y_{1:N}$ from Eq. (12) while $P_{N,K}$ is the distribution of $W_{1:N}$ from Eq. (13). If*

Assumption 2 and Condition 1 hold, then there exist positive constants C', C'', C''', C'''' depending only on $\{C_i\}_{i=1}^5$ such that

$$d_{TV}(P_{N,\infty}, P_{N,K}) \leq \frac{C' + C'' \ln^2 N + C''' \ln N \ln K + C'''' \ln K}{K}.$$

See Appendix G.1 for explicit values of the constants as well as the proof. Theorem 4.1 states that the AIFA approximation error grows as $O(\ln^2 N)$ with fixed K , and decreases as $O(\ln K/K)$ for fixed N . The bound accords with our intuition that, for fixed K , the error should increase as N increases: with more data, the expected number of latent components in the data increases, demanding finite approximations of increasingly larger sizes. In particular, $O(\ln N)$ is the standard Bayesian nonparametric growth rate for non-power law models. It is likely that the $O(\ln^2 N)$ factor can be improved to $O(\ln N)$ due to $O(\ln N)$ being the natural growth rate; more generally, we conjecture that the error directly depends on the expected number of latent components in a model for N observations. On the other hand, for fixed N , we expect that error should decrease as K increases and the approximation thus has greater capacity. This behavior also matches Theorem 3.1, which guarantees that sufficiently large finite models have small error.

We highlight that Theorem 4.1 provides upper bounds both (i) for approximations that were already known in the literature but where bounds were not already known, as in the case of the beta–negative binomial process, and (ii) for processes and approximations not previously studied in the literature in any form.

Lower bounds. From the upper bound in Theorem 4.1, we know how to set a sufficient number of atoms for accurate approximations: for the total variation to be less than some ϵ , we solve for the smallest K such that the right hand side of Theorem 4.1 is smaller than ϵ . We now derive lower bounds on the AIFA approximation error to characterize a *necessary* number of atoms for accurate approximations, by looking at worst-case observational likelihoods f . In particular, Theorem 4.1 implies that an AIFA with $K = O(\text{poly}(\ln N)/\epsilon)$ atoms suffices in approximating the target model to less than ϵ error. In Theorem 4.2 below, we establish that K must grow at least at a $\ln N$ rate in the worst case. In Theorem 4.3 below, we establish that the $1/\epsilon$ term is necessary. To the best of our knowledge, Theorems 4.2 and 4.3 are the *first* lower bounds on IFA approximation error for any process.

Our lower bounds apply to the beta–Bernoulli process with $d = 0$. Recall that $P_{N,\infty}$ is the distribution of $Y_{1:N}$ from Eq. (12) while $P_{N,K}$ is the distribution of $W_{1:N}$ from Eq. (13). In what follows, $P_{N,\infty}^{\text{BP}}$ refers to the marginal distribution of the observations that arises when we use the prior $\text{BP}(\gamma, \alpha, 0)$. Analogously, $P_{N,K}^{\text{BP}}$ is the observational distribution that arises when we use the AIFA $_K$ approximation in Example 3.1. The observational likelihood f will be clear from context. The worst-case observational likelihoods f are pathological. We leave to future work to lower bound the approximation error when more common likelihoods f , such as Gaussian or Dirichlet, are used.

For the first result, it will be useful to define the *growth function* for any $N \in \mathbb{N}$, $\alpha > 0$:

$$C(N, \alpha) := \sum_{n=1}^N \frac{\alpha}{n-1+\alpha}. \quad (18)$$

$C(N, \alpha)$ satisfies $\lim_{N \rightarrow \infty} C(N, \alpha)/(\alpha \ln N) = 1$; this asymptotic equivalence is a corollary of Lemma E.10 or Theorem 2.3 from Korwar and Hollander (1972). Our next result shows that

our AIFA approximation can be poor if the approximation level K is too small compared to the growth function $C(N, \alpha)$.

Theorem 4.2 ($\ln N$ is necessary). *For the beta–Bernoulli process model with $d = 0$, there exists an observation likelihood f , independent of K and N , such that for any N , if $K \leq 0.5\gamma C(N, \alpha)$, then*

$$d_{TV}(P_{N,\infty}^{BP}, P_{N,K}^{BP}) \geq 1 - \frac{C}{N^{\gamma\alpha/8}},$$

where C is a constant depending only on γ and α .

See Appendix G.2 for the proof. The intuition is that, with high probability, the number of features that manifest in the target $X_{1:N}$ is greater than $0.5\gamma C(N, \alpha)$. However, the finite model $Z_{1:N}$ has fewer than $0.5\gamma C(N, \alpha)$ components. Hence, there is an event where the target and approximation assign drastically different probability masses. Theorem 4.2 implies that as N grows, if the approximation level K fails to surpass the $0.5\gamma C(N, \alpha)$ threshold, then the total variation between the approximate and the target model remains bounded from zero; in fact, the error tends to one.

We next show that the $1/K$ factor in the upper bound from Theorem 4.1 is *tight* (up to logarithmic factors).

Theorem 4.3 (Lower bound of $1/K$). *For the beta–Bernoulli process model with $d = 0$, there exists an observation likelihood f , independent of K and N , such that for any N ,*

$$d_{TV}(P_{N,\infty}^{BP}, P_{N,K}^{BP}) \geq C \frac{1}{(1 + \gamma/K)^2} \frac{1}{K},$$

where C is a constant depending only on γ .

See Appendix G.2 for the proof. The intuition is that, under the pathological likelihood f , analyzing the AIFA approximation error is the same as analyzing the binomial–Poisson approximation error (Le Cam, 1960). We then show that $1/K$ is a lower bound using the techniques from Barbour and Hall (1984). Theorem 4.3 implies that an AIFA with $K = \Omega(1/\epsilon)$ atoms is necessary in the worst case.

Our lower bounds (which apply specifically to the beta–Bernoulli process) are much less general than our upper bounds. However, as a practical matter, generality in the lower bounds is not so crucial due to the different roles played by upper and lower bounds. Upper bounds give control over the approximation error; this control is what is needed to trust the approximation and to set the approximation level. Whether or not we have access to lower bounds, general-purpose upper bounds give us this control. Lower bounds, on the other hand, serve as a helpful check that the upper bounds are not too loose — and reassure us that we are not inefficiently using too many atoms in a too-large approximation. From that standpoint, the need for general-purpose lower bounds is not as pressing.

The dependence on the accuracy level in the $d = 0$ beta–Bernoulli process is worse for AIFAs than for TFAs. For example, consider the Bondesson approximation (Bondesson, 1982; Campbell et al., 2019) of $\text{BP}(\gamma, \alpha, 0)$; we will see next that this approximation is a TFA with excellent error bounds.

Example 4.3 (Bondesson approximation (Bondesson, 1982)). Fix $\alpha \geq 1$, let $E_l \stackrel{\text{i.i.d.}}{\sim} \text{Exp}(1)$, and let $\Gamma_k := \sum_{l=1}^k E_l$. The K -atom Bondesson approximation of $\text{BP}(\gamma, \alpha, 0)$ is a TFA $\sum_{k=1}^K \theta_k \delta_{\psi_k}$, where $\theta_k := V_k \exp(-\Gamma_k/\gamma\alpha)$, $V_k \stackrel{\text{i.i.d.}}{\sim} \text{Beta}(1, \alpha - 1)$, and $\psi_k \stackrel{\text{i.i.d.}}{\sim} H$.

The following result gives a bound on the error of the Bondesson approximation.

Proposition 4.4. (*Campbell et al., 2019, Appendix A.1*) For $\gamma > 0, \alpha \geq 1$, let Θ_K be distributed according to a level- K Bondesson approximation of $\text{BP}(\gamma, \alpha, 0)$, $R_n | \Theta_K \stackrel{i.i.d.}{\sim} \text{LP}(\ell; \Theta_K), T_n | R_n \stackrel{\text{indep}}{\sim} f(\cdot | R_n)$ with N observations. Let $Q_{N,K}$ be the distribution of the observations $T_{1:N}$. Then: $d_{TV}(P_{N,\infty}^{BP}, Q_{N,K}) \leq N\gamma \left(\frac{\gamma\alpha}{1+\gamma\alpha}\right)^K$.

Proposition 4.4 implies that a TFA with $K = O(\ln\{N/\epsilon\})$ atoms suffices in approximating the target model to less than ϵ error. Up to log factors in N , comparing the necessary $1/\epsilon$ level for an AIFA and the sufficient $\ln(1/\epsilon)$ level for a TFA, we conclude that the necessary size for an AIFA is exponentially larger than the sufficient size for a TFA, in the worst-case observational likelihood f .

4.2. Approximating a (hierarchical) Dirichlet process

So far we have analyzed AIFA error for CRM-based models. In this section, we analyze the error that arises from using a normalized AIFA as an approximation for an NCRM; here, we focus on a Dirichlet process — i.e., a normalized gamma process without power-law behavior. We first consider a generative model with the same number of layers as in previous sections. But we also consider a more complex generative model, with an additional layer — as is common in, e.g., text analysis. Indeed, one of the strengths of Bayesian modeling is the flexibility facilitated by hierarchical modeling, and a goal of probabilistic programming is to provide fast, automated inference for these more complex models.

Dirichlet process. The Dirichlet process is one of the most widely used nonparametric priors and arises as a normalized gamma process. The generalized gamma process CRM is characterized by the rate measure $\nu(d\theta) = \gamma \frac{\lambda^{1-d}}{\Gamma(1-d)} \theta^{-d-1} e^{-\lambda\theta} d\theta$. We denote its distribution as $\text{GP}(\gamma, \lambda, d)$. A normalized draw from $\text{GP}(\gamma, 1, 0)$ is Dirichlet-process distributed with mass parameter γ (Kingman, 1975; Ferguson, 1973). By Corollary 3.3, $\text{IFA}_K(H, \nu_K)$ with $\nu_K = \text{Gam}(\gamma/K, 1)$ converges to $\text{GP}(\gamma, 1, 0)$. Because the normalization of independent gamma random variables is a Dirichlet random variable, a normalized draw from $\text{IFA}_K(H, \nu_K)$ is equal in distribution to $\sum_{i=1}^K p_i \delta_{\psi_i}$ where $\psi_i \stackrel{i.i.d.}{\sim} H$ and $\{p_i\}_{i=1}^K \sim \text{Dir}(\{\gamma/K\} \mathbf{1}_K)$. We call this distribution the *finite symmetric Dirichlet* (FSD), and denote it as $\text{FSD}_K(\gamma, H)$.¹²

In the simplest use case, the Dirichlet process is used as the de Finetti measure for observations X_n ; i.e., $\Xi \sim \text{DP}, X_n | \Xi \stackrel{i.i.d.}{\sim} \Xi$ for $1 \leq n \leq N$. In Appendix H, we state error bounds when FSD_K replaces the Dirichlet process as the mixing measure that are analogous to the results in Section 4.1. The upper bound is similar to Theorem 4.1 in that the error grows as $O(\ln^2 N)$ with fixed K , and decreases as $O(\ln K/K)$ for fixed N . The lower bounds, which are the analogues of Theorems 4.2 and 4.3, state that $K = \Omega(\ln N)$ is necessary for accurate approximations, and that truncation-based approximations are better than FSD_K , in the worst case. In comparison to existing results (Ishwaran and Zarepour, 2000, 2002), Theorem 1 of Ishwaran and Zarepour (2000) does not bound the distance between observational processes, so it is not directly comparable to our error bound. We improve upon Theorem 4 of Ishwaran and Zarepour (2002), whose upper bound on the FSD approximation error lacks an explicit dependence on K or N . So, unlike our bounds, that bound cannot be inverted to determine a sufficient approximation level K .

Hierarchical Dirichlet process. In modern applications such as text analysis, practitioners use additional hierarchical levels to capture group structure in observed data. In

¹²The name “finite symmetric Dirichlet” comes from Kurihara, Welling and Teh (2007). See Ishwaran and James (2001, Section 2.2) for other names this distribution has had in the literature.

text, we might have D documents with N words in each. More, generally, we might have D groups (each indexed by d) with N observations (each indexed by n) each. We target the influential model of Wang, Paisley and Blei (2011); Hoffman et al. (2013), which is a variant of the hierarchical Dirichlet process (HDP; Teh et al., 2006) and which we refer to as the *modified HDP*. In the HDP, G is a population measure with $G \sim \text{DP}(\omega, H)$. The measure for the d -th subpopulation is $G_d | G \sim \text{DP}(\alpha, G)$; the concentrations ω and α are potentially different from each other. The modified HDP is defined in terms of the *truncated stick-breaking (TSB) approximation*:

Definition 4.5 (Stick-breaking approximation (Sethuraman, 1994)). For $i = 1, 2, \dots, K-1$, let $v_i \stackrel{\text{i.i.d.}}{\sim} \text{Beta}(1, \alpha)$. Set $v_K = 1$. Let $\xi_i = v_i \prod_{j=1}^{i-1} (1 - v_j)$. Let $\psi_k \stackrel{\text{i.i.d.}}{\sim} H$, and $\Xi_K = \sum_{k=1}^K \xi_k \delta_{\psi_k}$. We denote the distribution of Ξ_K as $\text{TSB}_K(\alpha, H)$.

In the modified HDP, the sub-population measure is distributed as $G_d | G \sim \text{TSB}_T(\alpha, G)$. Wang, Paisley and Blei (2011) and Hoffman et al. (2013) set T to be small so that inference in the modified HDP is more efficient than in the HDP, since the number of parameters per group is greatly reduced. From a modeling standpoint, small T is a reasonable assumption since documents typically manifest a small number of topics from the corpus, with the total number depending on the document length and independent of corpus size. For completeness, the generative process of the modified HDP is

$$\begin{aligned} G &\sim \text{DP}(\omega, H), \\ H_d | G &\stackrel{\text{i.i.d.}}{\sim} \text{TSB}_T(\alpha, G) && \text{across } d, \\ \beta_{dn} | H_d &\stackrel{\text{indep}}{\sim} H_d(\cdot) && \text{across } d, n \\ W_{dn} | \beta_{dn} &\stackrel{\text{indep}}{\sim} f(\cdot | \beta_{dn}) && \text{across } d, n. \end{aligned} \tag{19}$$

H_d contains at most T distinct atom locations, all shared with the base measure G .

The finite approximation we consider replaces the population-level Dirichlet process with FSD_K , keeping the other conditionals intact:¹³

$$\begin{aligned} G_K &\sim \text{FSD}_K(\omega, H), \\ F_d | G_K &\stackrel{\text{i.i.d.}}{\sim} \text{TSB}_T(\alpha, G_K) && \text{across } d, \\ \psi_{dn} | F_d &\stackrel{\text{indep}}{\sim} F_d(\cdot) && \text{across } d, n, \\ Z_{dn} | \psi_{dn} &\stackrel{\text{indep}}{\sim} f(\cdot | \psi_{dn}) && \text{across } d, n. \end{aligned} \tag{20}$$

Our contribution is analyzing the error of Eq. (20).

Let $P_{(N,D),\infty}$ be the distribution of the observations $\{W_{dn}\}$. Let $P_{(N,D),K}$ be the distribution of the observations $\{Z_{dn}\}$. We have the following bound on the total variation distance between $P_{(N,D),\infty}$ and $P_{(N,D),K}$.

Theorem 4.6 (Upper bound for modified HDP). *For some constants C', C'', C''', C'''' that depend only on ω ,*

$$d_{TV}(P_{(N,D),\infty}, P_{(N,D),K}) \leq \frac{C' + C'' \ln^2(DT) + C''' \ln(DT) \ln K + C'''' \ln K}{K}.$$

¹³Our construction in Eq. (20) is slightly different from Eqs. 5.5 and 5.6 in Fox et al. (2010). Our document-level process F_d contains at most T topics from the underlying corpus; by contrast, the Fox et al. (2010) document-level process contains as many topics as the corpus-level process. However, the novelty of Eq. (20) is incidental since the replacement of the population-level DP with the FSD in the modified HDP is analogous to the DP case.

See Appendix I.1 for explicit values of the constants as well as the theorem’s proof. For fixed K , Theorem 4.6 is independent of N , the number of observations in each group, but scales with the number of groups D like $O(\text{poly}(\ln D))$. For fixed D , the approximation error decreases to zero at rate no slower than $O(\ln K/K)$. The $O(\ln(DT))$ factor is related to the expected logarithmic growth rate of Dirichlet process mixture models (Arratia, Barbour and Tavaré, 2003, Section 5.2) in the following way. Since there are D groups, each manifesting at most T distinct atom locations from an underlying Dirichlet process prior, the situation is akin to generating DT samples from a common Dirichlet process prior. Hence, the expected number of unique samples is $O(\ln(DT))$. Similar to Theorem 4.1, we speculate that the $O(\ln^2(DT))$ factor can be improved to $O(\ln(DT))$. For error bounds of truncation-based approximations of hierarchical processes, such as the HDP, we refer to Lijoi, Prünster and Rigon (2020b, Theorem 1).

5. Conceptual benefits of finite approximations

Though approximation error lends itself more readily to analysis, ease-of-use considerations are often at the forefront of users’ choice of finite approximation in practice. Therefore, we next compare AIFAs to TFAs in this dimension. We see that AIFAs offer more straightforward updates in approximate inference algorithms and easier implementation of parallelism.

To reduce notation in this section, we let a term without subscripts represent the collection of all subscripted terms: $\rho := (\rho_k)_{k=1}^K$ denotes the collection of atom sizes, $\psi := (\psi_k)_{k=1}^K$ denotes the collection of atom locations, $x := (x_{n,k})_{k=1,n=1}^{K,N}$ denotes the latent trait counts of each observation,¹⁴ and $y := (y_n)_{n=1}^N$ denotes the observed data. We use a dot to collect terms across the corresponding subscript: $x_{.,k} := (x_{n,k})_{n=1}^N$ denotes trait counts across observations of the k -th trait. We next consider algorithms to approximate the posterior distribution $\mathbb{P}(\rho, \psi, x | y)$ of the finite approximation.

Gibbs sampling. When all latent parameters are continuous, Hamiltonian Monte Carlo methods are increasingly standard for performing Markov chain Monte Carlo (MCMC) posterior approximation (Hoffman and Gelman, 2014; Carpenter et al., 2017). However, due to the discreteness of the trait counts x , successful MCMC algorithms for CRMs or their approximations have been based largely on Gibbs sampling (Geman and Geman, 1984). In particular, blocked Gibbs sampling utilizing the natural Markov blanket structure is straightforward to implement when the complete conditionals $\mathbb{P}(\rho | x, \psi, y)$, $\mathbb{P}(x | \psi, \rho, y)$, and $\mathbb{P}(\psi | x, \rho, y)$ are easy to simulate from.¹⁵

Different finite approximations with the same number of atoms K change only $\mathbb{P}(\rho)$ in the generative model. So, of the conditionals, we expect only $\mathbb{P}(\rho | x, \psi, y)$ to differ across finite approximations. We next show in Proposition 5.1 that the form of $\mathbb{P}(\rho | x, \psi, y)$ is particularly tractable for AIFAs. Then we will discuss how Gibbs derivations are substantially more involved for TFAs.

¹⁴The usage of x in this section is different from the usage in the remaining sections: in Eq. (6), x is a single observation from the likelihood process.

¹⁵Because of the factorization $\mathbb{P}(x | \psi, \rho, y) = \prod_{n=1}^N \mathbb{P}(x_{n,.} | \psi, \rho, y_n)$, Gibbs sampling over the finite approximation can be an appealing technique even when Gibbs sampling over the marginal process is not. In particular, the wall-time of a Gibbs iteration for the finite approximation can be small by drawing $\mathbb{P}(x_{n,.} | \psi, \rho, y_n)$ in parallel. Meanwhile, any iteration to update the trait counts with the marginal process representation needs to sequentially process the data points, prohibiting speed up through parallelism.

Proposition 5.1 (Conditional conjugacy of AIFA). *Suppose the likelihood is an exponential family (Eq. (6)) and the AIFA prior ν_K is as in Corollary 3.3. Then the complete conditional of the atom sizes factorizes across atoms as:*

$$\mathbb{P}(\rho \mid x, \psi, y) = \prod_{k=1}^K \mathbb{P}(\rho_k \mid x_{\cdot,k}).$$

Furthermore, each $\mathbb{P}(\rho_k \mid x_{\cdot,k})$ is in the same exponential family as the AIFA prior, with density proportional to

$$\mathbf{1}\{\rho \in U\} \rho^{c/K + \sum_{n=1}^N \phi(x_{n,k}) - 1} \exp \left(\langle \psi + \sum_{n=1}^N t(x_{n,k}), \mu(\rho) \rangle + (\lambda + N)[-A(\rho)] \right). \quad (21)$$

See Appendix J.2 for the proof of Proposition 5.1. For common models — such as beta–Bernoulli, gamma–Poisson, and beta–negative binomial — we see that the complete conditionals over AIFA atom sizes are in forms that are well known and easy to simulate.

There are many different types of TFAs, but typical TFA Gibbs updates pose additional challenges. Even when $\mathbb{P}(\rho)$ is easy to sample from, $\mathbb{P}(\rho \mid x)$ can be intractable, as we see in the following example.

Example 5.1 (Stick-breaking approximation (Broderick, Jordan and Pitman, 2012; Paisley, Carin and Blei, 2011)). Consider the TFA for BP($\gamma, \alpha, 0$) given by

$$\Theta_K = \sum_{i=1}^K \sum_{j=1}^{C_i} V_{i,j}^{(i)} \prod_{l=1}^{i-1} (1 - V_{i,j}^{(l)}) \delta_{\psi_{ij}},$$

where $C_i \stackrel{\text{i.i.d.}}{\sim} \text{Poisson}(\gamma)$, $V_{i,j}^{(l)} \stackrel{\text{i.i.d.}}{\sim} \text{Beta}(1, \alpha)$ and $\psi_{i,j} \stackrel{\text{i.i.d.}}{\sim} H$. One can sample the atom sizes $V_{i,j}^{(i)} \prod_{l=1}^{i-1} (1 - V_{i,j}^{(l)})$. But there is no tractable way to sample from the conditional distribution $\mathbb{P}(\rho \mid x)$ because of the dependence on C_i as well as the entangled form of each ρ . Strategies to make sampling more tractable include introducing auxiliary round indicator variables r_k and marginalizing out the stick-breaking proportions (Broderick, Jordan and Pitman, 2012). However, the final model still contains one Gibbs conditional that is difficult to sample from (Broderick, Jordan and Pitman, 2012, Equation 37).

Other superposition-based approximations, like decoupled Bondesson or power-law (Campbell et al., 2019), present similar challenges due to the number of atoms per round variables C_i and the dependence among the atom sizes.

Mean-field variational inference (MFVI). Analogous to Hamiltonian Monte Carlo for MCMC, black-box variational methods are increasingly used for variational inference when the latent parameters are continuous (Ranganath, Gerrish and Blei, 2014; Kingma and Welling, 2014; Rezende, Mohamed and Wierstra, 2014; Burda, Grosse and Salakhutdinov, 2016; Kucukelbir et al., 2017; Bingham et al., 2018). Mean-field coordinate ascent updates (Wainwright and Jordan, 2008, Section 6.3) remain popular for cases with discrete variables, including the present trait counts x .¹⁶

¹⁶When discrete latent variables are present, black-box variational methods typically utilize enumeration strategies to marginalize out the discrete variables. There exists a tradeoff between user time and wall time. The user time is small since there is no need to derive update equations, but the wall time can be large depending on the enumeration strategy.

MFVI posits a factorized distribution q to approximate the exact posterior. In our case, we approximate $\mathbb{P}(\rho, \psi, x | y)$ with $q(\rho, \psi, x) = q_\rho(\rho)q_\psi(\psi)q_x(x)$. We focus on $q_\rho(\rho)$. For fixed $q_\psi(\psi)$ and $q_x(x)$, the optimal q_ρ^* minimizes the (reverse) Kullback-Leibler divergence between the posterior and $q_\rho^*q_\psi q_x$:

$$q_\rho^* := \underset{q_\rho}{\operatorname{argmin}} \operatorname{KL}(q_\rho(\cdot)q_\psi(\cdot)q_x(\cdot) \parallel \mathbb{P}(\cdot, \cdot, \cdot | y)). \quad (22)$$

Our next result shows that q_ρ^* takes a convenient form when using AIFAs.

Corollary 5.2 (AIFA optimal distribution is in exponential family). *Suppose the likelihood is an exponential family (Eq. (6)) and the AIFA prior ν_K is as in Corollary 3.3. Then, the density of q_ρ^* is given by*

$$q_\rho^*(\rho) = \prod_k \tilde{p}_k(\rho_k), \quad (23)$$

where each \tilde{p}_k has density at ρ_k proportional to

$$\mathbf{1}\{\rho_k \in U\} \rho_k^{c/K + \sum_n \mathbb{E}_{x_{n,k} \sim q_x} \phi(x_{n,k}) - 1} \exp \left\langle \left[\psi + \frac{\sum_n \mathbb{E}_{x_{n,k} \sim q_x} t(x_{n,k})}{\lambda + N} \right], \left[\begin{array}{c} \mu(\rho_k) \\ -A(\rho_k) \end{array} \right] \right\rangle \quad (24)$$

where $x_{n,k} \sim q_x$ denotes the marginal distribution of $x_{n,k}$ under $q_x(x)$.

That is, when using the AIFA, the optimal q_ρ^* factorizes across the K atoms, and each distribution is in the conjugate exponential family for the likelihood $\ell(x_{n,k} | \rho_k)$. Typically users will report summary statistics like means or variances of the variational approximations q_ρ^* . These are typically straightforward from the exponential family form.

The TFA case is much more complex and requires both more steps in the inference scheme as well as additional approximations. See Appendix J for two illustrative examples.

Parallelization. We end with a brief discussion on parallelization. In both Proposition 5.1 and Corollary 5.2, the update distribution for ρ factorizes across the K atoms. Hence, AIFA updates can be done in parallel across atoms, yielding speed-ups in wall-clock time, with the gains being greatest when there are many instantiated atoms. For TFAs, due to the complicating coupling among the atom rates, there is no such benefit from parallelization.

6. Empirical evaluation

In our experiments, we compare our AIFA constructions to TFAs and to other IFA constructions (Lee, James and Choi, 2016; Lee, Miscouridou and Caron, 2022) on a variety of synthetic and real-data examples. Even though our theory suggests better performance of TFAs than AIFAs for worst-case likelihoods, we find comparable performance of TFAs and AIFAs in predictive tasks (Sections 6.1 and 6.2). Likewise, we find comparable performance of AIFAs and alternative IFAs in predictive tasks (Section 6.3). However, we find that AIFAs can be used to learn model hyperparameters where alternative IFA approximations fail (Section 6.4). And we show that AIFAs can be used to learn model hyperparameters for new models, not previously explored in the BNP literature (Section 6.5).

In relation to prior studies, existing empirical work has compared IFAs and TFAs only for simpler models and smaller data sets (e.g., Doshi-Velez et al. (2009, Table 1,2) and Kurihara, Welling and Teh (2007, Figure 4)). Our comparison is grounded in models with more levels and analyzes datasets of much larger sizes. For instance, in our topic modeling application, we analyze nearly 1 million documents, while the comparison in Kurihara, Welling and Teh (2007) utilizes only 200 synthetic data points.

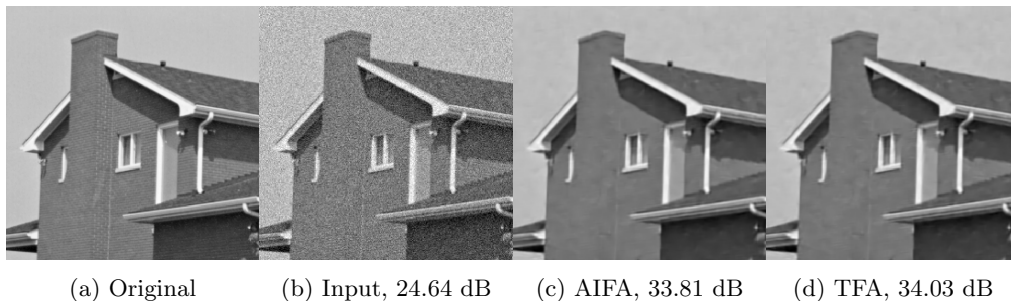


Fig 1: AIFA and TFA denoised images have comparable quality. **(a)** The noiseless image. **(b)** The corrupted image. **(c,d)** Sample denoised images from finite models with $K = 60$. We report PSNR (in dB) with respect to the noiseless image.

6.1. Image denoising with the beta-Bernoulli process

Our first experiments show comparable performance of the AIFA and TFA at an image denoising task with a CRM-based target model. We use MCMC for image denoising through dictionary learning because it is an application where finite approximations of BNP models — in particular the beta-Bernoulli process with $d = 0$ — have proven useful (Zhou et al., 2009). The observation likelihood in this dictionary learning model is not one of the worst cases in Section 4.1. We find that the performance of AIFAs and TFAs is comparable across K , and the posterior modes across TFA and AIFA models are similar to each other.

The goal of image denoising is to recover the original, noiseless image (e.g., Fig. 1a) from a corrupted one (e.g., Fig. 1b). The input image is first decomposed into small contiguous patches. The model assumes that each patch is a combination of latent *basis elements*. By estimating the coefficients expressing the combination, one can denoise the individual patches and ultimately the overall image. The beta-Bernoulli process allows simultaneous estimation of both basis elements and basis assignments. The number of extracted patches depends on both the patch size and the input image size. So even on the same input image, the analysis might process a varying number of “observations.” The nonparametric nature of the beta-Bernoulli process sidesteps the cumbersome problem of calibrating the number of basis elements for these different data set sizes, which can be large even for a relatively small image; for a 256×256 image like Fig. 1b, the number of extracted patches, N , is about 60,000. We quantify denoising quality by computing the peak signal-to-noise ratio (PNSR) between the original and the denoised image (Hore and Ziou, 2010). The higher the PNSR, the more similar the images.

We use Gibbs sampling to approximate the posterior distributions. To ensure stability and accuracy of the sampler, patches (i.e., observations) are gradually introduced in epochs, and the sampler modifies only the latent variables of the current epoch’s observations. See Appendix K.1 for more details about the finite approximations, the hyperparameter settings, and the inference algorithm.

Figs. 1c and 1d visually summarize the results of posterior inference for a particular image. We report experiments with other images in Appendix L.1. Our results across all images indicate that the AIFA and TFA perform similarly, and both approximations perform much better than the baseline (i.e., the noisy input image). Fig. 2 quantitatively confirms these qualitative findings; Fig. 2a shows that, for approximation levels we considered, the

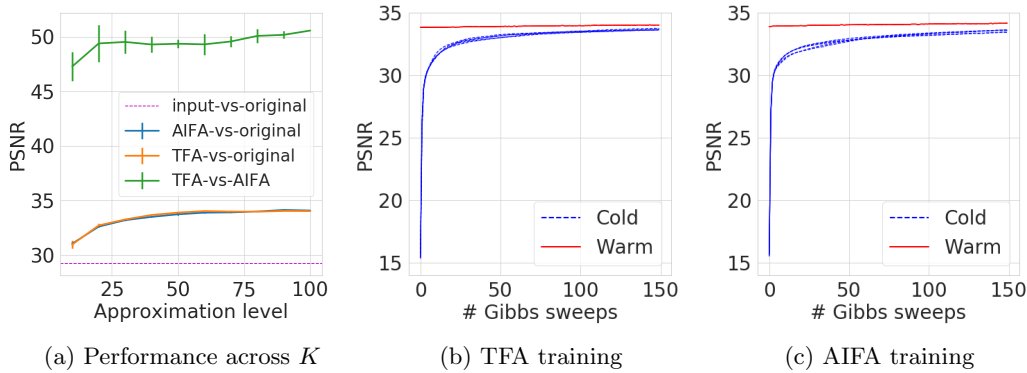


Fig 2: **(a)** Peak signal-to-noise ratio (PSNR) as a function of approximation level K . Error bars depict 1-standard-deviation ranges across 5 trials. **(b,c)** How PSNR evolves during inference across 10 trials, with 5 each starting from respectively cold or warm starts.

PSNR between either the TFA or AIFA output image and the original image are always very similar and substantially higher (between 30 and 35) than the PSNR between the original and corrupted image (below 30). In fact, each TFA denoised image is more similar to the AIFA denoised image than to the original image; the PSNR between the TFA and AIFA outputs is about 50. We also see from Fig. 2a that the quality of denoised images improves with increasing K . The improvement with K is largest for small K , and plateaus for larger values of K .

In addition to randomly initializing the latent variables at the beginning of the Gibbs sampler of one model (“cold start”), we can use the last configuration of latent variables visited in the other model as the initial state of the Gibbs sampler (“warm start”). In Fig. 2b, the warm-start curve uses the output of inference with the AIFA as an initial value for inference with the TFA; similarly, the warm-start curve of Fig. 2c uses the output with the TFA to initialize inference with the AIFA. For both approximations, $K = 60$. At the end of training, all latent variables for all patches have been assigned, so for the warm start experiment, we make all patches available from the start instead of gradually introducing patches. For both approximations, the Gibbs sampler initialized at the warm start visits candidate images that essentially have the same PSNR as the starting configuration; the PSNR values never deviate from the initial PSNR by more than 1%. The early iterates of the cold-start Gibbs sampler are noticeably lower in quality compared to the warm-start iterates, and the quality at the plateau is still lower than that of the warm start.¹⁷ Each PSNR trace corresponds to a different set of initial values and simulation of the conditionals. The variation across the 5 warm-start trials is small; the variation across the 5 cold-start trials is larger but still quite small. In all, the modes of TFA posterior are good initializations for inference with the AIFA model, and vice versa.

¹⁷Because the warm start represents the end of the training from the cold start with gradually introduced patches, the gap in final PSNR is due to the gradual patch introduction.

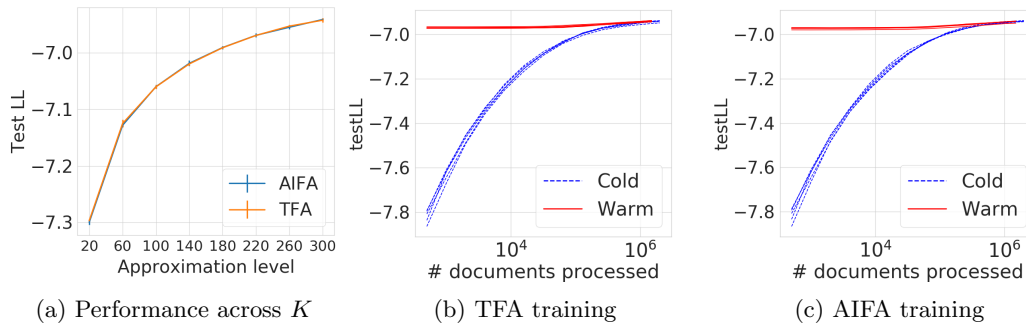


Fig 3: **(a)** Test log-likelihood (testLL) as a function of approximation level K . Error bars show 1 standard deviation across 5 trials. **(b,c)** TestLL change during inference.

6.2. Topic modelling with the modified hierarchical Dirichlet process

We next compare the performance of normalized AIFAs (namely, FSD_K) and TFAs (namely, TSB_K) in a DP-based model with additional hierarchy: the modified HDP from Section 4.2. As in Section 6.1, we find that the approximations perform similarly.

We use the modified HDP for topic modeling. We apply stochastic variational inference with mean-field factorization (Hoffman et al., 2013) to approximate the posterior over the latent topics. The training corpus consists of nearly one million documents from Wikipedia. We measure the quality of inferred topics via predictive log-likelihood on a set of 10,000 held-out documents. See Appendix K.2 for complete experimental details.

Fig. 3a shows that, as expected, the quality of the inferred topics improves as the approximation level grows. For a given approximation level, the quality of the topics learned using the TFA and the normalized AIFA are almost the same.

The warm start in this case corresponds to using variational parameters at the end of the other model’s training. Fig. 3b uses the outputs of inference with the normalized AIFA approximation as initial values for inference with the normalized TFA; similarly Fig. 3c uses the TFA to initialize inference with the AIFA. We fix the number of topics to $K = 300$ and run 5 trials each with the cold start and warm start, respectively. For both approximations, the test log-likelihood stays nearly the same for warm-start training iterates; the test log-likelihood for the iterates never deviate more than 0.5% from the initial value. The early iterates after the cold start are noticeably lower in quality compared to the warm iterates; however at the end of training, the test log-likelihoods are nearly the same. Each trace corresponds to a different set of initial values and ordering of data batches processed. The variation across either cold starts or warm starts is small. So, in sum, the modes of the TFA posterior are good initializations for inference with the AIFA model, and vice versa.

6.3. Comparing predictions across independent finite approximations

We next show that AIFAs have comparable predictive performance with other IFAs, namely the BFRY IFA and GenPar IFA. We consider a linear-Gaussian factor analysis model with the power-law beta-Bernoulli process (Griffiths and Ghahramani, 2011), where the AIFA, BFRY IFA, or GenPar IFA can be used directly.

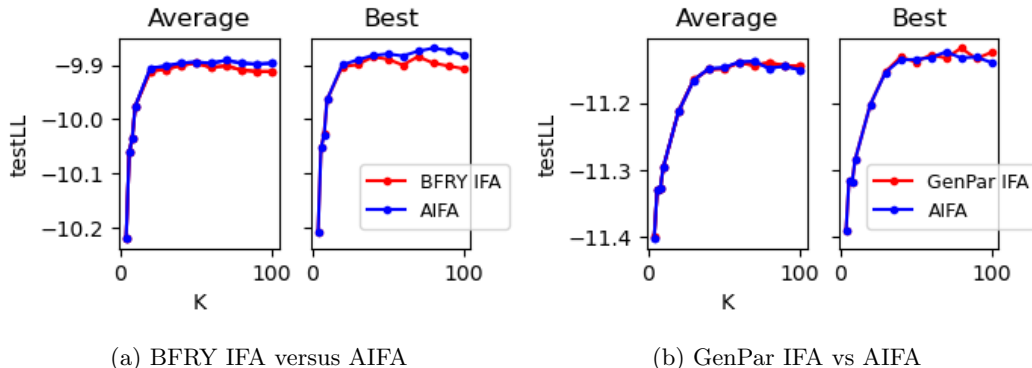


Fig 4: **(a)** The left panel shows the average predictive log-likelihood of the AIFA (blue) and BFRY IFA (red) as a function of the approximation level K ; the average is across 10 trials with different random seeds for the stochastic optimizer. The right panel shows highest predictive log-likelihood across the same 10 trials. **(b)** The panels are analogous to **(a)**, except the GenPar IFA is in red.

Recall that the BFRY IFA applies only when the concentration hyperparameter is zero, and the GenPar IFA applies only when the concentration parameter is positive. We consider it a strength of the AIFA that it applies to both cases (and the negative range of the concentration hyperparameter) simultaneously. Nonetheless, we here generate two separate synthetic datasets: one to compare the BFRY IFA with the AIFA and one to compare the GenPar IFA with the AIFA. In each case, we generate 2,000 data points from the full CRM model with a discount of $d = 0.6$. We use 1,500 for training and report predictive log-likelihood on the 500 held-out data points. For posterior approximation, we use automatic differentiation variational inference as implemented in Pyro (Bingham et al., 2018). To isolate the effect of the approximation type, we use “ideal” initialization conditions: we initialize the variational parameters using the latent features, assignments, and variances that generated the training set. See Appendix K.3 for more details about the BFRY IFA, GenPar IFA, and the approximate inference scheme. Fig. 4a shows that across approximation levels K , the predictive performances of the AIFA and BFRY IFA are similar. Likewise, Fig. 4b shows that the predictive performance of the AIFA and GenPar IFA are similar.

6.4. Discount estimation

We next show that AIFAs can reliably recover the beta process discount hyperparameter d , which governs the power law growth in the number of features. By contrast, we show that the BFRY IFA or GenPar IFA struggle at this task. In Appendix L.3, we show that the AIFA can also reliably estimate the mass and concentration hyperparameters.

We generate a synthetic dataset so that the ground truth hyperparameter values are known. The data takes the form of a binary matrix X , with N rows and \tilde{K} columns. We generate X from an Indian buffet process prior; recall that the Indian buffet process is the marginal process of a beta process CRM paired with Bernoulli likelihood. To learn the hyperparameter values with an AIFA, we maximize the marginal likelihood of the observed

matrix X implied by the AIFA. In particular, we compute the marginal likelihood by integrating the Bernoulli likelihood $\mathbb{P}(x_{n,k} | \theta_k)$ over θ_k distributed as the K -atom AIFA ν_K . To quantify the variability of the estimation procedure, we generate 50 feature matrices and compute the maximum likelihood estimate for each of these 50 trials. See Appendix K.4 for more experimental details.

Fig. 5a shows that we can use an AIFA to estimate the underlying discount for a variety of ground-truth discounts. Since the estimates and error bars are similar whether we use the AIFA (left) or full nonparametric process (right), we conclude that using the AIFA yields comparable inference to using the full process.

In theory, the marginal likelihood of the BFRY IFA can also be used to estimate the discount, but in practice we find that this approach is not straightforward and can yield unreliable estimates. At the time of writing, such an experiment had not yet been attempted; Lee, James and Choi (2016) focus on clustering models and do not discuss strategies to estimate any hyperparameter in a feature allocation model with a BFRY IFA. We are not aware of a closed-form formula for the marginal likelihood. Default schemes to numerically integrate $\mathbb{P}(0 | \theta_k)$ against the BFRY prior for θ_k fail because of overflow issues. $(KT(d)d/\gamma)^{1/d}$ is typically very large, especially for small d . Due to finite precision, $1 - \exp\left(- (Kd/\gamma)^{1/d} \frac{\theta}{1-\theta}\right)$ evaluates to 1 on the quadrature grid used by numerical integrators (Piessens et al., 2012). In this case, Eq. (4) behaves as θ^{-d-1} near 0, and thus the integral over θ diverges. To create the left panel of Fig. 5b, we view the marginal likelihood as an expectation and construct Monte Carlo estimates; we draw 10^5 BFRY samples to estimate the marginal likelihood, and we take the estimate’s logarithm as an approximation to the log marginal likelihood (red line). To quantify the uncertainty, we draw 100 batches of 10^5 samples (light red region). Even for this large number of Monte Carlo samples, the estimated log marginal likelihood curve is too noisy to be useful for hyperparameter estimation. By comparison, we can compute the log marginal likelihood analytically for the IBP (dashed black line); it is much smoother and features a clear minimum. Moreover, we can compute the AIFA log marginal likelihood via numerical integration (solid blue line); it is also very smooth and features a clear minimum.

We again consider the BFRY IFA and GenPar IFA separately and generate separate simulated data for each case due to their disjoint assumptions; we generate data with concentration $\alpha = 0$ for the BFRY IFA and with $\alpha > 0$ for the GenPar IFA. An experiment to recover a discount hyperparameter with the GenPar IFA, analogous to the experiment above with the BFRY IFA, has also not previously been attempted. There is no analytical formula for the GenPar IFA marginal likelihood, and we again encounter overflow when trying numerical integration. Therefore, we resort to Monte Carlo; we find that estimates of the log marginal likelihood are too noisy for practical use in recovering the discount (the right panel of Figure 5b).

6.5. Dispersion estimation

Finally, we show that the AIFA can straightforwardly be adapted to estimate hyperparameters in other BNP processes, not just the beta process. In particular we show that AIFAs can be used to learn the dispersion parameter τ in the novel Xgamma-CMP process that we introduced in Example 3.4. We consider a well-known application of BNP trait-allocation models to matrix-factorization-based topic modeling (Roychowdhury and Kulis, 2015). The observed data is a count matrix X , with N rows, representing documents, and V columns,

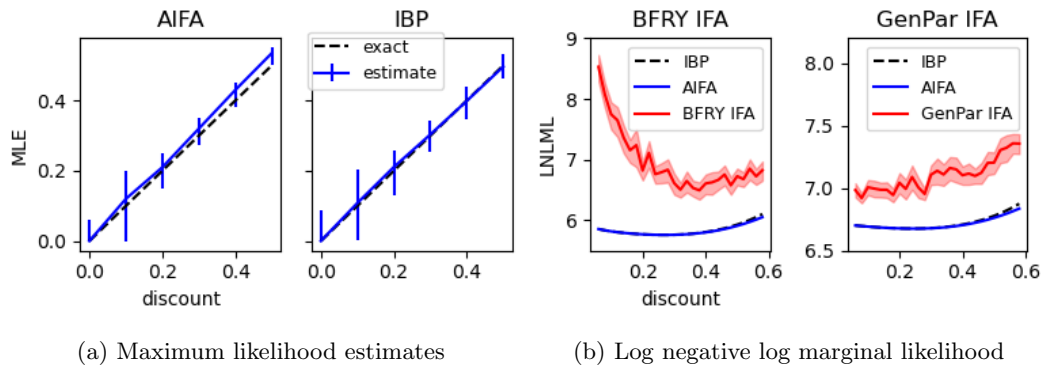


Fig 5: (a) We estimate the discount by maximizing the marginal likelihood of the AIFA (left) or the full process (right). The solid blue line is the median of the estimated discounts, while the lower and upper bounds of the error bars are the 20% and 80% quantiles. The black dashed line is the ideal value of the estimated discount, equal to the ground-truth discount. (b) In each panel, the solid red line is the average log of negative log marginal likelihood (LNLML) across batches. The light red region depicts two standard errors in either direction from the mean.

representing vocabulary words. We adjust the model of Roychowdhury and Kulis (2015) to use the Xgamma-CMP process of Example 3.4 instead of a gamma-Poisson process. The added flexibility of τ allows modeling trait count distributions that are over- or under-dispersed, which cannot be done with the gamma-Poisson process.

To have a notion of ground truth, we generate synthetic data (with $N = 600$) from a large AIFA (with $K = 500$) of the Xgamma-CMP process, which is a good approximation of the BNP limit.¹⁸ In each set of experiments, the data are overdispersed ($\tau < 1$) or underdispersed ($\tau > 1$). In this case, we take a Bayesian approach to estimating τ , and put a uniform prior on $\tau \in (0, 100]$ since τ must be strictly positive. For smaller values of K ($K = 50$ to $K = 150$), we approximate the posterior for the K -atom AIFA using Gibbs sampling. See Appendix K.5 for more details about the experimental setup.

Fig. 6 shows that the posterior approximation agrees with the ground truth on the dispersion type (over or under) in each case. We also see from the figures that the 95% credible intervals contain the ground-truth τ value in each case.

7. Discussion

We have provided a general construction of automated independent finite approximations (AIFAs) for completely random measures and their normalizations. Our construction provides novel finite approximations not previously seen in the literature. For processes without power-law behavior, we provide approximation error bounds; our bounds show that we can ensure accurate approximation by setting the number of atoms K to be (1) logarithmic in the number of observations N and (2) inverse to the error tolerance ϵ . We have discussed

¹⁸For the chosen number of documents N , let the number of traits with positive count be \hat{K} . There is no noticeable difference in the distribution of \hat{K} between $K = 500$ and $K > 500$. The rates of the inactive (zero count) traits are smaller than $1/N$.

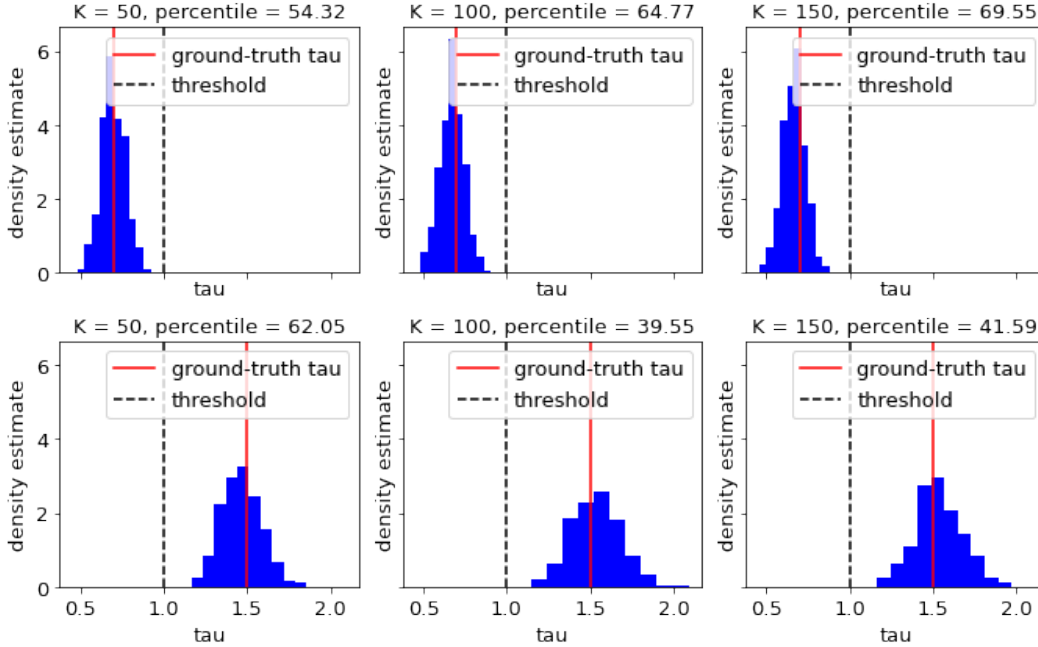


Fig 6: Blue histograms show posterior density estimates for τ from MCMC draws. The ground-truth τ (solid red line) is 0.7 in the overdispersed case (upper row) and 1.5 in the underdispersed case (lower row). The threshold $\tau = 1$ (dashed black line) marks the transition from overdispersion ($\tau < 1.0$) to underdispersion ($\tau > 1.0$). The percentile in each panel’s title is the percentile where the ground truth τ falls in the posterior draws. The approximation size K of the AIFA increases in the plots from left to right.

how the independence and automatic construction of AIFA atom sizes lead to convenient inference schemes. A natural competitor for AIFAs is a truncated finite approximation (TFA). We show that, for the worst case choice of observational likelihood and the same K , AIFAs can incur larger error than the corresponding TFAs. However, in our experiments, we find that the two methods have essentially the same performance in practice. Meanwhile, AIFAs are overall easier to work with than TFAs, whose coupled atoms complicate the development of inference schemes. Future work might extend our error bound analysis to conjugate exponential family CRMs with power-law behavior. An obstacle to upper bounds for the positive-discount case is the verification of the clauses in Condition 1. In the positive-discount case, the functions h and $M_{n,x}$, which describe the marginal representation of the nonparametric process, take forms that are straightforwardly amenable to analysis. But the function \tilde{h} , which describes the finite approximations, is complex. In general, \tilde{h} is equal to the ratio of two normalization constants of different AIFAs. The normalization constants can be computed numerically. However, to make theoretical statements such as the clauses in Condition 1, we need to prove their smoothness properties. Another direction is to tighten the error upper bound by focusing on specific, commonly-used observational likelihoods — in contrast to the worst-case analysis we provide here. Finally, more work is required to directly compare the size of error in the finite approximation to the size of error due to approximate

inference algorithms such as Markov chain Monte Carlo or variational inference.

Acknowledgments

Tin D. Nguyen, Jonathan Huggins, Lorenzo Masoero, and Tamara Broderick were supported in part by ONR grant N00014-17-1-2072, NSF grant CCF-2029016, ONR MURI grant N00014-11-1-0688, and a Google Faculty Research Award. Jonathan Huggins was also supported by the National Institute of General Medical Sciences of the National Institutes of Health under grant number R01GM144963 as part of the Joint NSF/NIGMS Mathematical Biology Program. The content is solely the responsibility of the authors and does not necessarily represent the official views of the National Institutes of Health.

References

- ACHARYA, A., GHOSH, J. and ZHOU, M. (2015). Nonparametric Bayesian factor analysis for dynamic count matrices. In *International Conference on Artificial Intelligence and Statistics*.
- ADELL, J. A. and LEKUONA, A. (2005). Sharp estimates in signed Poisson approximation of Poisson mixtures. *Bernoulli* **11** 47–65.
- ALDOUS, D. (1985). Exchangeability and related topics. *École d'Été de Probabilités de Saint-Flour XIII—1983* 1–198.
- ALZER, H. (1997). On some inequalities for the gamma and psi functions. *Mathematics of computation* **66** 373–389.
- ANTONIAK, C. E. (1974). Mixtures of Dirichlet processes with applications to Bayesian nonparametric problems. *The Annals of Statistics* **2** 1152–1174.
- ARBEL, J., DE BLASI, P. and PRÜNSTER, I. (2019). Stochastic approximations to the Pitman–Yor process. *Bayesian Analysis* **14** 1201–1219.
- ARBEL, J. and PRÜNSTER, I. (2017). A moment-matching Ferguson & Klass algorithm. *Statistics and Computing* **27** 3–17.
- ARRATIA, R., BARBOUR, A. D. and TAVARÉ, S. (2003). *Logarithmic combinatorial structures: a probabilistic approach* **1**. European Mathematical Society.
- BARBOUR, A. D. and HALL, P. (1984). On the rate of Poisson convergence. In *Mathematical Proceedings of the Cambridge Philosophical Society* **95** 473–480. Cambridge University Press.
- BERTOIN, J., FUJITA, T., ROYNETTE, B. and YOR, M. (2006). On a particular class of self-decomposable random variables: the durations of Bessel excursions straddling independent exponential times. *Probability and Mathematical Statistics* **26** 315–366.
- BINGHAM, E., CHEN, J. P., JANKOWIAK, M., OBERMEYER, F., PRADHAN, N., KARALETSOS, T., SINGH, R., SZERLIP, P., HORSFALL, P. and GOODMAN, N. D. (2018). Pyro: deep universal probabilistic programming. *Journal of Machine Learning Research*.
- BLACKWELL, D. and MACQUEEN, J. B. (1973). Ferguson distributions via Polya urn schemes. *The Annals of Statistics* **1** 353–355.
- BLEI, D. M., GRIFFITHS, T. L. and JORDAN, M. I. (2010). The nested Chinese restaurant process and Bayesian nonparametric inference of topic hierarchies. *Journal of the ACM* **57** 1–30.
- BONDESSON, L. (1982). On Simulation from Infinitely Divisible Distributions. *Advances in Applied Probability* **14** 855–869.

- BRIX, A. (1999). Generalized gamma measures and shot-noise Cox processes. *Advances in Applied Probability* **31** 929–953.
- BRODERICK, T., JORDAN, M. I. and PITMAN, J. (2012). Beta processes, stick-breaking and power laws. *Bayesian analysis* **7** 439–476.
- BRODERICK, T., PITMAN, J. and JORDAN, M. I. (2013). Feature allocations, probability functions, and paintboxes. *Bayesian Analysis* **8** 801–836.
- BRODERICK, T., WILSON, A. C. and JORDAN, M. I. (2018). Posteriors, conjugacy, and exponential families for completely random measures. *Bernoulli* **24** 3181–3221.
- BRODERICK, T., MACKEY, L., PAISLEY, J. and JORDAN, M. I. (2015). Combinatorial Clustering and the Beta Negative Binomial Process. *IEEE Transactions on Pattern Analysis and Machine Intelligence* **37** 290–306.
- BURDA, Y., GROSSE, R. B. and SALAKHUTDINOV, R. (2016). Importance Weighted Autoencoders. In *International Conference on Learning Representations*.
- CAMPBELL, T., CAI, D. and BRODERICK, T. (2018). Exchangeable trait allocations. *Electronic Journal of Statistics* **12** 2290–2322.
- CAMPBELL, T., HUGGINS, J. H., HOW, J. P. and BRODERICK, T. (2019). Truncated random measures. *Bernoulli* **25** 1256–1288.
- CANALE, A. and DUNSON, D. B. (2011). Bayesian kernel mixtures for counts. *Journal of the American Statistical Association* **106** 1528–1539.
- CANONNE, C. A short note on Poisson tail bounds. *Technical report available from <https://ccanonne.github.io/>*.
- CARPENTER, B., GELMAN, A., HOFFMAN, M. D., LEE, D., GOODRICH, B., BETANCOURT, M., BRUBAKER, M., GUO, J., LI, P. and RIDDELL, A. (2017). Stan: A Probabilistic Programming Language. *Journal of Statistical Software* **76** 1–32.
- DE VALPINE, P., TUREK, D., PACIOREK, C., ANDERSON-BERGMAN, C., TEMPLE LANG, D. and BODIK, R. (2017). Programming with models: writing statistical algorithms for general model structures with NIMBLE. *Journal of Computational and Graphical Statistics* **26** 403–413.
- DEVROYE, L. and JAMES, L. (2014). On simulation and properties of the stable law. *Statistical methods & applications* **23** 307–343.
- DOERR, B. and NEUMANN, F. (2019). *Theory of evolutionary computation: recent developments in discrete optimization*. Springer Nature.
- DOSHI-VELEZ, F., MILLER, K. T., VAN GAEL, J. and TEH, Y. W. (2009). Variational inference for the Indian buffet process. In *International Conference on Artificial Intelligence and Statistics*.
- FERGUSON, T. S. (1973). A Bayesian analysis of some nonparametric problems. *The Annals of Statistics* **1** 209–230.
- FERGUSON, T. S. and KLASS, M. J. (1972). A representation of independent increment processes without Gaussian components. *The Annals of Mathematical Statistics* **43** 1634–1643.
- FOX, E. B., SUDDERTH, E., JORDAN, M. I. and WILLSKY, A. S. (2010). A Sticky HDP-HMM with Application to Speaker Diarization. *The Annals of Applied Statistics* **5** 1020–1056.
- GELMAN, A. and RUBIN, D. B. (1992). Inference from Iterative Simulation Using Multiple Sequences. *Statistical Science* **7** 457–472.
- GEMAN, S. and GEMAN, D. (1984). Stochastic Relaxation, Gibbs Distributions, and the Bayesian Restoration of Images. *Pattern Analysis and Machine Intelligence, IEEE Transactions on* **6** 721–741.

- GILKS, W. R. and WILD, P. (1992). Adaptive rejection sampling for Gibbs sampling. *Journal of the Royal Statistical Society: Series C (Applied Statistics)* **41** 337–348.
- GNEDIN, A. V. (1998). On convergence and extensions of size-biased permutations. *Journal of Applied Probability* **35** 642–650.
- GORDON, L. (1994). A stochastic approach to the gamma function. *The American Mathematical Monthly* **101** 858–865.
- GRIFFITHS, T. L. and GHAHRAMANI, Z. (2011). The Indian buffet process: an introduction and review. *Journal of Machine Learning Research* **12** 1185–1224.
- HJORT, N. L. (1990). Nonparametric Bayes estimators based on beta processes in models for life history data. *The Annals of Statistics* **18** 1259–1294.
- HOFFMAN, M., BACH, F. R. and BLEI, D. M. (2010). Online learning for latent Dirichlet allocation. In *Advances in Neural Information Processing Systems*.
- HOFFMAN, M. D. and GELMAN, A. (2014). The No-U-Turn sampler: adaptively setting path lengths in Hamiltonian Monte Carlo. *Journal of Machine Learning Research* **15** 1593–1623.
- HOFFMAN, M. D., BLEI, D. M., WANG, C. and PAISLEY, J. (2013). Stochastic variational inference. *Journal of Machine Learning Research* **14** 1303–1347.
- HORE, A. and ZIOU, D. (2010). Image quality metrics: PSNR vs. SSIM. In *2010 20th International Conference on Pattern Recognition* 2366–2369. IEEE.
- ISHWARAN, H. and JAMES, L. F. (2001). Gibbs sampling methods for stick-breaking priors. *Journal of the American Statistical Association* **96** 161–173.
- ISHWARAN, H. and ZAREPOUR, M. (2000). Markov Chain Monte Carlo in Approximate Dirichlet and Beta Two-Parameter Process Hierarchical Models. *Biometrika* **87** 371–390.
- ISHWARAN, H. and ZAREPOUR, M. (2002). Exact and approximate sum representations for the Dirichlet process. *Canadian Journal of Statistics* **30** 269–283.
- JAMES, L. F. (2013). Stick-breaking PG(α, ζ)-generalized gamma processes. Available at [arXiv:1308.6570v3](https://arxiv.org/abs/1308.6570v3).
- JAMES, L. F. (2017). Bayesian Poisson calculus for latent feature modeling via generalized Indian Buffet Process priors. *The Annals of Statistics* **45** 2016–2045.
- JAMES, L. F., LIJOI, A. and PRÜNSTER, I. (2009). Posterior Analysis for Normalized Random Measures with Independent Increments. *Scandinavian Journal of Statistics* **36** 76–97.
- JOHNSON, N. L., KEMP, A. W. and KOTZ, S. (2005). *Univariate Discrete Distributions*. *Wiley Series in Probability and Statistics*. Wiley.
- JOHNSON, M. J. and WILLSKY, A. S. (2013). Bayesian nonparametric hidden semi-Markov models. *Journal of Machine Learning Research* **14** 673–701.
- KALLENBERG, O. (2002). *Foundations of modern probability*, 2nd ed. Springer, New York.
- KINGMA, D. P. and WELING, M. (2014). Auto-encoding variational Bayes. In *International Conference on Learning Representations*.
- KINGMAN, J. F. C. (1967). Completely random measures. *Pacific Journal of Mathematics* **21** 59–78.
- KINGMAN, J. F. C. (1975). Random discrete distributions. *Journal of the Royal Statistical Society B* **37** 1–22.
- KINGMAN, J. (1992). *Poisson Processes* **3**. Clarendon Press.
- KLINE, M. (1998). *Calculus: An Intuitive and Physical Approach*. *Dover Books on Mathematics*. Dover Publications.
- KORWAR, R. M. and HOLLANDER, M. (1972). Contributions to the theory of Dirichlet processes. *The Annals of Probability* **1** 705–711.

- KUCUKELBIR, A., TRAN, D., RANGANATH, R., GELMAN, A. and BLEI, D. M. (2017). Automatic Differentiation Variational Inference. *Journal of Machine Learning Research* **18** 1–45.
- KURIHARA, K., WELLING, M. and TEH, Y. W. (2007). Collapsed variational Dirichlet process mixture models. In *International Joint Conference on Artificial Intelligence*.
- LAST, G. and PENROSE, M. (2017). *Lectures on the Poisson Process. Institute of Mathematical Statistics Textbooks*. Cambridge University Press.
- LE CAM, L. (1960). An approximation theorem for the Poisson binomial distribution. *Pacific J. Math.* **10** 1181–1197.
- LEE, J., JAMES, L. F. and CHOI, S. (2016). Finite-dimensional BFRY priors and variational Bayesian inference for power law models. In *Advances in Neural Information Processing Systems*.
- LEE, J., MISCOURIDOU, X. and CARON, F. (2022). A unified construction for series representations and finite approximations of completely random measures. *Bernoulli*.
- LEVIN, D. A. and PERES, Y. (2017). *Markov chains and mixing times* **107**. American Mathematical Society.
- LIJOI, A., PRÜNSTER, I. and RIGON, T. (2020a). The Pitman–Yor multinomial process for mixture modelling. *Biometrika* **107** 891–906.
- LIJOI, A., PRÜNSTER, I. and RIGON, T. (2020b). Sampling Hierarchies of Discrete Random Structures. *Statistics and Computing* **30** 1591–1607.
- LIJOI, A. and PRÜNSTER, I. (2010). *Models beyond the Dirichlet process*. In *Bayesian Nonparametrics. Cambridge Series in Statistical and Probabilistic Mathematics* 80–136. Cambridge University Press.
- LIJOI, A., PRÜNSTER, I. and RIGON, T. (2023). Finite-dimensional Discrete Random Structures and Bayesian Clustering. *Journal of the American Statistical Association* **0** 1–13.
- LOEVE, M. (1956). Ranking limit problem. In *Proceedings of the Third Berkeley Symposium on Mathematical Statistics and Probability, Volume 2: Contributions to Probability Theory* 177–194.
- MINKA, T. B., SHMUELI, G., KADANE, J. B., BORLE, S. and BOATWRIGHT, P. Computing with the COM-Poisson distribution. *Technical report*.
- ORBANZ, P. (2010). Conjugate projective limits. Available at *arXiv:1012.0363v2*.
- PAISLEY, J., BLEI, D. M. and JORDAN, M. I. (2012). Stick-breaking beta processes and the Poisson process. In *International Conference on Artificial Intelligence and Statistics*.
- PAISLEY, J. and CARIN, L. (2009). Nonparametric factor analysis with beta process priors. In *International Conference on Machine Learning*.
- PAISLEY, J., CARIN, L. and BLEI, D. (2011). Variational inference for stick-breaking beta process priors. In *International Conference on Machine Learning*.
- PALLA, K., KNOWLES, D. A. and GHARAMANI, Z. (2012). An infinite latent attribute model for network data. In *International Conference on Machine Learning*.
- PERMAN, M., PITMAN, J. and YOR, M. (1992). Size-biased sampling of Poisson point processes and excursions. *Probability Theory and Related Fields* **92** 21–39.
- PIESSENS, R., DE DONCKER-KAPENGA, E., ÜBERHUBER, C. W. and KAHANER, D. K. (2012). *QUADPACK: a subroutine package for automatic integration* **1**. Springer Science & Business Media.
- PITMAN, J. (1995). Exchangeable and partially exchangeable random partitions. *Probability theory and related fields* **102** 145–158.
- PITMAN, J. (1996). Some developments of the Blackwell-MacQueen urn scheme. *Lecture Notes-Monograph Series* 245–267.

- PITMAN, J. and YOR, M. (1997). The two-parameter Poisson-Dirichlet distribution derived from a stable subordinator. *The Annals of Probability* 855–900.
- POLLARD, D. (2001). *A User's Guide to Measure Theoretic Probability*. Cambridge University Press.
- POLLARD, D. (2012). *Convergence of stochastic processes*. Springer Science & Business Media.
- RANGANATH, R., GERRISH, S. and BLEI, D. M. (2014). Black box variational inference. In *International Conference on Artificial Intelligence and Statistics*.
- REGAZZINI, E., LIJOI, A. and PRÜNSTER, I. (2003). Distributional results for means of normalized random measures with independent increments. *The Annals of Statistics* **31** 560–585.
- REZENDE, D. J., MOHAMED, S. and WIERSTRA, D. (2014). Stochastic backpropagation and approximate inference in deep generative models. In *International Conference on Machine Learning*.
- ROYCHOWDHURY, A. and KULIS, B. (2015). Gamma processes, stick-breaking, and variational inference. In *International Conference on Artificial Intelligence and Statistics*.
- SETHURAMAN, J. (1994). A constructive definition of Dirichlet priors. *Statistica Sinica* **4** 639–650.
- SHMUELI, G., MINKA, T. P., KADANE, J. B., BORLE, S. and BOATWRIGHT, P. (2005). A useful distribution for fitting discrete data: revival of the Conway–Maxwell–Poisson distribution. *Journal of the Royal Statistical Society: Series C (Applied Statistics)* **54** 127–142.
- STORN, R. and PRICE, K. (1997). Differential evolution—a simple and efficient heuristic for global optimization over continuous spaces. *Journal of global optimization* **11** 341.
- TEH, Y. W., GÖRÜR, D. and GHAHRAMANI, Z. (2007). Stick-breaking construction for the Indian buffet process. In *International Conference on Artificial Intelligence and Statistics*.
- TEH, Y. W. and GÖRÜR, D. (2009). Indian buffet processes with power-law behavior. In *Advances in Neural Information Processing Systems*.
- TEH, Y. W., JORDAN, M. I., BEAL, M. J. and BLEI, D. M. (2006). Hierarchical Dirichlet Processes. *Journal of the American Statistical Association* **101** 1566–1581.
- THIBAU, R. and JORDAN, M. I. (2007). Hierarchical beta processes and the Indian buffet process. In *International Conference on Artificial Intelligence and Statistics*.
- TITSIAS, M. (2008). The infinite gamma-Poisson feature model. In *Advances in Neural Information Processing Systems*.
- VIRTANEN, P., GOMMERS, R., OLIPHANT, T. E., HABERLAND, M., REDDY, T., COURNAPEAU, D., BUROVSKI, E., PETERSON, P., WECKESSER, W., BRIGHT, J., VAN DER WALT, S. J., BRETT, M., WILSON, J., MILLMAN, K. J., MAYOROV, N., NELSON, A. R. J., JONES, E., KERN, R., LARSON, E., CAREY, C. J., POLAT, İ., FENG, Y., MOORE, E. W., VANDERPLAS, J., LAXALDE, D., PERKTOLD, J., CIMRMAN, R., HENRIKSEN, I., QUINTERO, E. A., HARRIS, C. R., ARCHIBALD, A. M., RIBEIRO, A. H., PEDREGOSA, F., VAN MULBREGT, P. and SCI-PY 1.0 CONTRIBUTORS (2020). SciPy 1.0: Fundamental Algorithms for Scientific Computing in Python. *Nature Methods* **17** 261–272.
- WAINWRIGHT, M. J. and JORDAN, M. I. (2008). Graphical Models, Exponential Families, and Variational Inference. *Foundations and Trends® in Machine Learning* **1** 1–305.
- WANG, C., PAISLEY, J. and BLEI, D. (2011). Online variational inference for the hierarchical Dirichlet process. In *International Conference on Artificial Intelligence and Statistics*.
- ZHOU, M., CHEN, H., REN, L., SAPIRO, G., CARIN, L. and PAISLEY, J. W. (2009). Non-

parametric Bayesian dictionary learning for sparse image representations. In *Advances in Neural Information Processing Systems*.

ZHOU, M., HANNAH, L., DUNSON, D. and CARIN, L. (2012). Beta-negative binomial process and Poisson factor analysis. In *International Conference on Artificial Intelligence and Statistics*.

Appendix A: Additional examples of AIFA construction

Let $B(\alpha, \beta) = \frac{\Gamma(\alpha)\Gamma(\beta)}{\Gamma(\alpha+\beta)}$ denote the beta function.

Example A.1 (Beta prime process). Taking $V = \mathbb{R}_+$, $g(\theta) = (1+\theta)^{-1}$, $h(\theta; \eta) = (1+\theta)^{-\eta}$, and $Z(\xi, \eta) = B(\xi, \eta)$ in Theorem 3.1 yields the beta prime process of Broderick et al. (2015), which has rate measure

$$\nu(d\theta) = \frac{\gamma}{B(\eta, 1-d)} \theta^{-1-d} (1+\theta)^{-d-\eta} d\theta.$$

Since g is continuous, $g(0) = 1$, $1 \leq g(\theta) \leq 1+\theta$, and $h(\theta; \eta)$ is continuous and bounded on $[0, 1]$, Assumption 1 holds.

In the case of $d = 0$, the corresponding exponential family distribution is beta prime. With two placeholder parameters α and β , the beta prime density at $\theta > 0$ is

$$\text{Beta}'(\theta; \alpha, \beta) = \frac{\theta^{\alpha-1} (1+\theta)^{-\alpha-\beta}}{B(\alpha, \beta)}.$$

To construct AIFA using Corollary 3.3, we set $c = \gamma\eta$ and

$$\nu_K(\theta) = \text{Beta}'(\theta; \gamma\eta/K, \eta).$$

Example A.2 (Generalized gamma process). Taking $V = \mathbb{R}_+$, $g(\theta) = 1$, $h(\theta; \lambda) = e^{-\lambda\theta}$, and $Z(\xi, \lambda) = \Gamma(\xi)\lambda^{-\xi}$ in Theorem 3.1 yields the generalized gamma process, with rate measure

$$\nu(d\theta) = \gamma \frac{\lambda^{1-d}}{\Gamma(1-d)} \theta^{-d-1} e^{-\lambda\theta} d\theta.$$

Since $h(\theta; \eta)$ is continuous and bounded on $[0, 1]$, Assumption 1 holds.

In the case of $d = 0$ i.e. the gamma process, the corresponding exponential family distribution is gamma. To construct AIFA using Corollary 3.3, we set $c = \gamma\lambda$ and

$$\nu_K(\theta) = \text{Gamma}(\theta; \gamma\lambda/K, \lambda).$$

Example A.3 (PG(α, ζ)-generalized gamma process). Taking $V = \mathbb{R}_+^2$, $g(\theta) = 1$, $h(\theta; \eta) = e^{-(\eta_1\theta)^{\eta_2}}$, and $Z(\xi, \eta) = \Gamma(\xi/\eta_2)(\eta_1\eta_2)^{-\xi}$ in Theorem 3.1 yields the PG(α, ζ)-generalized gamma process whose rate measure is

$$\nu(d\theta) = \frac{\gamma(\eta_1\eta_2)^{1-d}}{\Gamma((1-d)/\eta_2)} \theta^{-d-1} e^{-(\eta_1\theta)^{\eta_2}} d\theta.$$

Since $h(\theta; \eta)$ is continuous and bounded on $[0, 1]$, Assumption 1 holds.

In the positive discount case, let $c = \frac{\gamma(\eta_1\eta_2)^{1-d}}{\Gamma((1-d)/\eta_2)}$, and the finite-dimensional distribution has density equalling

$$\frac{1}{Z_K} \theta^{c/K-1-d} S_{1/K}^{(1-1/K)} e^{-(\eta_1\theta)^{\eta_2}} d\theta,$$

where $Z_K := \int_0^\infty \theta^{c/K-1-d} S_{1/K}^{(1-1/K)} e^{-(\eta_1\theta)^{\eta_2}} d\theta$.

In the case of $d = 0$, the corresponding exponential family distribution is generalized gamma. With three placeholder parameters ξ' , η'_1 , and η'_2 , the generalized gamma density at $\theta > 0$ is

$$\text{GenGamma}(\theta; \xi', \eta'_1, \eta'_2) = \frac{(\eta'_2/\xi'\eta'_1)\theta^{\eta'_1-1} e^{-(\theta/\xi')^{\eta'_2}}}{\Gamma(\eta'_1/\eta'_2)}$$

To construct AIFA using Corollary 3.3, we set $c = \frac{\gamma\eta_1\eta_2}{\Gamma(\eta_2^{-1})}$ and

$$\nu_K(\theta) = \text{GenGamma}\left(\theta; \frac{1}{\eta_1}, \frac{\gamma\eta_1\eta_2}{K\Gamma(\eta_2^{-1})}, \eta_2\right).$$

Example A.4 (Extended gamma process). Taking $V = (0, \infty) \times (1, \infty)$, $g(\theta) = 1$, $h(\theta; \eta) = Z_\tau^{-c}(\theta)$, $U = [0, T]$, and $Z(\xi, \eta) = \int_0^\infty \theta^{\xi-1} Z_\tau^{-c}(\theta) d\theta$ in Theorem 3.1 yields the extended gamma process from Eq. (11). Since $g(\theta) = 1$, the second condition in Assumption 1 holds. For any τ and c , $Z_\tau^{-c}(\theta)$ is continuous and bounded on $[0, 1]$, so the third condition in Assumption 1 holds. As for the first condition, we note that $Z_\tau^{-c}(\theta) \leq (1 + \theta)^{-c}$, since the minimum of $Z_\tau(\theta)$ with respect to τ is $1 + \theta$, attained at $\tau = \infty$. Therefore, $Z(\xi, \eta)$ is finite if

$$\int_0^T \theta^{\xi-1} (1 + \theta)^{-c} d\theta$$

is finite. Since $(1 + \theta)^{-c} \leq 1$, the last integral is at most

$$\int_0^T \theta^{\xi-1} d\theta = \frac{T^\xi}{\xi},$$

which is finite. Hence, all three conditions of Assumption 1 hold, and we can apply Corollary 3.3. The AIFA is

$$\nu_K(\theta) = \frac{1}{Z_K} \theta^{\gamma/K-1} Z_\tau^{-c}(\theta) 1\{0 \leq \theta \leq T\} d\theta,$$

where Z_K is the normalization constant $Z_K = \int_0^T \theta^{\gamma/K-1} Z_\tau^{-c}(\theta) d\theta$. More generally, for $\gamma, c, \tau > 0$ and $T \geq 1$, we use the notation $\text{XGamma}(\gamma, c, \tau, T)$ to denote the real-valued distribution with density at θ equal to:

$$\text{XGamma}(\theta; \gamma, c, \tau, T) := \frac{\theta^{\gamma-1} Z_\tau^{-c}(\theta) 1\{0 \leq \theta \leq T\}}{\int_0^T \theta^{\gamma-1} Z_\tau^{-c}(\theta) d\theta}. \quad (\text{A.1})$$

Appendix B: Proofs of AIFA convergence

In this appendix, to highlight the fact that the i.i.d. distributions are different across K , we use $\rho_{K,i}$ to denote the i -th atom size in the approximation of level K i.e. the K -atom AIFA is

$$\Theta_K := \sum_{i=1}^K \rho_{K,i} \delta_{\psi_{K,i}}, \quad \rho_{K,i} \stackrel{\text{i.i.d.}}{\sim} \nu_K, \quad \psi_{K,i} \stackrel{\text{i.i.d.}}{\sim} H.$$

B.1. AIFA converges to CRM in distribution

We first state a more general construction than Theorem 3.1, and proceed to prove that result, as a proof of Theorem 3.1.

For the more general construction, we first generalize the $S_b(\theta)$ as in Theorem 3.1 with so-called approximate indicators.

Definition B.1. The parameterized function family $\{S_b\}_{b \in \mathbb{R}_+}$ is composed of *approximate indicators* if, for any $b \in \mathbb{R}_+$, $S_b(\theta)$ is a real, non-decreasing function such that $S_b(\theta) = 0$ for $\theta \leq 0$ and $S_b(\theta) = 1$ for $\theta \geq b$.

Valid examples of approximate indicators are the indicator function $S_b(\theta) = \mathbf{1}\{\theta > 0\}$ and the smoothed indicator function from Theorem 3.1. Some approximate indicators have a point of discontinuity; e.g., $S_b(\theta) = \mathbf{1}\{\theta > 0\}$. But the smoothed indicator is both continuous and differentiable; see Appendix B.2.

Theorem B.2. *Suppose Assumption 1 holds, and let $\{S_b\}_{b \in \mathbb{R}_+}$ be a family of approximate indicators. Fix $a > 0$, and let $(b_K)_{K \in \mathbb{N}}$ be a decreasing sequence such that $b_K \rightarrow 0$. For $c := \gamma h(0; \eta) / Z(1 - d, \eta)$, let*

$$\nu_K(d\theta) := \theta^{-1+cK^{-1}-dS_{b_K}(\theta-aK^{-1})} g(\theta)^{cK^{-1}-d} h(\theta; \eta) Z_K^{-1} d\theta$$

be a family of probability densities, where Z_K is chosen such that $\int \nu_K(d\theta) = 1$. If $\Theta_K \sim \text{IFA}_K(H, \nu_K)$, then $\Theta_K \xrightarrow{\mathcal{D}} \Theta$ as $K \rightarrow \infty$.

Theorem B.2 recovers Theorem 3.1 by setting S_b equaling the smoothed indicator, $a = 1$, and $b_K = 1/K$. See Appendix L.2 for discussions on the impact of the tuning hyperparameters on the performance of our IFA.

In order to prove Theorem B.2, we require a few auxiliary results.

Lemma B.3 (Kallenberg (2002, Lemma 12.1, Lemma 12.2 and Theorem 16.16)). *Let Θ be a random measure and $\Theta_1, \Theta_2, \dots$ a sequence of random measures. If for all measurable sets A and $t > 0$,*

$$\lim_{K \rightarrow \infty} \mathbb{E}[e^{-t\Theta_K(A)}] = \mathbb{E}[e^{-t\Theta(A)}],$$

then $\Theta_K \xrightarrow{\mathcal{D}} \Theta$.

For a density f , let $\mu(t, f) : \theta \mapsto (1 - e^{-t\theta})f(\theta)$. In results that follow we assume all measures on \mathbb{R}_+ have densities with respect to Lebesgue measure. We abuse notation and use the same symbol to denote the measure and the density.

Proposition B.4. *Let $\Theta \sim \text{CRM}(H, \nu)$ and for $K = 1, 2, \dots$, let $\Theta_K \sim \text{IFA}_K(H, \nu_K)$ where ν is a measure and ν_1, ν_2, \dots are probability measures on \mathbb{R}_+ , all absolutely continuous with respect to Lebesgue measure. If $\|\mu(1, n\nu_K) - \mu(1, \nu)\|_1 \rightarrow 0$, then $\Theta_K \xrightarrow{\mathcal{D}} \Theta$.*

Proof. Let $t > 0$ and A a measurable set. First, recall that the Laplace functional of the CRM Θ is

$$\mathbb{E}[e^{-t\Theta(A)}] = \exp \left\{ -H(A) \int_0^\infty \mu(t, \nu)(\theta) d\theta \right\}.$$

We have

$$\begin{aligned} \mathbb{E}[e^{-t\rho_{K,1} \mathbf{1}\{\psi_{K,1} \in A\}}] &= \mathbb{P}(\psi_{K,1} \in A) \mathbb{E}[e^{-t\rho_{K,1}}] + \mathbb{P}(\psi_{K,1} \notin A) \\ &= H(A) \mathbb{E}[e^{-t\rho_{K,1}}] + 1 - H(A) \\ &= 1 - H(A)(1 - \mathbb{E}[e^{-t\rho_{K,1}}]) \\ &= 1 - \frac{H(A)}{K} \int_0^\infty \mu(t, K\nu_K)(\theta) d\theta. \end{aligned}$$

Since $\frac{|1 - e^{-t\theta}|}{|1 - e^{-\theta}|} \leq \max(1, t)$, it follows by hypothesis that $\|\mu(t, K\nu_K) - \mu(t, \nu)\|_1 \rightarrow 0$. Thus,

by dominated convergence and the standard exponential limit,

$$\begin{aligned} \lim_{K \rightarrow \infty} \mathbb{E}[e^{-t\rho_{K,1}\mathbb{1}(\psi_{K,1} \in A)}]^{K} &= \lim_{K \rightarrow \infty} \left(1 - \frac{H(A)}{K} \int_0^\infty \mu(t, K\nu_K)(\theta) \, d\theta\right)^K \\ &= \exp \left\{ - \lim_{K \rightarrow \infty} H(A) \int_0^\infty \mu(t, K\nu_K)(\theta) \, d\theta \right\} \\ &= \exp \left\{ -H(A) \int_0^\infty \mu(t, \nu)(\theta) \, d\theta \right\}. \end{aligned}$$

Finally, by the independence of the random variables $\{\theta_{K,i}\}_{i=1}^K$ and $\{\psi_{K,i}\}_{i=1}^K$,

$$\lim_{K \rightarrow \infty} \mathbb{E}[e^{-t\Theta_K(A)}] = \lim_{K \rightarrow \infty} \mathbb{E}[e^{-t\rho_{K,1}\mathbb{1}(\psi_{K,1} \in A)}]^{K},$$

so the result follows from Lemma B.3. \square

Lemma B.5. *If there exist measures $\pi(\theta) \, d\theta$ and $\pi'(\theta) \, d\theta$ on \mathbb{R}_+ such that for some $\kappa > 0$ and c, c' ,*

1. *the measures μ, μ_1, μ_2, \dots have densities f, f_1, f_2, \dots with respect to π and densities f', f'_1, f'_2, \dots with respect to π' ,*
2. $\int_0^\kappa |f'(\theta) - f'_K(\theta)| \, d\theta \xrightarrow{K \rightarrow \infty} 0$,
3. $\sup_{\theta \in [\kappa, \infty)} |f(\theta) - f_K(\theta)| \xrightarrow{K \rightarrow \infty} 0$,
4. $\sup_{\theta \in [0, \kappa]} \pi'(\theta) \leq c' < \infty$, and
5. $\int_\kappa^\infty \pi(\theta) \, d\theta \leq c < \infty$,

then

$$\|\mu - \mu_K\|_1 \xrightarrow{K \rightarrow \infty} 0.$$

Proof. We have, using the assumptions and Hölder's inequality,

$$\begin{aligned} \|\mu - \mu_K\|_1 &= \int_0^\kappa |f'(\theta) - f'_K(\theta)| \pi'(d\theta) + \int_\kappa^\infty |f(\theta) - f_K(\theta)| \pi(d\theta) \\ &\leq \left(\sup_{\theta \in [0, \kappa]} \pi'(\theta) \right) \int_0^\kappa |f'(\theta) - f'_K(\theta)| \, d\theta \\ &\quad + \left(\sup_{\theta \in [\kappa, \infty)} |f(\theta) - f_K(\theta)| \right) \int_\kappa^\infty \pi(d\theta) \\ &\leq c' \int_0^\kappa |f'(\theta) - f'_K(\theta)| \, d\theta + c \sup_{\theta \in [\kappa, \infty)} |f(\theta) - f_K(\theta)|. \end{aligned}$$

The conclusion follows by the assumptions. \square

Proof of Theorem B.2. Note that since h is continuous and bounded on $[0, \epsilon]$, c as given in the theorem statement is finite. We will apply Lemma B.5 with $\kappa = \min(1, \epsilon)$, $\mu = \mu(1, \nu)$, $\mu_K = \mu(1, n\nu_K)$,

$$\pi(\theta) = \frac{\theta^{-d} g(\theta)^{1-d} h(\theta; \eta)}{Z(1-d, \eta)},$$

and $\pi'(\theta) := (\theta g(\theta))^d \pi(\theta)$. Because of the finiteness of $Z(\xi, \eta)$, item 5 of Lemma B.5, which asks for $\int_{\kappa}^{\infty} \pi(\theta) d\theta < \infty$, is satisfied. Thus, $f(\theta) = \gamma(1 - e^{-\theta})(\theta g(\theta))^{-1}$,

$$f_K(\theta) = nZ_K^{-1}(1 - e^{-\theta})\theta^{-1+cK^{-1}+d-dS_{b_K}(\theta-aK^{-1})}g(\theta)^{-1+cK^{-1}},$$

and $f'(\theta) = (\theta g(\theta))^{-d}f(\theta)$, and $f'_K(\theta) = (\theta g(\theta))^{-d}f_K(\theta)$.

We now note a few useful properties that we will use repeatedly in the proof. Observe that $(a/K)^{cK^{-1}} = 1 + o(1)$. The assumption that h is bounded and continuous implies that on $[0, a/K]$, $h(\theta; \eta) = h(0; \eta) + o(1)$. Similarly, for any $\delta > 0$, $g(\theta)$ is bounded and continuous for $\theta \in [0, \delta]$ and therefore, together with the fact that $g(0) = 1$, we can conclude that on $[0, a/K]$, $g(\theta) = 1 + o(1)$.

For the remainder of the proof we will consider K large enough that $aK^{-1} + 2b_K$ and cK^{-1} are less than κ . The normalizing constant Z_K can be written as

$$\begin{aligned} Z_K &= \int_0^{a/K} (\theta g(\theta))^{-1+cK^{-1}} \pi'(d\theta) \\ &\quad + \int_{a/K}^{\kappa} \theta^{-1+cK^{-1}-dS_{b_K}(\theta-aK^{-1})} g(\theta)^{-1+cK^{-1}} \pi'(d\theta) \\ &\quad + \int_{\kappa}^{\infty} (\theta g(\theta))^{-1+cK^{-1}-d} \pi'(d\theta). \end{aligned}$$

We rewrite each term in turn. For the first term,

$$\begin{aligned} \int_0^{a/K} \theta^{-1+cK^{-1}} g(\theta)^{-1+cK^{-1}} \pi'(d\theta) &= (c/\gamma + o(1)) \int_0^{a/K} \theta^{-1+cK^{-1}} d\theta \\ &= (c/\gamma + o(1)) \frac{K}{c} \left(\frac{a}{K} \right)^{cK^{-1}} \\ &= \frac{K}{\gamma} + o(K). \end{aligned}$$

Since $\kappa \leq 1$ and $S_{b_K} \in [0, 1]$, for $\theta \in [a/K, \kappa]$, $\theta^{-dS_{b_K}(\theta-aK^{-1})} \leq \theta^{-d}$. Since $g(0) = 1$, $c_* \leq 1$ and therefore $g(\theta)^{-1+cK^{-1}} \leq c_*^{-1+c}$. Hence the second term is upper bounded by

$$\begin{aligned} c_*^{-1+c} \int_{a/K}^{\kappa} \theta^{-1+cK^{-1}-d} \pi'(d\theta) &\leq c_*^{-1}(c/\gamma + O(1)) \frac{K^d}{a^d} \frac{K}{c} (\kappa^{cK^{-1}} - (a/K)^{cK^{-1}}) \\ &= O(K^d) \times O(\ln K) \\ &= o(K). \end{aligned}$$

For the third term,

$$\begin{aligned} \int_{\kappa}^{\infty} (\theta g(\theta))^{-1+cK^{-1}-d} \pi'(d\theta) &= \int_{\kappa}^{\infty} (\theta g(\theta))^{-1+cK^{-1}} \pi(d\theta) \\ &\leq (\kappa c_*)^{-1+cK^{-1}} \int_{\kappa}^{\infty} \pi(d\theta) \\ &\leq (\kappa c_*)^{-1}. \end{aligned}$$

Hence, $Z_K = \frac{K}{\gamma} + o(K)$ and $KZ_K^{-1} = \gamma(1 + e_K)$, where $e_K = o(1)$.

Next, we have

$$\begin{aligned}
& \sup_{\theta \in [\kappa, \infty)} |f(\theta) - f_K(\theta)| \\
&= \sup_{\theta \in [\kappa, \infty)} (1 - e^{-\theta})(\theta g(\theta))^{-1} |\gamma - K Z_K^{-1}(\theta g(\theta))^{cK^{-1}}| \\
&\leq \sup_{\theta \in [\kappa, \infty)} \gamma (\theta g(\theta))^{-1} |1 - (1 + e_K)(\theta g(\theta))^{cK^{-1}}| \\
&\leq \gamma \sup_{\theta \in [\kappa, \infty)} (\theta g(\theta))^{-1} |1 - (\theta g(\theta))^{cK^{-1}}| \\
&\quad + \gamma e_K \sup_{\theta \in [\kappa, \infty)} (\theta g(\theta))^{-1+cK^{-1}}.
\end{aligned} \tag{B.1}$$

To bound the two terms we will use the fact that if $\theta \geq \kappa$, then

$$\theta g(\theta) \geq \frac{\theta}{c^*(1+\theta)} \geq \frac{\kappa}{c^*(1+\kappa)} =: \tilde{\kappa}$$

and if $\theta \leq 1$ then $\theta g(\theta) \leq c_* \leq 1$. Hence, letting $\psi := \theta g(\theta)$, for the first term in Eq. (B.1) we have

$$\begin{aligned}
& \gamma \sup_{\theta \in [\kappa, \infty)} (\theta g(\theta))^{-1} |1 - (\theta g(\theta))^{cK^{-1}}| \\
&\leq \gamma \sup_{\psi \in [\tilde{\kappa}, \infty)} \psi^{-1} |1 - \psi^{cK^{-1}}| \\
&\leq \gamma \sup_{\psi \in [\tilde{\kappa}, 1]} \psi^{-1} |1 - \psi^{cK^{-1}}| + \gamma \sup_{\psi \in [1, \infty)} \psi^{-1} |1 - \psi^{cK^{-1}}| \\
&\leq \gamma \tilde{\kappa}^{-1} \sup_{\psi \in [\tilde{\kappa}, 1]} |1 - \psi^{cK^{-1}}| + \gamma \left(\frac{K-c}{K} \right)^{Kc^{-1}} \left| 1 - \frac{K}{K-c} \right| \\
&\leq \gamma \tilde{\kappa}^{-1} (1 - \tilde{\kappa}^{cK^{-1}}) + O(1) \times \frac{c}{K-c} \\
&= \gamma \tilde{\kappa}^{-1} \times o(1) + O(K^{-1}) \\
&\rightarrow 0.
\end{aligned}$$

Similarly, for the second term in Eq. (B.1) we have

$$\begin{aligned}
\gamma e_K \sup_{\theta \in [\kappa, \infty)} (\theta g(\theta))^{-1+cK^{-1}} &\leq \gamma e_K \sup_{\psi \in [\tilde{\kappa}, \infty)} \psi^{-1+cK^{-1}} \\
&\leq \gamma \tilde{\kappa}^{-1} e_K \\
&\rightarrow 0.
\end{aligned}$$

Since $g(\theta)$ is bounded on $[0, \kappa]$, $g(\theta)^{cK^{-1}} = 1 + o(1)$ and therefore $(1 + e_K)g(\theta)^{cK^{-1}} = 1 + e'_K$, where $e'_K = o(1)$. Using this observation together with the bound $(1 - e^{-\theta})\theta^{-1} \leq 1$, we have

$$\begin{aligned}
& \int_0^\kappa |f'(\theta) - f'_K(\theta)| d\theta = \int_0^\kappa (\theta g(\theta))^{-d} |f(\theta) - f_K(\theta)| d\theta \\
&= \int_0^\kappa (1 - e^{-\theta})(\theta g(\theta))^{-1-d} |\gamma - K Z_K^{-1} \theta^{cK^{-1}+d-dS_{b_K}(\theta-aK^{-1})} g(\theta)^{cK^{-1}}| d\theta
\end{aligned}$$

$$\begin{aligned}
&\leq \gamma [c^*(1 + \kappa)]^{1+d} \int_0^\kappa \theta^{-d} |1 - (1 + e'_K) \theta^{cK^{-1}+d-dS_{b_K}(\theta-aK^{-1})}| d\theta \\
&\leq \gamma \int_0^\kappa \theta^{-d} |1 - \theta^{cK^{-1}+d-dS_{b_K}(\theta-aK^{-1})}| d\theta + \gamma e'_K \int_0^\kappa \theta^{cK^{-1}+d-dS_{b_K}(\theta-aK^{-1})} d\theta. \quad (\text{B.2})
\end{aligned}$$

We bound the first integral in Eq. (B.2) in four parts: from 0 to aK^{-1} , from aK^{-1} to $aK^{-1} + b_K$, from $aK^{-1} + b_K$ to $\kappa - b_K$, and from $\kappa - b_K$ to κ . The first part is equal to

$$\begin{aligned}
\int_0^{aK^{-1}} \theta^{-d} |1 - \theta^{d+cK^{-1}}| d\theta &\leq \int_0^{aK^{-1}} \theta^{-d} + \theta^{cK^{-1}} d\theta \\
&= \frac{\theta^{1-d}}{1-d} + \frac{K}{c+K} \theta^{1+cK^{-1}} \Big|_0^{aK^{-1}} \\
&= \frac{1}{1-d} (aK^{-1})^{1-d} + \frac{K}{c+K} (aK^{-1})^{1+cK^{-1}} \\
&\rightarrow 0.
\end{aligned}$$

The second part is equal to

$$\begin{aligned}
\int_{aK^{-1}}^{aK^{-1}+b_K} \theta^{-d} |1 - \theta^{cK^{-1}+d-dS_{b_K}(\theta-aK^{-1})}| d\theta &\leq \int_{aK^{-1}}^{aK^{-1}+b_K} \theta^{-d} + \theta^{cK^{-1}-d} d\theta \\
&\leq 2 \int_{aK^{-1}}^{aK^{-1}+b_K} \theta^{-d} d\theta \\
&= \frac{2}{1-d} \theta^{1-d} \Big|_{aK^{-1}}^{aK^{-1}+b_K} \\
&= \frac{2}{1-d} \left[\left(\frac{a}{K} + b_K \right)^{1-d} - \left(\frac{a}{K} \right)^{1-d} \right] \\
&\rightarrow 0.
\end{aligned}$$

The third part is equal to

$$\begin{aligned}
\int_{aK^{-1}+b_K}^{\kappa-b_K} \theta^{-d} |1 - \theta^{cK^{-1}}| d\theta &= \int_{aK^{-1}+b_K}^{\kappa-b_K} \theta^{-d} - \theta^{cK^{-1}-d} d\theta \\
&= \frac{1}{1-d} \theta^{1-d} - \frac{K}{c+K(1-d)} \theta^{1-d+cK^{-1}} \Big|_{aK^{-1}+b_K}^{\kappa-b_K} \\
&= \frac{(\kappa - b_K)^{1-d}}{1-d} - \frac{K}{c+K(1-d)} (\kappa - b_K)^{1-d+cK^{-1}} \\
&\quad - \frac{(aK^{-1} + b_K)^{1-d}}{1-d} + \frac{K}{c+K} (aK^{-1} + b_K)^{1-d+cK^{-1}} \\
&\rightarrow 0.
\end{aligned}$$

The fourth part is equal to

$$\begin{aligned}
\int_{\kappa-b_K}^\kappa \theta^{-d} |1 - \theta^{cK^{-1}}| d\theta &\leq \int_{\kappa-b_K}^\kappa \theta^{-d} + \theta^{cK^{-1}-d} d\theta \\
&\rightarrow 0
\end{aligned}$$

using the same argument as the second part. The second integral in Eq. (B.2) is upper bounded by

$$\gamma e'_K \int_0^\kappa \theta^{cK^{-1}-dS_{b_K}(\theta-aK^{-1})} d\theta \leq \gamma e'_K \int_0^\kappa \theta^{-d} d\theta = \gamma e'_K \frac{\kappa^{1-d}}{1-d} = o(K).$$

Since $\sup_{\theta \in [0, \kappa]} \pi'(\theta) < \infty$ by the boundedness of g and h and π is a probability density by construction, conclude using Lemma B.5 that $\|\mu - \mu_K\|_1 \rightarrow 0$. It then follows from Lemma B.3 that $\Theta_K \xrightarrow{\mathcal{D}} \Theta$. \square

B.2. Differentiability of smoothed indicator

We show that

$$S_b(\theta) = \begin{cases} \exp\left(\frac{-1}{1-(\theta-b)^2/b^2} + 1\right) & \text{if } \theta \in (0, b) \\ \mathbf{1}[\theta > 0] & \text{otherwise.} \end{cases}$$

is differentiable over the whole real line. Since on the separate domains $(-\infty, 0)$, $(0, b)$, and (b, ∞) , the derivative exists and is continuous, we only need to show that the values of the derivative at $\theta = 0$ and $\theta = b$ from either side match.

To start, we show that $S_b(\theta)$ is continuous at $\theta = 0$ and $\theta = b$.

$$\begin{aligned} \lim_{\theta \rightarrow b^-} S_b(\theta) &= \exp\left(1 - \frac{1}{1-0}\right) = 1, \\ \lim_{\theta \rightarrow 0^+} S_b(\theta) &= \exp\left(1 - \frac{1}{\infty}\right) = 0. \end{aligned}$$

For $\theta = b$, the derivative from the right ($\theta \rightarrow b^+$) is 0 since constant function. The derivative on the interval $(0, b)$ equals

$$\frac{dS_b}{d\theta} = S_b(\theta) \frac{-1}{[(\theta-b)^2/b^2 - 1]^2} \frac{2(\theta-b)}{b^2}. \quad (\text{B.3})$$

The limit as we approach b from the left is 0 since $\lim_{\theta \rightarrow b^-} S_b(\theta) = 1$ and the term $(\theta - b)$ vanishes. So the one-sided derivative is continuous at $\theta = b$.

For $\theta = 0$, the derivative from the left ($\theta \rightarrow 0^-$) is 0 since also constant function. The limit of Eq. (B.3) as we approach 0 from the right is also 0. It suffices to show

$$\lim_{\theta \rightarrow 0^+} S_b(\theta) \frac{-1}{[(\theta-b)^2/b^2 - 1]^2} = 0.$$

Reparametrizing $x = \frac{1}{1-(\theta-b)^2/b^2}$, we have that $x \rightarrow \infty$ and $\theta \rightarrow 0^+$. The last limit becomes

$$\lim_{x \rightarrow \infty} \frac{\exp(-x)}{x^2} = 0,$$

which is true because the decay of the exponential function is faster than any polynomial.

The derivative defined over disjoint intervals are continuous at the boundary points, so the overall approximate indicator is differentiable.

B.3. Normalized AIFA EPPF converges to NCRM EPPF

Proof of Theorem 3.4. First, we show that the total mass of AIFA converges in distribution to the total mass of CRM. It suffices to consider $K \geq b$ so that the AIFA EPPF is non-zero since we only care about the asymptotic behavior of $p_K(n_1, n_2, \dots, n_b)$. Through Appendix B.1, we have shown that for all measurable sets A and $t > 0$, the Laplace functionals converge:

$$\lim_{K \rightarrow \infty} \mathbb{E}[e^{-t\Theta_K(A)}] = \mathbb{E}[e^{-t\Theta(A)}],$$

By choosing $A = \Psi$ i.e. the ground space, we have that $\Theta_K(\Psi)$ is the total mass of AIFA and $\Theta(\Psi)$ is the total mass of CRM

$$\Theta_K(\Psi) = \sum_{i=1}^K \rho_{K,i}, \quad \Theta(\Psi) = \sum_{i=1}^{\infty} \theta_i.$$

Since for any $t > 0$, the Laplace transform of $\Theta_K(\Psi)$ converges to that of $\Theta(\Psi)$, we conclude that $\Theta_K(\Psi)$ converges to $\Theta(\Psi)$ in distribution (Kallenberg, 2002, Theorem 5.3):

$$\sum_{i=1}^K \rho_{K,i} \xrightarrow{\mathcal{D}} \Theta(\Psi). \quad (\text{B.4})$$

Second, we show that the decreasing order statistics of AIFA atom sizes converges (in finite-dimensional distributions i.e., in f.d.d) to the decreasing order statistics of CRM atom sizes. For each K , the decreasing order statistics of AIFA atoms is denoted by $\{\rho_{K,(i)}\}_{i=1}^K$:

$$\rho_{K,(1)} \geq \rho_{K,(2)} \geq \dots \geq \rho_{K,(K)}.$$

We will leverage Loeve (1956, Theorem 4 and page 191) to find the limiting distribution $\{\rho_{K,(i)}\}_{i=1}^K$ as $K \rightarrow \infty$. It is easy to verify the conditions to use the theorem: because the sums $\sum_{i=1}^K \rho_{K,i}$ converge in distribution to a limit, we know that all the $\rho_{K,i}$'s are uniformly asymptotically negligible (Kallenberg, 2002, Lemma 15.13). Now, we discuss what the limits are. It is well-known that $\Theta(\Psi)$ is an infinitely divisible positive random variable with no drift component and Levy measure exactly $\nu(d\theta)$ (Perman, Pitman and Yor, 1992). In the terminology of Loeve (1956, Equation 2), the characteristics of $\Theta(\Psi)$ are $a = b = 0$ (no drift or Gaussian parts), $L(x) = 0$, and

$$M(x) = -\nu([x, \infty)).$$

Let I be a counting process *in reverse* over $(0, \infty)$ defined based on the Poisson point process $\{\theta_i\}_{i=1}^{\infty}$ in the following way. For any x , $I(x)$ is the number of points θ_i exceeding the threshold x :

$$I(x) := |\{i : \theta_i \geq x\}|.$$

We augment $I(0) = \infty$ and $I(\infty) = 0$. As a stochastic process, I has independent increments, in that for all $0 = t_0 < t_1 < \dots < t_k$, the increments $I(t_i) - I(t_{i-1})$ are independent, furthermore the law of the increments is $I(t_{i-1}) - I(t_i) \sim \text{Poisson}(M(t_i) - M(t_{i-1}))$. These properties are simple consequences of the counting measure induced by the Poisson point

process. According to [Loeve \(1956, Page 191\)](#), the limiting distribution of $\{\rho_{K,(i)}\}_{i=1}^K$ is governed by I , in the sense that for any fixed $t \in \mathbb{N}$, for any $x_1, x_2, \dots, x_t \in [0, \infty)$:

$$\begin{aligned} \lim_{K \rightarrow \infty} \mathbb{P}(\rho_{K,(1)} < x_1, \rho_{K,(2)} < x_2, \dots, \rho_{K,(t)} < x_t) \\ = \mathbb{P}(I(x_1) < 1, I(x_2) < 2, \dots, I(x_t) < t). \end{aligned} \quad (\text{B.5})$$

Because the θ_i 's induce I , we can relate the left hand side to the order statistics of the Poisson point process. We denote the decreasing order statistic of the $\{\theta_i\}_{i=1}^\infty$ as:

$$\theta_{(1)} \geq \theta_{(2)} \geq \dots \geq \theta_{(n)} \geq \dots$$

Clearly, for any $t \in \mathbb{N}$, the event that $I(x)$ exceeds t is the same as the top t jumps among the $\{\theta_i\}_{i=1}^\infty$ exceed x : $I(x) \geq t \iff \theta_{(t)} \geq x$. Therefore Eq. (B.5) can be rewritten as, for any fixed $t \in \mathbb{N}$, for any $x_1, x_2, \dots, x_t \in [0, \infty)$:

$$\lim_{K \rightarrow \infty} \mathbb{P}(\rho_{K,(1)} < x_1, \rho_{K,(2)} < x_2, \dots, \rho_{K,(t)} < x_t) = \mathbb{P}(\theta_{(1)} < x_1, \theta_{(2)} < x_2, \dots, \theta_{(t)} < x_t). \quad (\text{B.6})$$

It is well-known that convergence of the distribution function imply weak convergence — for instance, see [Pollard \(2012, Chapter III, Problem 1\)](#). Actually, from [Loeve \(1956, Theorem 5 and page 194\)](#), for any fixed $t \in \mathbb{N}$, the convergence in distribution of $\{\rho_{K,(i)}\}_{i=1}^t$ to $\{\theta_i\}_{i=1}^t$ holds jointly with the convergence of $\sum_{i=1}^K \rho_{K,(i)}$ to $\sum_{i=1}^\infty \theta_i$: the two conditions of the theorem, which are continuity of the distribution function of each $\rho_{K,i}$ and $M(0) = -\infty$ ¹⁹, are easily verified. Therefore, by the continuous mapping theorem, if we define the normalized atom sizes:

$$p_{K,(s)} := \frac{\rho_{K,(s)}}{\sum_{i=1}^K \rho_{K,i}}, \quad p_{(s)} := \frac{\theta_{(s)}}{\sum_{i=1}^\infty \theta_i},$$

we also have that the normalized decreasing order statistics converge:

$$(p_{K,i})_{i=1}^K \xrightarrow{f.d.d.} (p_{K,(i)})_{i=1}^\infty.$$

Finally we show that the EPPFs converge. In addition, if we define the *size-biased permutation* (in the sense of [Gnedin \(1998, Section 2\)](#)) of the normalized atom sizes:

$$\{\tilde{p}_{K,i}\} \sim \text{SBP}(p_{K,(s)}), \quad \{\tilde{p}_i\} \sim \text{SBP}(p_{(s)}),$$

then by [Gnedin \(1998, Theorem 1\)](#), the finite-dimensional distributions of the size-biased permutation also converges:

$$(\tilde{p}_{K,i})_{i=1}^K \xrightarrow{f.d.d.} (\tilde{p}_i)_{i=1}^\infty. \quad (\text{B.7})$$

[Pitman \(1996, Equation 45\)](#) gives the EPPF of $\Xi = \Theta/\Theta(\Psi)$:

$$p(n_1, n_2, \dots, n_b) = \mathbb{E} \left(\prod_{i=1}^b \tilde{p}_i^{n_i-1} \prod_{i=1}^{b-1} \left(1 - \sum_{j=1}^i \tilde{p}_j \right) \right),$$

Likewise, the EPPF of $\Xi_K = \Theta_K/\Theta_K(\Psi)$ is:

$$p_K(n_1, n_2, \dots, n_t) = \mathbb{E} \left(\prod_{i=1}^b \tilde{p}_{K,i}^{n_i-1} \prod_{i=1}^{b-1} \left(1 - \sum_{j=1}^i \tilde{p}_{K,j} \right) \right).$$

¹⁹There is a typo in [Loeve \(1956\)](#).

Since b is fixed, and each p_j is $[0, 1]$ valued, the mapping from the b -dimensional vector p to the product $\prod_{i=1}^b p_i^{n_i-1} \prod_{i=1}^{b-1} \left(1 - \sum_{j=1}^i p_j\right)$ is continuous and bounded. The choice of N , b , n_i have been fixed but arbitrary. Hence, the convergence in finite-dimensional distributions of in Eq. (B.7) imply that the EPPFs converge. \square

Appendix C: Marginal processes of exponential CRMs

The marginal process characterization describes the probabilistic model not through the two-stage sampling $\Theta \sim \text{CRM}(H, \nu)$ and $X_n | \Theta \stackrel{\text{i.i.d.}}{\sim} \text{LP}(\ell; \Theta)$, but through the conditional distributions $X_n | X_{n-1}, X_{n-2}, \dots, X_1$ i.e. the underlying Θ has been *marginalized out*. This perspective removes the need to infer a countably infinite set of target variables. In addition, the *exchangeability* between X_1, X_2, \dots, X_N i.e. the joint distribution's invariance with respect to ordering of observations (Aldous, 1985), often enables the development of inference algorithms, namely Gibbs samplers.

Broderick, Wilson and Jordan (2018, Corollary 6.2) derive the conditional distributions $X_n | X_{n-1}, X_{n-2}, \dots, X_1$ for general exponential family CRMs Eqs. (6) and (7).

Proposition C.1 (Target's marginal process (Broderick, Wilson and Jordan, 2018, Corollary 6.2)). *For any n , $X_n | X_{n-1}, \dots, X_1$ is a random measure with finite support.*

1. Let $\{\zeta_i\}_{i=1}^{K_{n-1}}$ be the union of atom locations in X_1, X_2, \dots, X_{n-1} . For $1 \leq m \leq n-1$, let $x_{m,j}$ be the atom size of X_m at atom location ζ_j . Denote $x_{n,i}$ to be the atom size of X_n at atom location ζ_i . The $x_{n,i}$'s are independent across i and the p.m.f. of $x_{n,i}$ at x is

$$h(x | x_{1:(n-1)}) = \frac{Z \left(-1 + \sum_{m=1}^{n-1} \phi(x_{m,i}) + \phi(x), \eta + \left(\frac{\sum_{m=1}^{n-1} t(x_{m,i}) + t(x)}{n} \right) \right)}{\kappa(x) Z \left(-1 + \sum_{m=1}^{n-1} \phi(x_{m,i}), \eta + \left(\frac{\sum_{m=1}^{n-1} t(x_{m,i})}{n-1} \right) \right)}.$$

2. For each $x \in \mathbb{N}$, X_n has $p_{n,x}$ atoms whose atom size is exactly x . The locations of each atom are iid H : as H is diffuse, they are disjoint from the existing union of atoms $\{\zeta_i\}_{i=1}^{K_{n-1}}$. $p_{n,x}$ is Poisson-distributed, independently across x , with mean:

$$M_{n,x} = \gamma' \kappa(0)^{n-1} \kappa(x) Z \left(-1 + (n-1)\phi(0) + \phi(x), \eta + \left(\frac{(n-1)t(0) + t(x)}{n} \right) \right).$$

In Proposition C.2, we state a similar characterization of $Z_n | Z_{n-1}, Z_{n-2}, \dots, Z_1$ for the finite-dimensional model in Eq. (13) and give the proof.

Proposition C.2 (Approximation's marginal process). *For any n , $Z_n | Z_{n-1}, \dots, Z_1$ is a random measure with finite support.*

1. Let $\{\zeta_i\}_{i=1}^{K_{n-1}}$ be the union of atom locations in Z_1, Z_2, \dots, Z_{n-1} . For $1 \leq m \leq n-1$, let $z_{m,j}$ be the atom size of Z_m at atom location ζ_j . Denote $z_{n,i}$ to be the atom size of Z_n

at atom location ζ_i . $z_{n,i}$'s are independently across i and the p.m.f. of $z_{n,i}$ at x is:

$$\begin{aligned} \tilde{h}(x | z_{1:(n-1)}) &= \\ \kappa(x) &\frac{Z\left(c/K - 1 + \sum_{m=1}^{n-1} \phi(z_{m,i}) + \phi(x), \eta + \binom{\sum_{m=1}^{n-1} t(z_{m,i}) + t(x)}{n}\right)}{Z\left(c/K - 1 + \sum_{m=1}^{n-1} \phi(z_{m,i}), \eta + \binom{\sum_{m=1}^{n-1} t(z_{m,i})}{n-1}\right)}. \end{aligned}$$

2. $K - K_{n-1}$ atom locations are generated iid from H . Z_n has $p_{n,x}$ atoms whose size is exactly x (for $x \in \mathbb{N} \cup \{0\}$) over these $K - K_{n-1}$ atom locations (the $p_{n,0}$ atoms whose atom size is 0 can be interpreted as not present in Z_n). The joint distribution of $p_{n,x}$ is a multinomial with $K - K_{n-1}$ trials, with success of type x having probability:

$$\begin{aligned} \tilde{h}(x | z_{1:(n-1)} = 0_{n-1}) &= \\ \kappa(x) &\frac{Z\left(c/K - 1 + (n-1)\phi(0) + \phi(x), \eta + \binom{(n-1)t(0) + t(x)}{n}\right)}{Z\left(c/K - 1 + (n-1)\phi(0), \eta + \binom{(n-1)t(0)}{n-1}\right)}. \end{aligned}$$

Proof of Proposition C.2. We only need to prove the conditional distributions for the atom sizes: that the K distinct atom locations are generated iid from the base measure is clear.

First we consider $n = 1$. By construction in Corollary 3.3, a priori, the trait frequencies $\{\rho_i\}_{i=1}^K$ are independent, each following the distribution:

$$\mathbb{P}(\rho_i \in d\theta) = \frac{\mathbf{1}\{\theta \in U\}}{Z(c/K - 1, \eta)} \theta^{c/K-1} \exp\left(\left\langle \eta, \binom{\mu(\theta)}{-A(\theta)} \right\rangle\right).$$

Conditioned on $\{\rho_i\}_{i=1}^K$, the atom sizes $z_{1,i}$ that Z_1 puts on the i -th atom location are independent across i and each is distributed as:

$$\mathbb{P}(z_{1,i} = x | \rho_i) = \kappa(x) \rho_i^{\phi(x)} \exp(\langle \mu(\rho_i), t(x) \rangle - A(\rho_i)).$$

Integrating out ρ_i , the marginal distribution for $z_{1,i}$ is:

$$\begin{aligned} \mathbb{P}(z_{1,i} = x) &= \int \mathbb{P}(z_{1,i} = x | \rho_i = \theta) \mathbb{P}(\rho_i \in d\theta) \\ &= \frac{\kappa(x)}{Z(c/K - 1, \eta)} \int_U \theta^{c/K-1+\phi(x)} \exp\left(\left\langle \eta + \binom{t(x)}{1}, \binom{\mu(\theta)}{-A(\theta)} \right\rangle\right) d\theta \\ &= \kappa(x) \frac{Z\left(c/K - 1 + \phi(x), \eta + \binom{t(x)}{1}\right)}{Z(c/K - 1, \eta)}, \end{aligned}$$

by definition of Z as the normalizer Eq. (8).

Now we consider $n \geq 2$. The distribution of $z_{n,i}$ only depends on the distribution of $z_{n-1,i}, z_{n-2,i}, \dots, z_{1,i}$ since the atom sizes across different atoms are independent of each other both a priori and a posteriori. The predictive distribution is an integral:

$$\mathbb{P}(z_{n,i} = x | z_{1:(n-1),i}) = \int \mathbb{P}(z_{n,i} = x | \rho_i) \mathbb{P}(\rho_i \in d\theta | z_{1:(n-1),i}).$$

Because the prior over ρ_i is conjugate for the likelihood $z_{i,j} | \rho_i$, and the observations $z_{i,j}$ are conditionally independent given ρ_i , the posterior $\mathbb{P}(\rho_i \in d\theta | z_{1:(n-1),i})$ is in the same exponential family but with different natural parameters:

$$\mathbf{1}\{\theta \in U\} \frac{\theta^{c/K-1+\sum_{m=1}^{n-1} \phi(z_{m,i})} \exp\left(\left\langle \eta + \left(\frac{\sum_{m=1}^{n-1} t(z_{m,i})}{n-1}\right), \begin{pmatrix} \mu(\theta) \\ -A(\theta) \end{pmatrix} \right\rangle\right) d\theta}{Z\left(c/K-1+\sum_{m=1}^{n-1} \phi(z_{m,i}), \eta + \left(\frac{\sum_{m=1}^{n-1} t(z_{m,i})}{n-1}\right)\right)}.$$

This means that the predictive distribution $\mathbb{P}(z_{n,i} = x | z_{1:(n-1),i})$ equals:

$$\begin{aligned} & \kappa(x) \frac{\int_U \theta^{c/K-1+\sum_{m=1}^{n-1} \phi(z_{m,i})+\phi(x)} \exp\left(\left\langle \eta + \left(\frac{\sum_{m=1}^{n-1} t(z_{m,i}) + t(x)}{n}\right), \begin{pmatrix} \mu(\theta) \\ -A(\theta) \end{pmatrix} \right\rangle\right) d\theta}{Z\left(c/K-1+\sum_{m=1}^{n-1} \phi(z_{m,i}), \eta + \left(\frac{\sum_{m=1}^{n-1} t(z_{m,i})}{n-1}\right)\right)} \\ &= \kappa(x) \frac{Z\left(c/K-1+\sum_{m=1}^{n-1} \phi(z_{m,i}) + \phi(x), \eta + \left(\frac{\sum_{m=1}^{n-1} t(z_{m,i}) + t(x)}{n}\right)\right)}{Z\left(c/K-1+\sum_{m=1}^{n-1} \phi(z_{m,i}), \eta + \left(\frac{\sum_{m=1}^{n-1} t(z_{m,i})}{n-1}\right)\right)}. \end{aligned}$$

The predictive distribution $\mathbb{P}(z_{n,i} = x | z_{1:(n-1),i})$ govern both the distribution of atom sizes for known atom locations and new atom locations. \square

Appendix D: Admissible hyperparameters of extended gamma process

We first describe the two desiderata of a useful Bayesian nonparametric model in more detail. The condition that the total mass of the rate measure needs to be infinite reads as

$$\int_0^\infty \nu(d\theta) = \infty$$

This is [Broderick, Wilson and Jordan \(2018, A1\)](#). To ensure that the number of active traits is almost surely finite, it suffices to ensure that the expected number of traits is finite. The condition that the expected number of active traits is finite reads as

$$\int_0^\infty (1 - Z_\tau^{-1}(\theta)) \nu(d\theta) < \infty.$$

This is [Broderick, Wilson and Jordan \(2018, A2\)](#): note that $Z_\tau^{-1}(\theta)$ is exactly the probability that a trait with rate θ does not manifest.

Lemma D.1 (Hyperparameters for extended gamma rate measure). *For any $\gamma > 0$, $c > 0$, $T \geq 1$, $\tau > 0$, for the rate measure $\nu(\theta)$ from Eq. (11) Then,*

- $\int_0^\infty \nu(d\theta) = \infty$.
- $\int_0^\infty [1 - Z_\tau^{-1}(\theta)] \nu(d\theta) < \infty$.

Proof of Lemma D.1. We observe that it suffices to show the two conclusions for $\gamma = 1$, since any positive scaling of the rate measure will preserve the finiteness (or infiniteness) of

the integrals. In addition, we can replace the upper limit of integration, ∞ , by T , since the rate measure is zero for $\theta > T$.

We begin with elementary observations about the monotonicity of $Z_\tau(\theta)$. $Z_\tau(\theta)$ is increasing in θ but decreasing in τ . In the limit of $\tau \rightarrow \infty$, $Z_\tau(\theta)$ approaches $1 + \theta$.

To prove the first statement, we use a simple lower bound on $\int_0^T \nu(d\theta)$, which holds since $T \geq 1$:

$$\begin{aligned} \int_0^T \theta^{-1} Z_\tau^{-c}(\theta) d\theta &\geq \int_0^1 \theta^{-1} Z_\tau^{-c}(\theta) d\theta \\ &\geq Z_\tau^{-c}(1) \int_0^1 \theta^{-1} d\theta = \infty. \end{aligned}$$

Since $Z_\tau(\theta)$ is increasing in θ , for all $\theta \in [0, 1]$, $Z_\tau^{-c}(\theta) \geq Z_\tau^{-c}(1) > 0$. There are many ways to show $\int_0^1 \theta^{-1} d\theta = \infty$ — the connection with the harmonic series is one.

To prove the second statement, we consider two cases separately.

In the first case, $\tau \leq 1.0$. We first show that, there exists a constant $\kappa > 0$ such that, for $\theta \in [0, 1]$:

$$1 - Z_\tau^{-1}(\theta) \leq \theta + \kappa\theta^2. \tag{D.1}$$

Consider the Taylor series of $Z_\tau(\theta)$. By recursion, the j th derivative of $Z_\tau(\theta)$ equals

$$\frac{d^j}{d\theta^j} Z_\tau(\theta) = \sum_{i=0}^{\infty} \left(\prod_{k=1}^i (j+k) \right)^{1-\tau} \frac{\theta^j}{(j!)^\tau}. \tag{D.2}$$

It is easy to check that the infinite sums in Eq. (D.2) converge for any θ . By absolute convergence theorems²⁰, it suffices to inspect $\theta > 0$. By the ratio test, subsequent terms have ratio

$$\frac{\theta^{j+1}}{[(j+1)!]^\tau} \left(\prod_{k=1}^i (j+1+k) \right)^{1-\tau} / \frac{\theta^j}{[(j!)!]^\tau} \left(\prod_{k=1}^i (j+k) \right)^{1-\tau} = \frac{\theta(j+1+i)^{1-\tau}}{j+1} \xrightarrow{j \rightarrow \infty} 0.$$

Clearly $Z_\tau(0) = 1$. Hence, for all θ close enough to 0, $Z_\tau(\theta)$ is strictly positive. Therefore, $Z_\tau^{-1}(\theta)$ also has derivatives of all orders in an open interval containing $[0, 1]$. Note that $\frac{d}{d\theta} Z_\tau(\theta)|_{\theta=0} = 1$. Therefore

$$\frac{d}{d\theta} Z_\tau^{-1}(\theta)|_{\theta=0} = \frac{-\frac{d}{d\theta} Z_\tau(\theta)|_{\theta=0}}{Z_\tau^2(0)} = -1.$$

By Taylor's theorem Kline (1998, Section 20.3), for any $\theta \in [0, 1]$, there exists a y between 0 and θ such that

$$Z_\tau^{-1}(\theta) = 1 - \theta + \frac{1}{2} \left(\frac{d^2}{d\theta^2} Z_\tau^{-1}(\theta) \Big|_{\theta=y} \right) \theta^2.$$

It is clear that the second derivative $\frac{d^2}{d\theta^2} Z_\tau^{-1}(\theta) \Big|_{\theta=y}$ is bounded by a constant independent of y for $y \in [0, 1]$, since

$$\frac{d^2}{d\theta^2} Z_\tau^{-1}(\theta) = \frac{\frac{d^2}{d\theta^2} Z_\tau(\theta)}{Z_\tau^2(\theta)} - 2 \left(\frac{d}{d\theta} Z_\tau(\theta) \right)^2 \frac{1}{Z_\tau^3(\theta)},$$

²⁰see, e.g. https://www.whitman.edu/mathematics/calculus_online/section11.06.html

with the $Z_\tau(\theta)$ being at least 1 and the derivatives being bounded. This shows Eq. (D.1). Therefore:

$$\begin{aligned} \int_0^T [1 - Z_\tau^{-1}(\theta)]\nu(d\theta) &\leq \int_0^1 [1 - Z_\tau^{-1}(\theta)]\theta^{-1}Z_\tau^{-c}(\theta)d\theta + \int_1^T \theta^{-1}Z_\tau^{-c}(\theta)d\theta \\ &= A + B. \end{aligned}$$

We use the estimate $1 - Z_\tau^{-1}(\theta)\theta + \kappa\theta^2$ in the first part (A):

$$\int_0^1 [1 - Z_\tau^{-1}(\theta)]\theta^{-1}Z_\tau^{-c}(\theta)d\theta \leq \int_0^1 (1 + \kappa\theta)Z_\tau^{-c}(\theta)d\theta.$$

Since $Z_\tau^{-c}(\theta) \leq \exp(-c\theta)$, it is true that A is finite. For the second part (B), we again use the upper bound $Z_\tau^{-c}(\theta) \leq \exp(-c\theta)$ and also $\theta^{-1} \leq 1$ to conclude that B is finite. Overall $A + B$ is finite.

In the second case, $\tau > 1.0$. Since $Z_\tau(\theta) \leq Z_1(\theta)$, $1 - Z_\tau^{-1}(\theta) \leq 1 - Z_1^{-1}(\theta) = 1 - \exp(-\theta)$. In addition, since $Z_\tau(\theta) \geq Z_\infty(\theta)$, we also have $Z_\tau^{-c}(\theta) \leq Z_\infty^{-c} = \frac{1}{(1+\theta)^c}$. Hence

$$\int_0^T [1 - Z_\tau^{-1}(\theta)]\nu(d\theta) \leq \int_0^T (1 - \exp(-\theta))\theta^{-1} \frac{1}{(1+\theta)^c} d\theta.$$

Observe that for any positive θ , $(1 - \exp(-\theta))\theta^{-1} \leq 1$. Therefore

$$\int_0^T [1 - Z_\tau^{-1}(\theta)]\nu(d\theta) \leq \int_0^T \frac{1}{(1+\theta)^c} d\theta.$$

The integrand $\frac{1}{(1+\theta)^c}$ is continuous and upper bounded on $[0, T]$, so the overall integral is finite. □

Appendix E: Technical lemmas

E.1. Concentration

Lemma E.1 (Modified upper tail Chernoff bound). *Let $X = \sum_{i=1}^n X_i$, where $X_i = 1$ with probability p_i and $X_i = 0$ with probability $1 - p_i$, and all X_i are independent. Let μ be an upper bound on $E(X) = \sum_{i=1}^n p_i$. Then for all $\delta > 0$:*

$$\mathbb{P}(X \geq (1 + \delta)\mu) \leq \exp\left(-\frac{\delta^2}{2 + \delta}\mu\right).$$

Proof of Lemma E.1. The proof relies on the regular upper tail Chernoff bound (Doerr and Neumann, 2019, Theorem 1.10.1) and an argument using stochastic domination. We pad the first n Poisson trials that define X with additional trials $X_{n+1}, X_{n+2}, \dots, X_{n+m}$. m is the smallest natural number such that $\frac{\mu - \mathbb{E}[X]}{m} \leq 1$. Each X_{n+i} is a Bernoulli with probability $\frac{\mu - \mathbb{E}[X]}{m}$, and the trials are independent. Then $Y = X + \sum_{j=1}^m X_{n+j}$ is itself the sum of Poisson trials with mean exactly μ , so the regular Chernoff bound applies:

$$\mathbb{P}(Y \geq (1 + \delta)\mu) \leq \exp\left(-\frac{\delta^2}{2 + \delta}\mu\right),$$

where we used (Doerr and Neumann, 2019, Equation 1.10.13) and the simple observation that $2/3\delta < \delta$. By construction, X is stochastically dominated by Y , so the tail probabilities of X are upper bounded by the tail probabilities of Y . \square

Lemma E.2 (Lower tail Chernoff bound (Doerr and Neumann, 2019, Theorem 1.10.5)). *Let $X = \sum_{i=1}^n X_i$, where $X_i = 1$ with probability p_i and $X_i = 0$ with probability $1 - p_i$, and all X_i are independent. Let $\mu := E(X) = \sum_{i=1}^n p_i$. Then for all $\delta \in (0, 1)$:*

$$\mathbb{P}(X \leq (1 - \delta)\mu) \leq \exp(-\mu\delta^2/2).$$

Lemma E.3 (Tail bounds for Poisson distribution). *If $X \sim \text{Poisson}(\lambda)$ then for any $x > 0$:*

$$\mathbb{P}(X \geq \lambda + x) \leq \exp\left(-\frac{x^2}{2(\lambda + x)}\right),$$

and for any $0 < x < \lambda$:

$$\mathbb{P}(X \leq \lambda - x) \leq \exp\left(-\frac{x^2}{2\lambda}\right).$$

Proof of Lemma E.3. For $x \geq -1$, let $\psi(x) := 2((1+x)\ln(1+x) - x)/x^2$.

We first inspect the upper tail bound. If $X \sim \text{Poisson}(\lambda)$, for any $x > 0$, Pollard (2001, Exercise 3 p.272) implies that:

$$\mathbb{P}(X \geq \lambda + x) \leq \exp\left(-\frac{x^2}{2\lambda}\psi\left(\frac{x}{\lambda}\right)\right).$$

To show the upper tail bound, it suffices to prove that $\frac{x^2}{2\lambda}\psi\left(\frac{x}{\lambda}\right)$ is greater than $\frac{x^2}{2(\lambda+x)}$. In general, we show that for $u \geq 0$:

$$(u+1)\psi(u) - 1 \geq 0. \tag{E.1}$$

The denominator of $(u+1)\psi(u) - 1$ is clearly positive. Consider the numerator of $(u+1)\psi(u) - 1$, which is $g(u) := 2((u+1)^2 \ln(u+1) - u(u+1) - u^2)$. Its 1st and 2nd derivatives are:

$$\begin{aligned} g'(u) &= 4(u+1)\ln(u+1) - 2u + 1 \\ g''(u) &= 4\ln(u+1) + 2. \end{aligned}$$

Since $g''(u) \geq 0$, $g'(u)$ is monotone increasing. Since $g'(0) = 1$, $g'(u) > 0$ for $u \geq 0$, hence $g(u)$ is monotone increasing. Because $g(0) = 0$, we conclude that $g(u) \geq 0$ for $u > 0$ and Eq. (E.1) holds. Plugging in $u = x/\lambda$:

$$\psi\left(\frac{x}{\lambda}\right) \geq \frac{1}{1 + \frac{x}{\lambda}} = \frac{\lambda}{x + \lambda},$$

which shows $\frac{x^2}{2\lambda}\psi\left(\frac{x}{\lambda}\right) \geq \frac{x^2}{2(\lambda+x)}$.

Now we inspect the lower tail bound. We follow the proof of Canonne, Theorem 1. We first argue that:

$$\mathbb{P}(X \leq \lambda - x) \leq \exp\left(-\frac{x^2}{2\lambda}\psi\left(-\frac{x}{\lambda}\right)\right). \tag{E.2}$$

For any θ , the moment generating function $\mathbb{E}[\exp(\theta X)]$ is well-defined and well-known:

$$\mathbb{E}[\exp(\theta X)] := \exp(\lambda(\exp(\theta) - 1)).$$

Therefore:

$$\begin{aligned} \mathbb{P}(X \leq \lambda - x) &\leq \mathbb{P}(\exp(\theta X) \leq \exp(\theta(\lambda - x))) \leq \mathbb{P}(\exp(\theta(\lambda - x - X)) \geq 1) \\ &\leq \exp(\theta(\lambda - x))\mathbb{E}[\exp(-\theta X)], \end{aligned}$$

where we have used Markov's inequality.

We now aim to minimize $\exp(\theta(\lambda - x))\mathbb{E}[\exp(-\theta X)]$ as a function of θ . Its logarithm is:

$$\lambda(\exp(-\theta) - 1) + \theta(\lambda - x).$$

This is a convex function, whose derivative vanishes at $\theta = -\ln(1 - \frac{x}{\lambda})$. Overall this means the best upper bound on $\mathbb{P}(X \leq \lambda - x)$ is:

$$\exp\left(-\lambda\left(\frac{x}{\lambda} + \left(1 - \frac{x}{\lambda}\right)\ln\left(1 - \frac{x}{\lambda}\right)\right)\right),$$

which is exactly the right hand side of Eq. (E.2). Hence to demonstrate the lower tail bound, it suffices to show that:

$$\psi\left(-\frac{x}{\lambda}\right) \geq 1.$$

More generally, we show that for $-1 \leq u \leq 0$, $\psi(u) - 1 \geq 0$. Consider the numerator of $\psi(u) - 1$, which is $h(u) := 2((1 + u)\ln(1 + u) - u) - u^2$. The first two derivatives are:

$$\begin{aligned} h'(u) &= 2(1 + \ln(1 + u)) - 2u \\ h''(u) &= \frac{2}{1 + u} - 2 \end{aligned}$$

Since $h''(u) \geq 0$, $h(u)$ is convex on $[-1, 0]$. Note that $h(0) = 0$. Also, by simple continuity argument, $h(-1) = 2$. Therefore, h is non-negative on $[0, 1]$, meaning that $\psi(u) \geq 1$. \square

Lemma E.4 (Multinomial-Poisson approximation). *Let $\{p_i\}_{i=1}^{\infty}$, $p_i \geq 0$, $\sum_{i=1}^{\infty} p_i < 1$. Suppose there are n independent trials: in each trial, success of type i has probability p_i . Let $X = \{X_i\}_{i=1}^{\infty}$ be the number of type i successes after n trial. Let $Y = \{Y_i\}_{i=1}^{\infty}$ be independent Poisson random variables, where Y_i has mean np_i . Then, there exists a coupling $(\widehat{X}, \widehat{Y})$ of P_X and P_Y such that*

$$\mathbb{P}(\widehat{X} \neq \widehat{Y}) \leq n \left(\sum_{i=1}^{\infty} p_i \right)^2.$$

Furthermore, the joint distribution $(\widehat{X}, \widehat{Y})$ naturally disintegrates i.e. the conditional distribution $\widehat{X} | \widehat{Y}$ exists.

Proof of Lemma E.4. First, we recognize that both X and Y can be sampled in two steps.

- Regarding X , first sample $N_1 \sim \text{Binom}(n, \sum_{i=1}^{\infty} p_i)$. Then, for each $1 \leq k \leq N_1$, independently sample Z_k where $\mathbb{P}(Z_k = i) = \frac{p_i}{\sum_{j=1}^{\infty} p_j}$. Then, $X_i = \sum_{k=1}^{N_1} \mathbf{1}\{Z_k = i\}$ for each i .

- Regarding Y , first sample $N_2 \sim \text{Poisson}(n \sum_{i=1}^{\infty} p_i)$. Then, for each $1 \leq k \leq N_2$, independently sample T_k where $\mathbb{P}(T_k = i) = \frac{p_i}{\sum_{j=1}^{\infty} p_j}$. Then, $Y_i = \sum_{k=1}^{N_2} \mathbf{1}\{T_k = i\}$ for each i .

The two-step sampling perspective for X comes from rejection sampling: to generate a success of type k , we first generate some type of success, and then re-calibrate to get the right proportion for type k . The two-step perspective for Y comes from the thinning property of Poisson distribution (Last and Penrose, 2017, Exercise 1.5). The thinning property implies that for any finite index set \mathcal{K} , all $\{Y_i\}$ for $i \in \mathcal{K}$ are mutually independent and marginally, $Y_i \sim \text{Poisson}(np_i)$. Hence the whole collection $\{Y_i\}_{i=1}^{\infty}$ are independent Poissons and the mean of Y_i is np_i .

Observing that the conditional $X | N_1 = n$ is the same as $Y | N_2 = n$, we propose the coupling that essentially proves propagation rule Lemma E.8. The proposed coupling $(\widehat{X}, \widehat{Y})$ is that

- Sample $(\widehat{N}_1, \widehat{N}_2)$ from the maximal coupling that attains d_{TV} between the two distributions: $\text{Binom}(n, \sum_{i=1}^{\infty} p_i)$ and $\text{Poisson}(n \sum_{i=1}^{\infty} p_i)$.
- If $\widehat{N}_1 = \widehat{N}_2$, let the common value be n , sample $\widehat{X} | \widehat{N}_1 = n$ and set $\widehat{Y} = \widehat{X}$. Else $\widehat{N}_1 \neq \widehat{N}_2$, independently sample $\widehat{X} | \widehat{N}_1$ and $\widehat{Y} | \widehat{N}_2$.

From the classic binomial-Poisson approximation (Le Cam, 1960), we know that

$$\mathbb{P}(\widehat{N}_1 \neq \widehat{N}_2) = d_{\text{TV}}(P_{N_1}, P_{N_2}) \leq n \left(\sum_{i=1}^{\infty} p_i \right)^2,$$

which guarantees that

$$\mathbb{P}(\widehat{X} \neq \widehat{Y}) \leq n \left(\sum_{i=1}^{\infty} p_i \right)^2.$$

Alternatively, we can sample from the conditional $\widehat{X} | \widehat{Y}$ in the following way. From \widehat{Y} , compute \widehat{N}_2 , which is just $\sum_{x=1}^{\infty} \widehat{Y}_x$. Sample \widehat{N}_1 from the conditional distribution $\widehat{N}_1 | \widehat{N}_2$ of the maximal coupling that attains the binomial-Poisson total variation. If $\widehat{N}_1 = \widehat{N}_2$, set $\widehat{X} = \widehat{Y}$. Else sample \widehat{X} from the conditional $\widehat{X} | \widehat{N}_1$. It is straightforward to verify that this is the conditional $\widehat{X} | \widehat{Y}$ of the joint $(\widehat{X}, \widehat{Y})$ described above. \square

Lemma E.5 (Total variation between Poissons (Adell and Lekuona, 2005, Corollary 3.1)). *Let P_1 be the Poisson distribution with mean s , P_2 the Poisson distribution with mean t . Then:*

$$d_{\text{TV}}(P_1, P_2) \leq 1 - \exp(-|s - t|) \leq |s - t|.$$

E.2. Total variation

We will frequently use the following relationship between total variation and coupling. For two distributions P_X and P_Y over the same measurable space, it is well-known that the total variation distance between P_X and P_Y is at most the infimum over joint distributions $(\widehat{X}, \widehat{Y})$ which are couplings of P_X and P_Y :

$$d_{\text{TV}}(P_X, P_Y) \leq \inf_{\widehat{X}, \widehat{Y} \text{ coupling of } P_X, P_Y} \mathbb{P}(\widehat{X} \neq \widehat{Y}).$$

When P_X and P_Y are discrete distributions, the inequality is actual equality, and there exists couplings that attain the equality (Levin and Peres, 2017, Proposition 4.7).

We first state the chain rule, which will be applied to compare joint distributions that admit densities.

Lemma E.6 (Chain rule). *Suppose P_{X_1, Y_1} and P_{X_2, Y_2} are two distributions that have densities with respect to a common measure over the ground space $\mathcal{A} \times \mathcal{B}$. Then:*

$$d_{TV}(P_{X_1, Y_1}, P_{X_2, Y_2}) \leq d_{TV}(P_{X_1}, P_{X_2}) + \sup_{a \in \mathcal{A}} d_{TV}(P_{Y_1 | X_1=a}, P_{Y_2 | X_2=a}).$$

Proof of Lemma E.6. Because both P_{X_1, Y_1} and P_{X_2, Y_2} have densities, total variation distance is half of L_1 distance between the densities:

$$\begin{aligned} d_{TV}(P_{X_1, Y_1}, P_{X_2, Y_2}) &= \frac{1}{2} \int_{\mathcal{A} \times \mathcal{B}} |P_{X_1, Y_1}(a, b) - P_{X_2, Y_2}(a, b)| \, dadb \\ &= \frac{1}{2} \int_{\mathcal{A} \times \mathcal{B}} |P_{X_1, Y_1}(a, b) - P_{X_2}(a)P_{Y_1 | X_1}(b | a) \\ &\quad + P_{X_2}(a)P_{Y_1 | X_1}(b | a) - P_{X_2, Y_2}(a, b)| \, dadb \\ &\leq \frac{1}{2} \int_{\mathcal{A} \times \mathcal{B}} P_{Y_1 | X_1}(b | a) |P_{X_1}(a) - P_{X_2}(a)| \\ &\quad + P_{X_2}(a) |P_{Y_1 | X_1}(b | a) - P_{Y_2 | X_2}(b | a)| \, dadb \\ &= \frac{1}{2} \int_{\mathcal{A} \times \mathcal{B}} P_{Y_1 | X_1}(b | a) |P_{X_1}(a) - P_{X_2}(a)| \, dadb \\ &\quad + \frac{1}{2} \int_{\mathcal{A} \times \mathcal{B}} P_{X_2}(a) |P_{Y_1 | X_1}(b | a) - P_{Y_2 | X_2}(b | a)| \, dadb, \end{aligned}$$

where we have used triangle inequality. Regarding the first term, using Fubini:

$$\begin{aligned} &\frac{1}{2} \int_{\mathcal{A} \times \mathcal{B}} P_{Y_1 | X_1}(b | a) |P_{X_1}(a) - P_{X_2}(a)| \, dadb \\ &= \frac{1}{2} \int_{a \in \mathcal{A}} \left(\int_{b \in \mathcal{B}} P_{Y_1 | X_1}(b | a) \, db \right) |P_{X_1}(a) - P_{X_2}(a)| \, da \\ &= \frac{1}{2} \int_{a \in \mathcal{A}} |P_{X_1}(a) - P_{X_2}(a)| \, da \\ &= d_{TV}(P_{X_1}, P_{X_2}). \end{aligned}$$

Regarding the second term:

$$\begin{aligned} &\frac{1}{2} \int_{\mathcal{A} \times \mathcal{B}} P_{X_2}(a) |P_{Y_1 | X_1}(b | a) - P_{Y_2 | X_2}(b | a)| \, dadb \\ &= \int_{a \in \mathcal{A}} \left(\frac{1}{2} \int_{b \in \mathcal{B}} |P_{Y_1 | X_1}(b | a) - P_{Y_2 | X_2}(b | a)| \, db \right) P_{X_2}(a) \, da \\ &\leq \left(\sup_{a \in \mathcal{A}} d_{TV}(P_{Y_1 | X_1=a}, P_{Y_2 | X_2=a}) \right) \int_{a \in \mathcal{A}} P_{X_2}(a) \, da \\ &= \sup_{a \in \mathcal{A}} d_{TV}(P_{Y_1 | X_1=a}, P_{Y_2 | X_2=a}). \end{aligned}$$

The sum between the first and second upper bound gives the total variation chain rule. \square

An important consequence of Lemma E.6 is when the distributions being compared have natural independence structures.

Lemma E.7 (Product rule). *Let P_{X_1, Y_1} and P_{X_2, Y_2} be discrete distributions. In addition, suppose P_{X_1, Y_1} factorizes into $P_{X_1} P_{Y_1}$ and similarly $P_{X_2, Y_2} = P_{X_2} P_{Y_2}$. Then:*

$$d_{TV}(P_{X_1, Y_1}, P_{X_2, Y_2}) \leq d_{TV}(P_{X_1}, P_{X_2}) + d_{TV}(P_{Y_1}, P_{Y_2}).$$

Proof of Lemma E.7. Since P_{X_1, Y_1} and P_{X_2, Y_2} are discrete distributions, we can apply Lemma E.6 (the common measure is the counting measure). Because each joint distribution P_{X_i, Y_i} factorizes into $P_{X_i} P_{Y_i}$, for any $a \in \mathcal{A}$, the right most term in the inequality of Lemma E.6 simplifies into

$$\sup_{a \in \mathcal{A}} d_{TV}(P_{Y_1 | X_1=a}, P_{Y_2 | X_2=a}) = d_{TV}(P_{Y_1}, P_{Y_2}),$$

since $P_{Y_1} = P_{Y_1 | X_1=a}$ and $P_{Y_2} = P_{Y_2 | X_2=a}$ for any a . \square

We call the next lemma the propagation rule, which applies even if distributions do not have densities.

Lemma E.8 (Propagation rule). *Suppose P_{X_1, Y_1} and P_{X_2, Y_2} are two distributions over the same measurable space. Suppose that the conditional $Y_2 | X_2 = a$ is the same as the conditional $Y_1 | X_1 = a$, which we just denote as $Y | X = a$. Then:*

$$d_{TV}(P_{Y_1}, P_{Y_2}) \leq \inf_{\widehat{X}_1, \widehat{X}_2 \text{ coupling of } P_{X_1}, P_{X_2}} \mathbb{P}(\widehat{X}_1 \neq \widehat{X}_2).$$

If P_{X_1} and P_{X_2} are discrete distributions, we also have:

$$d_{TV}(P_{Y_1}, P_{Y_2}) \leq d_{TV}(P_{X_1}, P_{X_2}).$$

Proof of Lemma E.8. Let $(\widehat{X}_1, \widehat{X}_2)$ be any coupling of P_{X_1} and P_{X_2} . The following two-step process generates a coupling of P_{Y_1} and P_{Y_2} :

- Sample $(\widehat{X}_1, \widehat{X}_2)$.
- If $\widehat{X}_1 = \widehat{X}_2$, let the common value be x . Sample \widehat{Y}_1 from the conditional distribution $Y | X = x$, and set $\widehat{Y}_2 = \widehat{Y}_1$. Else if $\widehat{X}_1 \neq \widehat{X}_2$, independently sample \widehat{Y}_1 from $Y | X = \widehat{X}_1$ and \widehat{Y}_2 from $Y | X = \widehat{X}_2$.

It is easy to verify that the tuple $(\widehat{Y}_1, \widehat{Y}_2)$ is a coupling of P_{Y_1} and P_{Y_2} . In addition, $(\widehat{Y}_1, \widehat{Y}_2)$ has the property that

$$\mathbb{P}(\widehat{Y}_1 \neq \widehat{Y}_2, \widehat{X}_1 = \widehat{X}_2) = 0,$$

since conditioned on $\widehat{X}_1 = \widehat{X}_2$, the values of \widehat{Y}_1 and \widehat{Y}_2 always agree. Therefore:

$$\mathbb{P}(\widehat{Y}_1 \neq \widehat{Y}_2) = \mathbb{P}(\widehat{Y}_1 \neq \widehat{Y}_2, \widehat{X}_1 \neq \widehat{X}_2) \leq \mathbb{P}(\widehat{X}_1 \neq \widehat{X}_2).$$

This means that $d_{TV}(P_{Y_1}, P_{Y_2})$ is small:

$$d_{TV}(P_{Y_1}, P_{Y_2}) \leq \mathbb{P}(\widehat{X}_1 \neq \widehat{X}_2).$$

So far $(\widehat{X}_1, \widehat{X}_2)$ has been an arbitrary coupling between P_{X_1} and P_{X_2} . The final step is taking the infimum on the right hand side over couplings. When P_{X_1} and P_{X_2} are discrete distributions, the infimum over couplings is equal to the total variation distance. \square

The final lemma is the reduction rule, which says that the a larger collection of random variables, in general, has larger total variation distance than a smaller one.

Lemma E.9 (Reduction rule). *Suppose P_{X_1, Y_1} and P_{X_2, Y_2} are two distributions over the same measurable space $\mathcal{A} \times \mathcal{B}$. Then:*

$$d_{TV}(P_{X_1, Y_1}, P_{X_2, Y_2}) \geq d_{TV}(P_{X_1}, P_{X_2}).$$

Proof of Lemma E.9. By definition,

$$d_{TV}(P_{X_1}, P_{X_2}) = \sup_{\text{measurable } A} |P_{X_1}(A) - P_{X_2}(A)|.$$

For any measurable A , the product $A \times \mathcal{B}$ is also measurable. In addition:

$$P_{X_1}(A) - P_{X_2}(A) = P_{X_1, Y_1}(A, \mathcal{B}) - P_{X_2, Y_2}(A, \mathcal{B}).$$

Therefore, for any A ,

$$|P_{X_1}(A) - P_{X_2}(A)| \leq d_{TV}(P_{X_1, Y_1}, P_{X_2, Y_2}),$$

since $P_{X_1, Y_1}(A, \mathcal{B}) - P_{X_2, Y_2}(A, \mathcal{B})$ is the difference in probability mass for one measurable event. The final step is taking supremum of the left hand side. \square

E.3. Miscellaneous

Lemma E.10 (Order of growth of harmonic-like sums).

$$\alpha [\ln N + \ln(\alpha + 1) - \psi(\alpha)] \geq \sum_{n=1}^N \frac{\alpha}{n - 1 + \alpha} \geq \alpha(\ln N - \psi(\alpha) - 1).$$

where ψ is the digamma function.

Proof of Lemma E.10. Because of the digamma function identity $\psi(z + 1) = \psi(z) + 1/z$ for $z > 0$, we have:

$$\sum_{n=1}^N \frac{\alpha}{n - 1 + \alpha} = \alpha[\psi(\alpha + N) - \psi(\alpha)]$$

Gordon (1994, Theorem 5) says that

$$\psi(\alpha + N) \geq \ln(\alpha + N) - \frac{1}{2(\alpha + N)} - \frac{1}{12(\alpha + N)^2} \geq \ln N - 1.$$

Gordon (1994, Theorem 5) also says that

$$\psi(\alpha + N) \leq \ln(\alpha + N) \leq \ln((\alpha + 1)N) = \ln(1 + \alpha) + \ln N,$$

where it's a simple proof that $\alpha + N \leq \alpha N + N = (\alpha + 1)N$ when $\alpha > 0, N \geq 1$ \square

We list a collection of technical lemmas that are used when verifying Condition 1 for the recurring examples.

The first set assists in the beta-Bernoulli model.

- For $\alpha > 0$ and $i = 1, 2, 3, \dots$:

$$\frac{1}{i + \alpha - 1} \leq 2 \left(\frac{1}{2\alpha} \mathbf{1}\{i = 1\} + \frac{1}{i} \mathbf{1}\{i > 1\} \right). \quad (\text{E.3})$$

- For $m, x, y > 0$, $m \leq y$:

$$\left| \frac{m+x}{y+x} - \frac{m}{y} \right| \leq \frac{x}{y}. \quad (\text{E.4})$$

Proof of Eq. (E.3). If $i = 1$, $\frac{1}{i+\alpha-1} = \frac{1}{\alpha}$. If $i \geq 1$, $\frac{1}{i+\alpha-1} \leq \frac{1}{i-1} \leq \frac{2}{i}$. \square

Proof of Eq. (E.4).

$$\left| \frac{m+x}{y+x} - \frac{m}{y} \right| = \left| \frac{(m+x)y - m(y+x)}{y(y+x)} \right| = \left| \frac{x(y-m)}{y(y+x)} \right| \leq \frac{x}{y}.$$

\square

The second set aid in the gamma–Poisson model.

- For $x \in [0, 1)$;

$$(1-x) \ln(1-x) + x \geq 0. \quad (\text{E.5})$$

- For $x \in (0, 1)$, for $p \geq 0$:

$$(1-x)^p + p \frac{x}{1-x} \geq 1. \quad (\text{E.6})$$

- For $\lambda > 0$, for $m > 0, t > 1, x > 0$:

$$d_{TV}(\text{NB}(m, t^{-1}), \text{NB}(m+x, t^{-1})) \leq x \frac{1/t}{1-1/t}, \quad (\text{E.7})$$

where $\text{NB}(r, \theta)$ is the negative binomial distribution.

- For $y \in \mathbb{N}$, $K > m > 0$:

$$\left| \frac{m}{y} - K \frac{\Gamma(m/K + y)}{\Gamma(m/K) y!} \right| \leq e \frac{m^2}{K}. \quad (\text{E.8})$$

where e is the Euler constant and $\Gamma(y)$ is the gamma function.

Proof of Eq. (E.5). Set $g(x)$ to $(1-x) \ln(1-x) + x$. Then its derivative is $g'(x) = -\ln(1-x) \geq 0$, meaning the function is monotone increasing. Since $g(0) = 0$, it's true that $g(x) \geq 0$ over $[0, 1)$. \square

Proof of Eq. (E.6). Let $f(p) = (1-x)^p + p \frac{x}{1-x} - 1$. Then $f'(p) = \ln(1-x)(1-x)^p + \frac{x}{1-x}$. Also $f''(p) = (\ln(1-x))^2(1-x)^p > 0$. So $f'(p)$ is monotone increasing. At $p = 0$, $f'(0) = \ln(1-x) + \frac{x}{1-x} \geq 0$. Therefore $f'(p) \geq 0$ for all p . So $f(p)$ is increasing. Since $f(0) = 0$, it's true that $f(p) \geq 0$ for all p . \square

Proof of Eq. (E.7). It is known that $\text{NB}(r, \theta)$ is a Poisson stopped sum distribution ([Johnson, Kemp and Kotz, 2005](#), Equation 5.15):

- $N \sim \text{Poisson}(-r \ln(1-\theta))$.
- $Y_i \stackrel{i.i.d.}{\sim} \text{Log}(\theta)$ where the $\text{Log}(\theta)$ distribution's pmf at k equals $\frac{-\theta^k}{k \ln(1-\theta)}$.
- $\sum_{i=1}^N Y_i \sim \text{NB}(r, \theta)$.

Therefore, by the propagation rule Lemma E.8, to compare $\text{NB}(m, t^{-1})$ with $\text{NB}(m + x, t^{-1})$, it suffices to compare the two generating Poissons.

$$\begin{aligned} & d_{TV}(\text{NB}(m, t^{-1}), \text{NB}(m + x, t^{-1})) \\ & \leq d_{TV}(\text{Poisson}(-m \ln(1 - t^{-1}), \text{Poisson}(-(m + x) \ln(1 - t^{-1}))) \\ & \leq -\ln(1 - t^{-1})x \leq x \frac{t^{-1}}{1 - t^{-1}}. \end{aligned}$$

We have used the fact that total variation distance between Poissons is dominated by their different in means Lemma E.5 and Eq. (E.5). □

Proof of Eq. (E.8). Since $\Gamma\left(\frac{m}{K} + y\right) = \left(\prod_{j=0}^{y-1} \left(\frac{m}{K} + j\right)\right) \Gamma\left(\frac{m}{K}\right) = \Gamma\left(\frac{m}{K}\right) \frac{m}{K} \prod_{j=1}^{y-1} \left(\frac{m}{K} + j\right)$, we have:

$$\left| \frac{m}{y} - K \frac{\Gamma(m/K + y)}{\Gamma(m/K)y!} \right| = \frac{m}{y} \left(\prod_{j=1}^{y-1} \frac{m/K + j}{j} - 1 \right).$$

We inspect the product in more detail.

$$\begin{aligned} \prod_{j=1}^{y-1} \frac{m/K + j}{j} &= \prod_{j=1}^{y-1} \left(1 + \frac{m/K}{j} \right) \leq \prod_{j=1}^{y-1} \exp\left(\frac{m/K}{j}\right) \\ &= \exp\left(\frac{m}{K} \sum_{j=1}^{y-1} \frac{1}{j}\right) \leq \exp\left(\frac{m}{K} (\ln y + 1)\right) = (ey)^{m/K}. \end{aligned}$$

where the $(y - 1)$ -th Harmonic sum is bounded by $\ln y + 1$. Therefore

$$\left| \frac{m}{y} - K \frac{\Gamma(m/K + y)}{\Gamma(m/K)y!} \right| \leq \frac{m}{y} \left((ey)^{m/K} - 1 \right).$$

We quickly prove that for any $u \geq 1, 0 < a < 1$, we have

$$u^a - 1 \leq a(u - 1).$$

Truly, consider the function $g(u) = a(u - 1) - u^a + 1$. The derivative is $g'(u) = a - au^{a-1} = a(1 - u^{a-1})$. Since $a \in (0, 1)$ and $u \geq 1$, $g'(u) > 0$. Therefore $g(u)$ is monotone increasing. Since $g(1) = 0$, we have reached the conclusion. Applying to our situation:

$$(ey)^{m/K} - 1 \leq \frac{m}{K}(ey - 1).$$

In all:

$$\left| \frac{m}{y} - K \frac{\Gamma(m/K + y)}{\Gamma(m/K)y!} \right| \leq e \frac{m^2}{K}.$$

□

The third set aid in the beta-negative binomial model.

- For $x > 0, z \geq y > 1$:

$$B(x, y) - B(x, z) \leq (z - y)B(x + 1, y - 0.5) \leq (z - y)B(x + 1, y - 1). \quad (\text{E.9})$$

- For any $r > 0$, $b \geq 1$:

$$\sum_{y=1}^{\infty} \frac{\Gamma(y+r)}{y!\Gamma(r)} B(y, b+r) \leq \frac{r}{b-0.5}. \quad (\text{E.10})$$

- For $b \geq 1$, for any $c > 0$, for any $K \geq c$:

$$\left| 1 - \frac{\Gamma(b)}{\Gamma(b+c/K)} \right| \leq \frac{c}{K} (2 + \ln b). \quad (\text{E.11})$$

- For $b > 1$, $c > 0$, $K \geq 2c(\ln b + 2)$:

$$\left| c - \frac{K}{B(c/K, b)} \right| \leq \frac{c}{K} (3 \ln b + 8). \quad (\text{E.12})$$

Proof of Eq. (E.9). First we prove that for any $x \in [0, 1)$:

$$\sqrt{1-x} \ln(1-x) + x \geq 0.$$

Truly, let $g(x)$ be the function on the left hand side. Then its derivative is

$$g'(x) = \frac{2\sqrt{1-x} - \ln(1-x) - 2}{2\sqrt{1-x}}.$$

Denote the numerator function by $h(x)$. Its derivative is

$$h'(x) = \frac{1}{1-x} - \frac{1}{\sqrt{1-x}} \geq 0,$$

since $x \in [0, 1]$ meaning h is monotone increasing. Since $h(0) = 0$, it means $h(x) \geq 0$. This means $g'(x) \geq 0$ i.e. g itself is monotone increasing. Since $g(0) = 0$ it's true that $g(x) \geq 0$ for all $x \in [0, 1)$.

Second we prove that for all $x \in [0, 1]$, for all $p \geq 0$:

$$(1-x)^p + p \frac{x}{\sqrt{1-x}} - 1 \geq 0. \quad (\text{E.13})$$

Truly, let $f(p) = (1-x)^p + p \frac{x}{\sqrt{1-x}} - 1$. Then $f'(p) = \ln(1-x)(1-x)^p + \frac{x}{\sqrt{1-x}}$. Also $f''(p) = (\ln(1-x))^2(1-x)^p > 0$. So $f'(p)$ is monotone increasing. At $p = 0$, $f'(0) = \ln(1-x) + \frac{x}{\sqrt{1-x}} > 0$. Therefore $f'(p) \geq 0$ for all p . So $f(p)$ is increasing. Since $f(0) = 0$, it's true that $f(p) \geq 0$ for all p .

We finally prove the inequality about beta functions.

$$\begin{aligned} B(x, y) - B(x, z) &= \int_0^1 \theta^{x-1} (1-\theta)^{y-1} (1 - (1-\theta)^{z-y}) d\theta \\ &\leq \int_0^1 \theta^{x-1} (1-\theta)^{y-1} (z-y)\theta(1-\theta)^{-0.5} d\theta \\ &= (z-y) \int_0^1 \theta^x (1-\theta)^{y-1.5} d\theta = (z-y)B(x+1, y-0.5). \end{aligned}$$

where we have use $1 - (1-\theta)^{z-y} \leq (z-y)\theta(1-\theta)^{-1/2}$ from Eq. (E.13). As for $B(x+1, y-0.5) \leq B(x+1, y-1)$, it is because of the monotonicity of the beta function. \square

Proof of Eq. (E.10).

$$\begin{aligned}
\sum_{y=1}^{\infty} \frac{\Gamma(y+r)}{y!\Gamma(r)} B(y, b+r) &= \int_0^1 \sum_{y=1}^{\infty} \frac{\Gamma(y+r)}{y!\Gamma(r)} \theta^{y-1} (1-\theta)^{b+r-1} d\theta \\
&= \int_0^1 \theta^{-1} \left(\sum_{y=1}^{\infty} \frac{\Gamma(y+r)}{y!\Gamma(r)} \theta^y \right) (1-\theta)^{b+r-1} d\theta \\
&= \int_0^1 \left(\theta^{-1} \left(\frac{1}{(1-\theta)^r} - 1 \right) \right) (1-\theta)^{b+r-1} d\theta \\
&= \int_0^1 (\theta^{-1} (1 - (1-\theta)^r)) (1-\theta)^{b-1} d\theta \\
&\leq \int_0^1 \theta^{-1} r \frac{\theta}{\sqrt{1-\theta}} (1-\theta)^{b-1} d\theta \\
&= r \int_0^1 (1-\theta)^{b-1.5} d\theta = \frac{r}{b-0.5},
\end{aligned}$$

where the identity $\sum_{y=1}^{\infty} \frac{\Gamma(y+r)}{y!\Gamma(r)} \theta^y = \frac{1}{(1-\theta)^r} - 1$ is due to the normalization constant for negative binomial distributions, and we also used Eq. (E.13) on $1 - (1-\theta)^r$. \square

Proof of Eq. (E.11). First we prove that:

$$1 - \frac{\Gamma(b)}{\Gamma(b+c/K)} \leq \frac{c}{K} (2 + \ln b).$$

The recursion defining $\Gamma(b)$ allows us to write:

$$1 - \frac{\Gamma(b)}{\Gamma(b+c/K)} = 1 - \left(\prod_{i=1}^{\lfloor b \rfloor - 1} \frac{b-i}{b+c/K-i} \right) \frac{\Gamma(b - \lfloor b \rfloor + 1)}{\Gamma(b+c/K - \lfloor b \rfloor + 1)}.$$

The argument proceeds in one of two ways. If $\frac{\Gamma(b - \lfloor b \rfloor + 1)}{\Gamma(b+c/K - \lfloor b \rfloor + 1)} \geq 1$, then we have:

$$\begin{aligned}
1 - \frac{\Gamma(b)}{\Gamma(b+c/K)} &\leq 1 - \prod_{i=1}^{\lfloor b \rfloor - 1} \frac{b-i}{b+c/K-i} \\
&= \left(1 - \frac{b-1}{b+c/K-1} \right) + \frac{b-1}{b+c/K-1} - \left(\prod_{i=1}^{\lfloor b \rfloor - 1} \frac{b-i}{b+c/K-i} \right) \\
&= \frac{c}{K} \frac{1}{b+c/K-1} + \frac{b-1}{b+c/K-1} \left(1 - \prod_{i=2}^{\lfloor b \rfloor - 1} \frac{b-i}{b+c/K-i} \right) \\
&\leq \frac{c}{K} \frac{1}{b-1} + \left(1 - \prod_{i=2}^{\lfloor b \rfloor - 1} \frac{b-i}{b+c/K-i} \right) \\
&\leq \dots \leq \frac{c}{K} \sum_{i=1}^{\lfloor b \rfloor - 1} \frac{1}{b-i} \leq \frac{c}{K} (\ln b + 1).
\end{aligned}$$

Else, $\frac{\Gamma(b-\lfloor b \rfloor+1)}{\Gamma(b+c/K-\lfloor b \rfloor+1)} < 1$ and we write:

$$\begin{aligned} & 1 - \frac{\Gamma(b)}{\Gamma(b+c/K)} \\ &= 1 - \frac{\Gamma(b-\lfloor b \rfloor+1)}{\Gamma(b+c/K-\lfloor b \rfloor+1)} + \frac{\Gamma(b-\lfloor b \rfloor+1)}{\Gamma(b+c/K-\lfloor b \rfloor+1)} \left(1 - \prod_{i=1}^{\lfloor b \rfloor-1} \frac{b-i}{b+c/K-i} \right) \\ &\leq \left(1 - \frac{\Gamma(b-\lfloor b \rfloor+1)}{\Gamma(b+c/K-\lfloor b \rfloor+1)} \right) + \frac{c}{K}(\ln b + 1). \end{aligned}$$

We now argue that for all $x \in [1, 2)$, for all $K \geq c$, $1 - \frac{\Gamma(x)}{\Gamma(x+c/K)} \leq \frac{c}{K}$. By convexity of $\Gamma(x)$, we know that $\Gamma(x) \geq \Gamma(x+c/K) - \frac{c}{K}\Gamma'(x+c/K)$. Hence $\frac{\Gamma(x)}{\Gamma(x+c/K)} \geq 1 - \frac{c}{K} \frac{\Gamma'(x+c/K)}{\Gamma(x+c/K)}$. Since $x+c/K \in [1, 3)$ and $\psi(y) = \frac{\Gamma'(y)}{\Gamma(y)}$, the digamma function, is a monotone increasing function (it is the derivative of a $\ln \Gamma(x)$, which is also convex), $\left| \frac{\Gamma'(x+c/K)}{\Gamma(x+c/K)} \right| \leq \left| \frac{\Gamma'(3)}{\Gamma(3)} \right| \leq 1$. Applying this to $x = b - \lfloor b \rfloor + 1$, we conclude that:

$$1 - \frac{\Gamma(b)}{\Gamma(b+c/K)} \leq \frac{c}{K}(2 + \ln b).$$

We now show that:

$$\frac{\Gamma(b)}{\Gamma(b+c/K)} - 1 \geq -\frac{c}{K}(\ln b + \ln 2).$$

Convexity of $\Gamma(y)$ means that:

$$\Gamma(b) \geq \Gamma(b+c/K) - \frac{c}{K}\Gamma'(b+c/K) \rightarrow \frac{\Gamma(b)}{\Gamma(b+c/K)} - 1 \geq -\frac{c}{K} \frac{\Gamma'(b+c/K)}{\Gamma(b+c/K)}.$$

From Alzer (1997, Equation 2.2), we know that $\psi(x) \leq \ln(x)$ for positive x . Therefore:

$$-\frac{c}{K} \frac{\Gamma'(b+c/K)}{\Gamma(b+c/K)} \geq -\frac{c}{K} \ln(b+c/K) \geq -\frac{c}{K}(\ln b + \ln 2)$$

since $b + \frac{c}{K} \leq 2b$.

We combine two sides of the inequality to conclude that the absolute value is at most $\frac{c}{K}(2 + \ln b)$. \square

Proof of Eq. (E.12).

$$\begin{aligned} \left| c - \frac{K}{B(c/K, b)} \right| &= c \left| \frac{K/c}{\Gamma(c/K)} \frac{\Gamma(c/K+b)}{\Gamma(b)} - 1 \right| \\ &= c \left| \frac{K/c}{\Gamma(c/K)} \left(\frac{\Gamma(c/K+b)}{\Gamma(b)} - 1 \right) + \left(\frac{K/c}{\Gamma(c/K)} - 1 \right) \right| \\ &\leq c \left(\frac{K/c}{\Gamma(c/K)} \left| \frac{\Gamma(c/K+b)}{\Gamma(b)} - 1 \right| + \left| \frac{K/c}{\Gamma(c/K)} - 1 \right| \right). \end{aligned}$$

On the one hand:

$$\frac{K/c}{\Gamma(c/K)} = \frac{\Gamma(1)}{\Gamma(1+c/K)}.$$

From Eq. (E.11), we know:

$$\left| \frac{\Gamma(1)}{\Gamma(1 + c/K)} - 1 \right| \leq \frac{2c}{K}.$$

On the other hand, let $y = \Gamma(b)/\Gamma(c/K + b)$. Then:

$$\left| \frac{\Gamma(c/K + b)}{\Gamma(b)} - 1 \right| = \left| \frac{1}{y} - 1 \right| = \frac{|1 - y|}{y}.$$

Again using Eq. (E.11), $|1 - y| \leq \frac{c}{K}(2 + \ln b)$. Since $K \geq 2c(\ln b + 2)$, $\frac{c}{K}(2 + \ln b)$ is at most 0.5, meaning $|1 - y| \leq 0.5$ and $y \geq 0.5$. Therefore

$$\left| \frac{\Gamma(c/K + b)}{\Gamma(b)} - 1 \right| \leq \frac{2c}{K}(2 + \ln b).$$

In all:

$$\begin{aligned} \left| c - \frac{K}{B(c/K, b)} \right| &\leq c \left(\left(1 + \frac{2c}{K} \right) 2 \frac{c}{K} (2 + \ln b) + \frac{2c}{K} \right) \\ &\leq \frac{c}{K} (3 \ln b + 8). \end{aligned}$$

□

Appendix F: Verification of upper bound's assumptions for additional examples

Recall the definitions of h , \tilde{h} , and $M_{n,x}$ for exponential family CRM-likelihood in Appendix C.

F.1. Gamma-Poisson with zero discount

First we write down the functions in Condition 1 for non-power-law gamma-Poisson. This requires expressing the rate measure and likelihood in exponential-family form:

$$\ell(x | \theta) = \frac{1}{x!} \theta^x \exp(-\theta), \quad \nu(d\theta) = \gamma \lambda \theta^{-1} \exp(-\lambda \theta),$$

which means that $\kappa(x) = 1/x!$, $\phi(x) = x$, $\mu(\theta) = 0$, $A(\theta) = \theta$. This leads to the normalizer

$$Z = \int_0^\infty \theta^\xi \exp(-\lambda \theta) d\theta = \Gamma(\xi + 1) \lambda^{-(\xi+1)}.$$

Therefore, h is

$$\begin{aligned} h(x_n = x | x_{1:(n-1)}) &= \frac{1}{x!} \frac{\Gamma(-1 + \sum_{i=1}^{n-1} x_i + x + 1) (\lambda + n)^{-1 + \sum_{i=1}^{n-1} x_i + x + 1}}{\Gamma(-1 + \sum_{i=1}^{n-1} x_i + 1) (\lambda + n - 1)^{-1 + \sum_{i=1}^{n-1} x_i + 1}} \\ &= \frac{1}{x!} \frac{\Gamma(\sum_{i=1}^{n-1} x_i + x)}{\Gamma(\sum_{i=1}^{n-1} x_i)} \left(\frac{1}{\lambda + n} \right)^x \left(1 - \frac{1}{\lambda + n} \right)^{\sum_{i=1}^{n-1} x_i}, \end{aligned}$$

and similarly \tilde{h} is

$$\begin{aligned}\tilde{h}(x_n = x | x_{1:(n-1)}) &= \frac{1}{x!} \frac{\Gamma(-1 + \sum_{i=1}^{n-1} x_i + x + 1 + \gamma\lambda/K)(\lambda + n)^{-1 + \sum_{i=1}^{n-1} x_i + x + 1 + \gamma\lambda/K}}{\Gamma(-1 + \sum_{i=1}^{n-1} x_i + 1 + \gamma\lambda/K)(\lambda + n - 1)^{-1 + \sum_{i=1}^{n-1} x_i + 1 + \gamma\lambda/K}} \\ &= \frac{1}{x!} \frac{\Gamma(\sum_{i=1}^{n-1} x_i + x + \gamma\lambda/K)}{\Gamma(\sum_{i=1}^{n-1} x_i + \gamma\lambda/K)} \left(\frac{1}{\lambda + n}\right)^x \left(1 - \frac{1}{\lambda + n}\right)^{\sum_{i=1}^{n-1} x_i + \gamma\lambda/K},\end{aligned}$$

and $M_{n,x}$ is

$$M_{n,x} = \gamma\lambda \frac{1}{x!} \Gamma(x)(\lambda + n)^{-x} = \frac{\gamma\lambda}{x(\lambda + n)^x}.$$

Now, we state the constants so that gamma–Poisson satisfies Condition 1, and give the proof.

Proposition F.1 (Gamma–Poisson satisfies Condition 1). *The following hold for arbitrary $\gamma, \lambda > 0$. For any n :*

$$\begin{aligned}\sum_{x=1}^{\infty} M_{n,x} &\leq \frac{\gamma\lambda}{n-1+\lambda}, \\ \sum_{x=1}^{\infty} \tilde{h}(x | x_{1:(n-1)} = 0_{n-1}) &\leq \frac{\gamma\lambda}{n-1+\lambda}.\end{aligned}$$

For any K :

$$\sum_{x=0}^{\infty} \left| h(x | x_{1:(n-1)}) - \tilde{h}(x | x_{1:(n-1)}) \right| \leq \frac{2\gamma\lambda}{K} \frac{1}{n-1+\lambda}.$$

For any $K \geq \gamma\lambda$:

$$\sum_{x=1}^{\infty} \left| M_{n,x} - K\tilde{h}(x | x_{1:(n-1)} = 0_{n-1}) \right| \leq \frac{\gamma^2\lambda + e\gamma^2\lambda^2}{K} \frac{1}{n-1+\lambda}.$$

Proof of Proposition F.1. The growth rate condition of the target model is simple:

$$\sum_{x=1}^{\infty} M_{n,x} = \gamma\lambda \sum_{x=1}^{\infty} \frac{1}{x(\lambda + n)^x} \leq \gamma\lambda \sum_{x=1}^{\infty} \frac{1}{(\lambda + n)^x} = \frac{\gamma\lambda}{n-1+\lambda}.$$

The growth rate condition of the approximate model is also simple:

$$\begin{aligned}\sum_{x=1}^{\infty} \tilde{h}(x | x_{1:(n-1)} = 0_{n-1}) &= 1 - \tilde{h}(0 | x_{1:(n-1)} = 0_{n-1}) = 1 - \left(1 - \frac{1}{\lambda + n}\right)^{\gamma\lambda/K} \\ &\leq \frac{\gamma\lambda}{K} \frac{(\lambda + n)^{-1}}{1 - (\lambda + n)^{-1}} = \frac{1}{K} \frac{\gamma\lambda}{n-1+\lambda},\end{aligned}$$

where we have used Eq. (E.6) with $p = \frac{\gamma\lambda}{K}$, $x = (\lambda + n)^{-1}$.

For the total variation between h and \tilde{h} condition, observe that h and \tilde{h} are p.m.f.'s of negative binomial distributions, namely:

$$\begin{aligned}h(x | x_{1:(n-1)}) &= \text{NB} \left(x \mid \sum_{i=1}^{n-1} x_i, (\lambda + n)^{-1} \right), \\ \tilde{h}(x | x_{1:(n-1)}) &= \text{NB} \left(x \mid \sum_{i=1}^{n-1} x_i + \gamma\lambda/K, (\lambda + n)^{-1} \right).\end{aligned}$$

The two negative binomial distributions have the same success probability and only differ in the number of trials. Hence using Eq. (E.7), we have:

$$\sum_{x=0}^{\infty} \left| h(x | x_{1:(n-1)}) - \tilde{h}(x | x_{1:(n-1)}) \right| \leq 2 \frac{\gamma\lambda}{K} \frac{(\lambda+n)^{-1}}{1 - (\lambda+n)^{-1}} = \frac{2\gamma\lambda}{K} \frac{1}{n-1+\lambda},$$

where the factor 2 reflects how total variation distance is 1/2 the L_1 distance between p.m.f's.

For the total variation between $M_{n,\cdot}$ and $K\tilde{h}(\cdot | 0)$ condition,

$$\begin{aligned} & \sum_{x=1}^{\infty} \left| M_{n,x} - K\tilde{h}(x | x_{1:(n-1)} = 0_{n-1}) \right| \\ &= \sum_{x=1}^{\infty} \frac{1}{(\lambda+n)^x} \left| \frac{\gamma\lambda}{x} - K \frac{\Gamma(\gamma\lambda/K + x)}{\Gamma(\gamma\lambda/K)x!} \left(1 - \frac{1}{\lambda+n}\right)^{\gamma\lambda/K} \right| \\ &\leq \sum_{x=1}^{\infty} \frac{1}{(\lambda+n)^x} \left(\left| \frac{\gamma\lambda}{x} \left(1 - \left(1 - \frac{1}{\lambda+n}\right)^{\gamma\lambda/K}\right) \right| + \left| \frac{\gamma\lambda}{x} - K \frac{\Gamma(\gamma\lambda/K + x)}{\Gamma(\gamma\lambda/K)x!} \right| \right). \end{aligned}$$

Using Eq. (E.7) we can upper bound:

$$1 - \left(1 - \frac{1}{\lambda+n}\right)^{\gamma\lambda/K} \leq \frac{\gamma\lambda}{K} \frac{1}{\lambda+n-1},$$

while Eq. (E.8) gives the upper bound:

$$\left| \frac{\gamma\lambda}{x} - K \frac{\Gamma(\gamma\lambda/K + x)}{\Gamma(\gamma\lambda/K)x!} \right| \leq \frac{e\gamma^2\lambda^2}{K}.$$

This means:

$$\begin{aligned} & \sum_{x=1}^{\infty} \left| M_{n,x} - K\tilde{h}(x | x_{1:(n-1)} = 0_{n-1}) \right| \\ &\leq \sum_{x=1}^{\infty} \frac{1}{(\lambda+n)^x} \frac{\gamma\lambda}{x} \frac{\gamma\lambda}{K} \frac{1}{\lambda+n-1} + \sum_{x=1}^{\infty} \frac{1}{(\lambda+n)^x} \frac{e\gamma^2\lambda^2}{K} \\ &\leq \frac{\gamma^2\lambda^2}{K} \frac{1}{(\lambda+n-1)^2} + \frac{e\gamma^2\lambda^2}{K} \frac{1}{\lambda+n-1} \\ &\leq \frac{\gamma^2\lambda + e\gamma^2\lambda^2}{K} \frac{1}{n-1+\lambda}. \end{aligned}$$

□

F.2. Beta-negative binomial with zero discount

First we write down the functions in Condition 1 for non-power-law beta-negative binomial. This requires expressing the rate measure and likelihood in exponential-family form:

$$\begin{aligned} \ell(x | \theta) &= \frac{\Gamma(x+r)}{x!\Gamma(r)} \theta^x \exp(r \ln(1-\theta)), \\ \nu(d\theta) &= \gamma\alpha\theta^{-1} \exp(\ln(1-\theta)(\alpha-1)) \mathbf{1}\{\theta \leq 1\}, \end{aligned}$$

which means that $\kappa(x) = \Gamma(x+r)/\Gamma(r)x!$, $\phi(x) = x$, $\mu(\theta) = 0$, $A(\theta) = -r \ln(1-\theta)$. This leads to the normalizer:

$$Z = \int_0^1 \theta^\xi (1-\theta)^{r\lambda} d\theta = B(\xi+1, r\lambda+1).$$

To match the parametrizations, we need to set $\lambda = \frac{\alpha-1}{r}$ i.e. $r\lambda = \alpha-1$. Therefore, h is

$$h(x_n = x | x_{1:(n-1)}) = \frac{\Gamma(x+r)}{x!\Gamma(r)} \frac{B(\sum_{i=1}^{n-1} x_i + x, rn + \alpha)}{B(\sum_{i=1}^{n-1} x_i, r(n-1) + \alpha)},$$

and \tilde{h} is

$$\tilde{h}(x_n = x | x_{1:(n-1)}) = \frac{\Gamma(x+r)}{x!\Gamma(r)} \frac{B(\gamma\alpha/K + \sum_{i=1}^{n-1} x_i + x, rn + \alpha)}{B(\gamma\alpha/K + \sum_{i=1}^{n-1} x_i, r(n-1) + \alpha)},$$

and $M_{n,x}$ is

$$M_{n,x} = \gamma\alpha \frac{\Gamma(x+r)}{x!\Gamma(r)} B(x, rn + \alpha).$$

Now, we state the constants so that beta-negative binomial satisfies Condition 1, and give the proof.

Proposition F.2 (Beta-negative binomial satisfies Condition 1). *The following hold for any $\gamma > 0$ and $\alpha > 1$. For any n :*

$$\sum_{x=1}^{\infty} M_{n,x} \leq \frac{\gamma\alpha}{n-1 + (\alpha-0.5)/r}.$$

For any n , any K :

$$\sum_{x=1}^{\infty} \tilde{h}(x | x_{1:(n-1)} = 0_{n-1}) \leq \frac{1}{K} \frac{4\gamma\alpha}{n-1 + (\alpha-0.5)/r}.$$

For any K :

$$\sum_{x=0}^{\infty} \left| h(x | x_{1:(n-1)}) - \tilde{h}(x | x_{1:(n-1)}) \right| \leq 2 \frac{\gamma\alpha}{K} \frac{1}{n-1 + \alpha/r}.$$

For any n , for $K \geq \gamma\alpha(3 \ln(r(n-1) + \alpha) + 8)$:

$$\begin{aligned} & \sum_{x=1}^{\infty} \left| M_{n,x} - K \tilde{h}(x | x_{1:(n-1)} = 0_{n-1}) \right| \\ & \leq \frac{\gamma\alpha}{K} \frac{(4\gamma\alpha + 3) \ln(rn + \alpha + 1) + (10 + 2r)\gamma\alpha + 24}{n-1 + (\alpha-0.5)/r}. \end{aligned}$$

Proof of Proposition F.2. The growth rate condition for the target model is easy to verify:

$$\sum_{x=1}^{\infty} M_{n,x} = \gamma\alpha \sum_{x=1}^{\infty} \frac{\Gamma(x+r)}{\Gamma(r)x!} B(x, rn + \alpha) \leq \gamma\alpha \frac{r}{r(n-1) + \alpha - 0.5},$$

where we have used Eq. (E.10) with $b = r(n-1) + \alpha$.

As for the growth rate condition of the approximate model,

$$\begin{aligned} \sum_{x=1}^{\infty} \tilde{h}(x | x_{1:(n-1)} = 0_{n-1}) &= 1 - \tilde{h}(0 | x_{1:(n-1)} = 0_{n-1}) = 1 - \frac{B(\gamma\alpha/K, rn + \alpha)}{B(\gamma\alpha/K, r(n-1) + \alpha)} \\ &= \frac{B(\gamma\alpha/K, r(n-1) + \alpha) - B(\gamma\alpha/K, rn + \alpha)}{B(\gamma\alpha/K, r(n-1) + \alpha)}. \end{aligned}$$

The numerator is small because of Eq. (E.9) where $x = \gamma\alpha/K, y = r(n-1) + \alpha, z = rn + \alpha$:

$$\begin{aligned} B(\gamma\alpha/K, r(n-1) + \alpha) - B(\gamma\alpha/K, rn + \alpha) &\leq rB(\gamma\alpha/K + 1, r(n-1) + \alpha - 0.5) \\ &\leq rB(1, r(n-1) + \alpha - 0.5) \\ &= \frac{1}{n-1 + (\alpha - 0.5)/r}. \end{aligned}$$

The denominator is large because Eq. (E.12) with Eq. (E.12) with $c = \gamma\alpha, b = r(n-1) + \alpha$:

$$\frac{1}{B(\gamma\alpha/K, r(n-1) + \alpha)} \leq \frac{4\gamma\alpha}{K}.$$

Combining the two give yields

$$\sum_{x=1}^{\infty} \tilde{h}(x | x_{1:(n-1)} = 0_{n-1}) \leq \frac{1}{K} \frac{4\gamma\alpha}{n-1 + (\alpha - 0.5)/r}.$$

For the total variation between h and \tilde{h} condition, we first discuss how each function can be expressed a p.m.f. of so-called beta negative binomial i.e., BNB (Johnson, Kemp and Kotz, 2005, Section 6.2.3) distribution. Let $A = \sum_{i=1}^{n-1} x_i$. Observe that:

$$\frac{\Gamma(x+r)}{\Gamma(r)x!} \frac{B(A+x, rn+\alpha)}{B(A, r(n-1)+\alpha)} = \frac{\Gamma(A+r)}{\Gamma(A)x!} \frac{B(r+x, A+r(n-1)+\alpha)}{B(r, r(n-1)+\alpha)}. \quad (\text{F.1})$$

The random variable V_1 whose p.m.f at x appears on the right hand side of Eq. (F.1) is the result of a two-step sampling procedure:

$$P \sim \text{Beta}(r, r(n-1) + \alpha), \quad V_1 | P \sim \text{NB}(A; P).$$

We denote such a distribution as $V_1 \sim \text{BNB}(A; r, r(n-1) + \alpha)$. An analogous argument applies to \tilde{h} :

$$P \sim \text{Beta}(r, r(n-1) + \alpha), \quad V_2 | P \sim \text{NB}\left(A + \frac{\gamma\alpha}{K}; P\right).$$

Therefore:

$$\begin{aligned} h(x | x_{1:(n-1)}) &= \text{BNB}(x | A; r, r(n-1) + \alpha) \\ \tilde{h}(x | x_{1:(n-1)}) &= \text{BNB}\left(x | A + \frac{\gamma\alpha}{K}; r, r(n-1) + \alpha\right). \end{aligned}$$

We now bound the total variation between the BNB distributions. Because they have a common mixing distribution, we can upper bound the distance with an integral using simple

triangle inequalities:

$$\begin{aligned}
d_{\text{TV}}(h, \tilde{h}) &= \frac{1}{2} \sum_{x=0}^{\infty} |\mathbb{P}(V_1 = x) - \mathbb{P}(V_2 = x)| \\
&= \frac{1}{2} \sum_{x=0}^{\infty} \left| \int_0^1 (\mathbb{P}(V_1 = x | P = p) - \mathbb{P}(V_2 = x | P = p)) \mathbb{P}(P \in dp) \right| \\
&\leq \int_0^1 \left(\frac{1}{2} \sum_{x=0}^{\infty} |\mathbb{P}(V_1 = x | P = p) - \mathbb{P}(V_2 = x | P = p)| \right) \mathbb{P}(P \in dp) \\
&= \int_0^1 d_{\text{TV}}(\text{NB}(A, p), \text{NB}(A + \gamma\alpha/K, p)) \mathbb{P}(P \in dp).
\end{aligned}$$

For any p , we use Eq. (E.7) to upper bound the total variation distance between negative binomial distributions. Therefore:

$$\begin{aligned}
d_{\text{TV}}(h, \tilde{h}) &\leq \int_0^1 \frac{\gamma\alpha}{K} \frac{p}{1-p} \mathbb{P}(P \in dp) \\
&= \frac{\gamma\alpha}{K} \frac{1}{B(r, r(n-1) + \alpha)} \int_0^1 p^r (1-p)^{r(n-1) + \alpha - 2} dp \\
&= \frac{\gamma\alpha}{K} \frac{B(r+1, r(n-1) + \alpha - 1)}{B(r, r(n-1) + \alpha)} = \frac{\gamma\alpha}{K} \frac{1}{n-1 + \alpha/r}.
\end{aligned}$$

Finally, we verify the condition between $K\tilde{h}$ and $M_{n,\cdot}$, which is showing that the following sum is small:

$$\sum_{x=1}^{\infty} \frac{\Gamma(x+r)}{x! \Gamma(r)} \left| \gamma\alpha B(x, rn + \alpha) - K \frac{B(\gamma\alpha/K + x, rn + \alpha)}{B(\gamma\alpha/K, r(n-1) + \alpha)} \right|.$$

We look at the summand for $x = 1$ and the summation from $x = 2$ through ∞ separately. For $x = 1$, we prove that:

$$\frac{\Gamma(r+1)}{\Gamma(r)} \left| \gamma\alpha B(1, rn + \alpha) - K \frac{B(\gamma\alpha/K + 1, rn + \alpha)}{B(\gamma\alpha/K, r(n-1) + \alpha)} \right| \leq \frac{4r\gamma^2\alpha^2}{K} \frac{2 + \ln(rn + \alpha + 1)}{rn + \alpha}. \quad (\text{F.2})$$

Expanding gives:

$$\begin{aligned}
&\left| \gamma\alpha B(1, rn + \alpha) - K \frac{B(1 + \gamma\alpha/K, rn + \alpha)}{B(\gamma\alpha/K, r(n-1) + \alpha)} \right| \\
&= \frac{|\gamma\alpha B(1, rn + \alpha) B(\gamma\alpha/K, r(n-1) + \alpha) - KB(1 + \gamma\alpha/K, rn + \alpha)|}{B(\gamma\alpha/K, r(n-1) + \alpha)}. \quad (\text{F.3})
\end{aligned}$$

We look at the numerator of the right hand side in Eq. (F.3):

$$\begin{aligned}
&\left| \gamma\alpha B(1, rn + \alpha) \frac{\Gamma(\gamma\alpha/K) \Gamma(r(n-1) + \alpha)}{\Gamma(\gamma\alpha/K + r(n-1) + \alpha)} - K \frac{\Gamma(1 + \gamma\alpha/K) \Gamma(rn + \alpha)}{\Gamma(1 + \gamma\alpha/K + rn + \alpha)} \right| \\
&= \gamma\alpha \Gamma(\gamma\alpha/K) \left| \frac{1}{rn + \alpha} \frac{\Gamma(r(n-1) + \alpha)}{\Gamma(\gamma\alpha/K + r(n-1) + \alpha)} - \frac{\Gamma(rn + \alpha)}{\Gamma(\gamma\alpha/K + 1 + rn + \alpha)} \right|
\end{aligned}$$

$$\begin{aligned}
&= \frac{\gamma\alpha\Gamma(\gamma\alpha/K)}{rn+\alpha} \left| \frac{\Gamma(r(n-1)+\alpha)}{\Gamma(\gamma\alpha/K+r(n-1)+\alpha)} - \frac{\Gamma(rn+\alpha+1)}{\Gamma(\gamma\alpha/K+1+rn+\alpha)} \right| \\
&\leq \frac{\gamma\alpha\Gamma(\gamma\alpha/K)}{rn+\alpha} \left(\left| \frac{\Gamma(r(n-1)+\alpha)}{\Gamma(\gamma\alpha/K+r(n-1)+\alpha)} - 1 \right| + \left| \frac{\Gamma(rn+\alpha+1)}{\Gamma(\gamma\alpha/K+1+rn+\alpha)} - 1 \right| \right) \\
&\leq \frac{\gamma\alpha\Gamma(\gamma\alpha/K)}{rn+\alpha} \frac{2\gamma\alpha}{K} (2 + \ln(rn+\alpha+1)),
\end{aligned}$$

where we have used Eq. (E.11) with $c = \gamma\alpha$ and $b = r(n-1) + \alpha$ or $b = rn + \alpha + 1$. In all, Eq. (F.3) is upper bounded by:

$$\begin{aligned}
&\frac{2\gamma^2\alpha^2}{rn+\alpha} \frac{2 + \ln(rn+\alpha+1)}{K} \frac{\Gamma(\gamma\alpha/K)}{B(\gamma\alpha/K, r(n-1)+\alpha)} \\
&= \frac{2\gamma^2\alpha^2}{rn+\alpha} \frac{2 + \ln(rn+\alpha+1)}{K} \frac{\Gamma(\gamma\alpha/K+r(n-1)+\alpha)}{\Gamma(r(n-1)+\alpha)} \\
&\leq \frac{4\gamma^2\alpha^2}{K} \frac{2 + \ln(rn+\alpha+1)}{rn+\alpha},
\end{aligned}$$

since $\frac{\Gamma(r(n-1)+\alpha)}{\Gamma(r(n-1)+\alpha+\gamma\alpha/K)} \geq 1 - \frac{\gamma\alpha}{K} (2 + \ln(r(n-1)+\alpha)) \geq 0.5$ with $K \geq 2\gamma\alpha(2 + \ln(r(n-1)+\alpha))$. Combining with $\Gamma(r+1)/\Gamma(r) = r$, this is the proof of Eq. (F.2).

We now move onto the summands from $x = 2$ to ∞ . By triangle inequality:

$$\left| \gamma\alpha B(x, rn+\alpha) - K \frac{B(\gamma\alpha/K+x, rn+\alpha)}{B(\gamma\alpha/K, r(n-1)+\alpha)} \right| \leq T_1(x) + T_2(x),$$

where:

$$\begin{aligned}
T_1(x) &:= B(x, rn+\alpha) \left| \gamma\alpha - \frac{K}{B(\gamma\alpha/K, r(n-1)+\alpha)} \right|, \\
T_2(x) &:= K \frac{|B(x, rn+\alpha) - B(\frac{\gamma\alpha}{K} + x, rn+\alpha)|}{B(\gamma\alpha/K, r(n-1)+\alpha)}.
\end{aligned}$$

The helper inequalities we have proven once again are useful:

$$\begin{aligned}
\left| \gamma\alpha - \frac{K}{B(\gamma\alpha/K, r(n-1)+\alpha)} \right| &\leq \frac{\gamma\alpha}{K} (3\ln(r(n-1)+\alpha) + 8) \\
\frac{K}{B(\gamma\alpha/K, r(n-1)+\alpha)} &\leq \gamma\alpha + \frac{\gamma\alpha}{K} (3\ln(r(n-1)+\alpha) + 8) \leq 2\gamma\alpha, \\
|B(x, rn+\alpha) - B(\gamma\alpha/K+x, rn+\alpha)| &\leq \frac{\gamma\alpha}{K} B(x-1, rn+\alpha+1)
\end{aligned}$$

since $K \geq \gamma\alpha(3\ln(r(n-1)+\alpha) + 8)$, we have applied Eq. (E.12) in the first and second inequality and Eq. (E.9) in the third one. So for each $x \geq 2$, each summand is at most

$$\begin{aligned}
&\frac{\gamma\alpha(3\ln(r(n-1)+\alpha) + 8)}{K} \frac{\Gamma(x+r)}{x!\Gamma(r)} B(x, rn+\alpha) \\
&+ \frac{2\gamma^2\alpha^2}{K} \frac{\Gamma(x+r)}{x!\Gamma(r)} B(x-1, rn+\alpha+1).
\end{aligned}$$

To upper bound the summation from $x = 2$ to ∞ , it suffices to bound:

$$\sum_{x=2}^{\infty} \frac{\Gamma(x+r)}{\Gamma(r)x!} B(x, rn+\alpha) \leq \sum_{x=1}^{\infty} \frac{\Gamma(x+r)}{\Gamma(r)x!} B(x, rn+\alpha) \leq \frac{r}{r(n-1)+\alpha-0.5},$$

and:

$$\begin{aligned} \sum_{x=2}^{\infty} \frac{\Gamma(x+r)}{\Gamma(r)x!} B(x-1, rn+\alpha+1) &\leq r \sum_{x=2}^{\infty} \frac{\Gamma(x-1+r+1)}{\Gamma(r+1)(x-1)!} B(x-1, rn+\alpha+1) \\ &\leq r \sum_{z=1}^{\infty} \frac{\Gamma(z+r+1)}{\Gamma(r+1)z!} B(z, rn+\alpha+1) \\ &\leq \frac{r(r+1)}{r(n-1)+\alpha-0.5}, \end{aligned}$$

where we have used Eq. (E.10) in each upper bound. So the summation from $x = 2$ to ∞ is upper bounded by:

$$\frac{\gamma\alpha(3\ln(r(n-1)+\alpha)+8)}{K} \frac{r}{r(n-1)+\alpha-0.5} + \frac{2\gamma^2\alpha^2}{K} \frac{r(r+1)}{r(n-1)+\alpha-0.5} \quad (\text{F.4})$$

Eqs. (F.2) and (F.4) combine to give:

$$\begin{aligned} &\sum_{x=1}^{\infty} \left| M_{n,x} - K\tilde{h}(x \mid x_{1:(n-1)} = 0_{n-1}) \right| \\ &\leq \frac{\gamma\alpha(4\gamma\alpha+3)\ln(rn+\alpha+1) + (10+2r)\gamma\alpha + 24}{K(n-1+(\alpha-0.5)/r)}. \end{aligned}$$

□

Appendix G: Proofs of CRM bounds

G.1. Upper bound

Proof of Theorem 4.1. We first give explicit formulas for the constants C' , C'' , C''' , C'''' . Let β be the smallest positive constant where $\beta^2/(1+\beta) \geq 4/C_1$. Such constant exists because $\beta^2/(1+\beta)$ is an increasing function. The constants are

$$\begin{aligned} C' &= (\beta+1)C_1 \ln(1+1/C_1) [4C_1 \ln(1+1/C_1) + C_5] \\ &\quad + C_1^2 \psi_1(C_1) + \exp(2C_1(\psi(C_1)+1)) \\ &\quad + (\beta+1)2C_1 \ln(1+1/C_1) + C_2C_3, \end{aligned}$$

and

$$\begin{aligned} C'' &= (\beta+1)C_1(2C_1+C_4) + [(\beta+1)C_1+C_2]/\ln 2 \\ &\quad + (\beta+1)[C_1(4C_1 \ln(1+1/C_1) + C_5) + (2C_1+C_4)C_1 \ln(1+1/C_1)]/\ln 2, \end{aligned}$$

and

$$\begin{aligned} C''' &= (\beta+1)2C_1^2 \ln(1+1/C_1), \\ C'''' &= (\beta+1)2C_1^2 \ln(1+1/C_1) + (\beta+1)C_1. \end{aligned}$$

By the end of the proof, the reasoning for these constants will be clear.

We will focus on the case where the approximation level K is $\Omega(\ln N)$:

$$K \geq \max \{(\beta + 1) \max(C(K, C_1), C(N, C_1)), C_2(\ln N + C_3)\}, \quad (\text{G.1})$$

where $C(N, \alpha)$ is the growth function from Eq. (18). To see why it is sufficient, consider the case where $K < \max \{(\beta + 1) \max(C(K, C_1), C(N, C_1)), C_2(\ln N + C_3)\}$. This implies that K is smaller than a sum

$$\begin{aligned} K &< (\beta + 1)(C(N, C_1) + C(K, C_1)) + C_2(\ln N + C_3) \\ &\leq [(\beta + 1)C_1 + C_2] \ln N + (\beta + 1)C_1 \ln K + (\beta + 1)2C_1 \ln(1 + 1/C_1) + C_2C_3 \end{aligned}$$

where we have used upper bound on the growth function from Lemma E.10. Total variation distance is always upper bounded by 1. Hence, $d_{\text{TV}}(P_{N,\infty}, P_{N,K})$ is at most

$$\frac{[(\beta + 1)C_1 + C_2] \ln N + (\beta + 1)C_1 \ln K + (\beta + 1)2C_1 \ln(1 + 1/C_1) + C_2C_3}{K}$$

which is smaller than

$$\frac{\hat{C}^{(0)} + \hat{C}^{(1)} \ln^2 N + \hat{C}^{(2)} \ln K}{K} \quad (\text{G.2})$$

where

$$\begin{aligned} \hat{C}^{(0)} &= (\beta + 1)2C_1 \ln(1 + 1/C_1) + C_2C_3, \\ \hat{C}^{(1)} &= [(\beta + 1)C_1 + C_2] / \ln 2, \\ \hat{C}^{(2)} &= (\beta + 1)C_1. \end{aligned}$$

In the sequel, we will only consider the situation in Eq. (G.1).

First, we argue that it suffices to bound the total variation distance between the *trait-allocation matrices* coming from the target model and the approximate model. Given the latent measures X_1, X_2, \dots, X_N from the target model, we can read off the feature-allocation matrix F , which has N rows and as many columns as there are unique atom locations among the X_i 's:

1. The i -th row of F records the atom sizes of X_i .
2. Each column corresponds to an atom location: the locations are sorted first according to the index of the first measure X_i to manifest it (counting from 1, 2, ...), and then its atom size in X_i .

For illustration, suppose $X_1 = 3\delta_{\psi_1} + 4\delta_{\psi_2} + 4\delta_{\psi_3}$, $X_2 = 2\delta_{\psi_1} + \delta_{\psi_3} + \delta_{\psi_4} + 2\delta_{\psi_5}$ and $X_3 = 6\delta_{\psi_2} + 2\delta_{\psi_3} + \delta_{\psi_5} + 2\delta_{\psi_6} + 3\delta_{\psi_7}$. Then the associate trait-allocation matrix has 3 rows and 7 columns and has entries equal to

$$\begin{bmatrix} 3 & 4 & 4 & 0 & 0 & 0 & 0 \\ 2 & 0 & 1 & 1 & 2 & 0 & 0 \\ 0 & 6 & 2 & 0 & 1 & 2 & 3 \end{bmatrix}. \quad (\text{G.3})$$

The marginal process that described the atom sizes of $X_n | X_{n-1}, X_{n-2}, \dots, X_1$ in Proposition C.1 is also the description of how the rows of F are generated. The joint distribution X_1, X_2, \dots, X_n can be two-step sampled. First, the trait-allocation matrix F is sampled. Then, the atom locations are drawn iid from the base measure H : each column of F is assigned an atom location, and the latent measure X_i has atom size $F_{i,j}$ on the j th atom

location. A similar two-step sampling generates Z_1, Z_2, \dots, Z_n , the latent measures under the approximate model: the distribution over the feature-allocation matrix F' follows Proposition C.2 instead of Proposition C.1, but conditioned on the feature-allocation matrix, the process generating atom locations and constructing latent measures is exactly the same. In other words, this implies that the conditional distributions $Y_{1:N} | F$ and $W_{1:N} | F'$ when $F = F'$ are the same, since both models have the same the observational likelihood f given the latent measures 1 through N . Denote P_F to be the distribution of the feature-allocation matrix under the target model, and $P_{F'}$ the distribution of the feature-allocation matrix under the approximate model. Lemma E.8 implies that

$$d_{\text{TV}}(P_{N,\infty}, P_{N,K}) \leq \inf_{F, F' \text{ coupling of } P_F, P_{F'}} \mathbb{P}(F \neq F'). \quad (\text{G.4})$$

Next, we parametrize the trait-allocation matrices in a way that is convenient for the analysis of total variation distance. Let J be the number of columns of F . Our parametrization involves $d_{n,x}$, for $n \in [N]$ and $x \in \mathbb{N}$, and s_j , for $j \in [J]$:

1. For $n = 1, 2, \dots, N$:
 - (a) If $n = 1$, for each $x \in \mathbb{N}$, $d_{1,x}$ counts the number of columns j where $F_{1,j} = x$.
 - (b) For $n \geq 2$, for each $x \in \mathbb{N}$, let $J_n = \{j : \forall i < n, F_{i,j} = 0\}$ i.e. no observation before n manifests the atom locations indexed by columns in J_n . For each $x \in \mathbb{N}$, $d_{n,x}$ counts the number of columns $j \in J_n$ where $F_{n,j} = x$.
2. For $j = 1, 2, \dots, J$, let $I_j = \min\{i : F_{i,j} > 0\}$ i.e. the first row to manifest the j -th atom location. Let $s_j = F_{I_j:N,j}$ i.e. the history of the j -th atom location.

In words, $d_{n,x}$ is the number of atom locations that is first instantiated by the individual n and each atom has size x , while s_j is the history of the j -th atom location. $\sum_{n=1}^N \sum_{x=1}^{\infty} d_{n,x}$ is exactly J , the number of columns. For the example in Eq. (G.3):

1. For $n = 1, 2, \dots, 3$:
 - (a) For $n = 1$, $d_{1,1} = d_{1,2} = d_{1,j} = 0$ for $j > 4$. $d_{1,3} = 1$, $d_{1,4} = 2$.
 - (b) For $n = 2$, $d_{2,1} = 1$, $d_{2,2} = 1$, $d_{2,j} = 0$ for $j > 2$.
 - (c) For $n = 3$, $d_{3,1} = 0$, $d_{3,2} = 1$, $d_{3,3} = 1$, $d_{3,j} = 0$ for $j > 3$.
2. For $j = 1, 2, \dots, 7$, $s_1 = [3, 2, 0]$, $s_2 = [4, 0, 6]$, $s_3 = [4, 1, 2]$, $s_4 = [1, 0]$, $s_5 = [2, 1]$, $s_6 = [2]$, $s_7 = [3]$.

We use the short-hand d to refer to the collection of $d_{n,x}$ and s the collection of s_j . There is a one-to-one mapping between (d, s) and the trait-allocation matrix f , since we can read-off (d, s) from f and use (d, s) to reconstruct f . Let (D, S) be the distribution of d and s under the target model, while (D', S') is the distribution under the approximate model. We have that

$$d_{\text{TV}}(P_{N,\infty}, P_{N,K}) \leq \inf_{(D,S),(D',S') \text{ coupling of } P_{D,S}, P_{D',S'}} \mathbb{P}((D, S) \neq (D', S')).$$

To find an upper bound on $d_{\text{TV}}(P_{N,\infty}, P_{N,K})$, we will demonstrate a joint distribution such that $\mathbb{P}((D, S) \neq (D', S'))$ is small. The rest of the proof is dedicated to that end. To start, we only assume that (D, S, D', S') is a proper coupling, in that marginally $(D, S) \sim P_{D,S}$ and $(D', S') \sim P_{D',S'}$. As we progress, gradually more structure is added to the joint distribution (D, S, D', S') to control $\mathbb{P}((D, S) \neq (D', S'))$.

We first decompose $\mathbb{P}((D, S) \neq (D', S'))$ into other probabilistic quantities which can be analyzed using Condition 1. Define the *typical* set:

$$\mathcal{D}^* = \left\{ d : \sum_{n=1}^N \sum_{x=1}^{\infty} d_{n,x} \leq (\beta + 1) \max(C(K, C_1), C(N, C_1)) \right\}.$$

$d \in \mathcal{D}^*$ means that the trait-allocation matrix f has a small number of columns. The claim is that:

$$\mathbb{P}((D, S) \neq (D', S')) \leq \mathbb{P}(D \neq D') + \mathbb{P}(S \neq S' \mid D = D', D \in \mathcal{D}^*) + \mathbb{P}(D \notin \mathcal{D}^*). \quad (\text{G.5})$$

This is true from basic properties of probabilities and conditional probabilities:

$$\begin{aligned} & \mathbb{P}((D, S) \neq (D', S')) \\ &= \mathbb{P}(D \neq D') + \mathbb{P}(S \neq S', D = D') \\ &= \mathbb{P}(D \neq D') + \mathbb{P}(S \neq S', D = D', D \in \mathcal{D}^*) + \mathbb{P}(S \neq S', D = D', D \notin \mathcal{D}^*) \\ &\leq \mathbb{P}(D \neq D') + \mathbb{P}(S \neq S' \mid D = D', D \in \mathcal{D}^*) + \mathbb{P}(D \notin \mathcal{D}^*), \end{aligned}$$

The three ideas behind this upper bound are the following. First, because of the growth condition, we can analyze the atypical set probability $\mathbb{P}(D \notin \mathcal{D}^*)$. Second, because of the total variation between h and \tilde{h} , we can analyze $\mathbb{P}(S \neq S' \mid D = D', D \in \mathcal{D}^*)$. Finally, we can analyze $\mathbb{P}(D \neq D')$ because of the total variation between $K\tilde{h}$ and $M_{n,\cdot}$. In what follows we carry out the program.

Atypical set probability. The $\mathbb{P}(D \notin \mathcal{D}^*)$ term in Eq. (G.5) is easiest to control. Under the target model Proposition C.1, the $D_{i,x}$'s are independent Poissons with mean $M_{i,x}$, so the sum $\sum_{i=1}^N \sum_{x=1}^{\infty} D_{i,x}$ is itself a Poisson with mean $M = \sum_{i=1}^N \sum_{x=1}^{\infty} M_{i,x}$. Because of Lemma E.3, for any $x > 0$:

$$\mathbb{P}\left(\sum_{i=1}^N \sum_{x=1}^{\infty} D_{i,x} > M + x\right) \leq \exp\left(-\frac{x^2}{2(M+x)}\right).$$

For the event $\mathbb{P}(D \notin \mathcal{D}^*)$, $M + x = (\beta + 1) \max(C(K, C_1), C(N, C_1))$, $M \leq C(N, C_1)$ due to Eq. (14), so that $x \geq \beta \max(C(K, C_1), C(N, C_1))$. Therefore:

$$\mathbb{P}(D \notin \mathcal{D}^*) \leq \exp\left(-\frac{\beta^2}{2(\beta+1)} \max(C(K, C_1), C(N, C_1))\right). \quad (\text{G.6})$$

Difference between histories. To minimize the difference probability between the histories of atom sizes i.e. the $\mathbb{P}(S \neq S' \mid D = D', D \in \mathcal{D}^*)$ term in Eq. (G.5), we will use Eq. (16). The claim is, there exists a coupling of $S' \mid D'$ and $S \mid D$ such that:

$$\mathbb{P}(S \neq S' \mid D = D', D \in \mathcal{D}^*) \leq \frac{(\beta + 1) \max(C(K, C_1), C(N, C_1))}{K} C(N, C_1). \quad (\text{G.7})$$

Fix some $d \in \mathcal{D}^*$ — since we are in the typical set, the number of columns in the trait-allocation matrix is at most $(\beta + 1) \max(C(K, C_1), C(N, C_1))$. Conditioned on $D = d$, there is a finite number of history variables S , one for each atom location; similar for conditioning

of S' on $D' = d$. For both the target and the approximate model, the density of the joint distribution factorizes:

$$\begin{aligned}\mathbb{P}(S = s | D = d) &= \prod_{j=1}^J \mathbb{P}(S_j = s_j | D = d) \\ \mathbb{P}(S' = s | D' = d) &= \prod_{j=1}^J \mathbb{P}(S'_j = s_j | D' = d),\end{aligned}$$

since in both marginal processes, the atom sizes for different atom locations are independent of each other. Each S_j (or S'_j) only takes values from a countable set. Therefore, by Lemma E.7,

$$d_{\text{TV}}(P_{S|D=d}, P_{S'|D'=d}) \leq \sum_{j=1}^J d_{\text{TV}}(P_{S_j|D=d}, P_{S'_j|D'=d}).$$

We inspect each $d_{\text{TV}}(P_{S_j|D=d}, P_{S'_j|D'=d})$. Fixing d also fixes I_j , the first row to manifest the j -th atom location. The history s_j is then a $N - I_j + 1$ dimensional integer vector, whose t th entry is the atom size over the j th atom location of the $t + I_j - 1$ row. Because of Eq. (16), we know that conditioned on the same partial history $S_j(1 : (t-1)) = S'_j(1 : (t-1)) = s$, the distributions $S_j(t)$ and $S'_j(t)$ are very similar. The conditional distribution $S_j(t) | D = d, S_j(1 : (t-1)) = s$ is governed by h Proposition C.1 while $S'_j(t) | D' = d, S'_j(1 : (t-1)) = s$ is governed by \tilde{h} Proposition C.2. Hence:

$$d_{\text{TV}}\left(P_{S_j(t) | D=d, S_j(1:(t-1))=s}, P_{S'_j(t) | D'=d, S'_j(1:(t-1))=s}\right) \leq 2 \frac{1}{K} \frac{C_1}{t + I_j - 2 + C_1},$$

for any partial history s . To use this conditional bound, we repeatedly use Lemma E.6 to compare the joint $S_j = (S_j(1), S_j(2), \dots, S_j(N - I_j + 1))$ with the joint $S'_j = (S'_j(1), S'_j(2), \dots, S'_j(N - I_j + 1))$, peeling off one layer of random variables (indexed by t) at a time.

$$\begin{aligned}d_{\text{TV}}(P_{S_j|D=d}, P_{S'_j|D'=d}) &\leq \sum_{t=1}^{N-I_j+1} \max_s d_{\text{TV}}\left(P_{S_j(t) | D=d, S_j(1:(t-1))=s}, P_{S'_j(t) | D'=d, S'_j(1:(t-1))=s}\right) \\ &\leq \sum_{t=1}^{N-I_j+1} 2 \frac{1}{K} \frac{C_1}{t + I_j - 2 + C_1} \\ &\leq 2 \frac{C(N, C_1)}{K}.\end{aligned}$$

Multiplying the right hand side by $(\beta + 1) \max(C(K, C_1), C(N, C_1))$, the upper bound on J , we arrive at the same upper bound for the total variation between $P_{S|D=d}$ and $P_{S'|D'=d}$ in Eq. (G.7). Furthermore, our analysis of the total variation can be back-tracked to construct the coupling between the conditional distributions $S | D = d$ and $S' | D' = d$ which attains that small probability of difference because all the distributions being analyzed are discrete. Since the choice of conditioning $d \in \mathcal{D}^*$ was arbitrary, we have actually shown Eq. (G.7).

Difference between new atom sizes. Finally, to control the difference probability for the distribution over new atom sizes i.e. the $\mathbb{P}(D \neq D')$ term in Eq. (G.5), we will utilize

Eqs. (15) and (17). For each n , define the short-hand $d_{1:n}$ to refer to the collection $d_{i,x}$ for $i \in [n]$, $x \in \mathbb{N}$, and the typical sets:

$$\mathcal{D}_n^* = \left\{ d_{1:n} : \sum_{i=1}^n \sum_{x=1}^{\infty} d_{i,x} \leq (\beta + 1) \max(C(K, C_1), C(N, C_1)) \right\}.$$

The type of expansion performed in Eq. (G.5) can be done once here to see that:

$$\begin{aligned} & \mathbb{P}(D \neq D') \\ &= \mathbb{P}((D_{1:(N-1)}, D_N) \neq (D'_{1:(N-1)}, D'_N)) \\ &\leq \mathbb{P}(D_{1:(N-1)} \neq D'_{1:(N-1)}) \\ &\quad + \mathbb{P}(D_N \neq D'_N \mid D_{1:(N-1)} = D'_{1:(N-1)}, D_{1:(N-1)} \in \mathcal{D}_{n-1}^*) \\ &\quad + \mathbb{P}(D_{1:(N-1)} \notin \mathcal{D}_{n-1}^*). \end{aligned}$$

Apply the expansion once more to $\mathbb{P}(D_{1:(N-1)} \neq D'_{1:(N-1)})$, then to $\mathbb{P}(D_{1:(N-2)} \neq D'_{1:(N-2)})$. If we define:

$$B_j = \mathbb{P}(D_j \neq D'_j \mid D_{1:(j-1)} = D'_{1:(j-1)}, D_{1:(j-1)} \in \mathcal{D}_{j-1}^*),$$

with the special case B_1 simply being $\mathbb{P}(D_1 \neq D'_1)$, then:

$$\mathbb{P}(D \neq D') \leq \sum_{j=1}^N B_j + \sum_{j=2}^N \mathbb{P}(D_{1:(j-1)} \notin \mathcal{D}_{j-1}^*). \quad (\text{G.8})$$

The second summation in Eq. (G.8), comprising of only atypical probabilities, is easier to control. For any j , since $\sum_{i=1}^{j-1} \sum_{x=1}^{\infty} D_{i,x} \leq \sum_{i=1}^N \sum_{x=1}^{\infty} D_{i,x}$, $\mathbb{P}(D_{1:(j-1)} \notin \mathcal{D}_{j-1}^*) \leq \mathbb{P}(D \notin \mathcal{D}^*)$, so a generous upper bound for the contribution of all the atypical probabilities including the first one from Eq. (G.6) is

$$\begin{aligned} & \mathbb{P}(D \notin \mathcal{D}^*) + \sum_{j=2}^N \mathbb{P}(D_{1:(j-1)} \notin \mathcal{D}_{j-1}^*) \\ &\leq \exp\left(-\left(\frac{\beta^2}{2(\beta+1)} \max(C(K, C_1), C(N, C_1)) - \ln N\right)\right). \end{aligned}$$

By Lemma E.10, $\max(C(K, C_1), C(N, C_1)) \geq C_1(\max(\ln N, \ln K) - C_1(\psi(C_1) + 1))$. Since we have set β so that $\frac{\beta^2}{\beta+1} C_1 = 4$, we have

$$\begin{aligned} \frac{\beta^2}{2(\beta+1)} \max(C(K, C_1), C(N, C_1)) - \ln N &\geq 2 \max(\ln N, \ln K) - 2C_1(\psi(C_1) + 1) - \ln N \\ &\geq \ln K - 2C_1(\psi(C_1) + 1). \end{aligned}$$

meaning the overall atypical probabilities is at most

$$\mathbb{P}(D \notin \mathcal{D}^*) + \sum_{j=2}^N \mathbb{P}(D_{1:(j-1)} \notin \mathcal{D}_{j-1}^*) \leq \frac{\exp(2C_1(\psi(C_1) + 1))}{K}. \quad (\text{G.9})$$

As for the first summation in Eq. (G.8), we look at the individual B_j 's. For any fixed $d_{1:(j-1)} \in \mathcal{D}_{j-1}^*$, we claim that there exists a coupling between the conditionals $D_j \mid D_{1:(j-1)} =$

$d_{1:(j-1)}$ and $D'_j | D'_{1:(j-1)} = d_{1:(j-1)}$ such that $\mathbb{P}(D_j \neq D'_j | D_{1:(j-1)} = D'_{1:(j-1)} = d_{1:(j-1)})$ is at most

$$\frac{C_1^2}{K} \frac{1}{(j-1+C_1)^2} + [C_4 \ln j + C_5 + (\beta+1) \max(C(K, C_1), C(N, C_1))] \frac{1}{j-1+C_1}. \quad (\text{G.10})$$

Because the upper bound holds for arbitrary values $d_{1:(j-1)}$, the coupling actually ensures that, as long as $D_{1:(j-1)} = D'_{1:(j-1)}$ for some value in \mathcal{D}_{j-1}^* , the probability of difference between D_j and D'_j is small i.e. B_j is at most the right hand side.

We demonstrate the existence of a distribution $U = \{U_x\}_{x=1}^\infty$ of independent Poisson random variables, such that both the total variation between $P_{D_j | D_{1:(j-1)}=d_{1:(j-1)}}$ and P_U and the total variation between $P_{D'_j | D'_{1:(j-1)}=d_{1:(j-1)}}$ and P_U are small. Here, each U_x has mean:

$$\mathbb{E}(U_x) = \left(K - \sum_{i=1}^{j-1} \sum_{y=1}^{\infty} d_{i,y} \right) \tilde{h}(x | x_{1:(j-1)} = 0).$$

On the one hand, conditioned on $D'_{1:(j-1)} = d_{1:(j-1)}$, $D'_j = \{D'_{j,x}\}_{x=1}^\infty$ is the joint distribution of types of successes of type x , where there are $K - \sum_{i=1}^{j-1} \sum_{x=1}^{\infty} d_{i,x}$ independent trials and types x success has probability $\tilde{h}(x | x_{1:(j-1)} = 0)$ by Proposition C.2. Because of Lemma E.4 and Eq. (15):

$$\begin{aligned} \mathbb{P}(D'_j \neq U | D'_{1:(j-1)} = d_{1:(j-1)}) &\leq \left(K - \sum_{i=1}^{j-1} \sum_{y=1}^{\infty} d_{i,y} \right) \left(\sum_{x=1}^{\infty} \tilde{h}(x | x_{1:(j-1)} = 0) \right)^2 \\ &\leq K \left(\frac{1}{K} \frac{C_1}{j-1+C_1} \right)^2 \\ &\leq \frac{C_1^2}{K} \frac{1}{(j-1+C_1)^2}. \end{aligned} \quad (\text{G.11})$$

On the other hand, conditioned on $D_{1:(j-1)}$, $D_j = \{D_{j,x}\}_{x=1}^\infty$ consists of independent Poissons, where the mean of $D_{j,x}$ is $M_{j,x}$ by Proposition C.1. We show that there exists a coupling of P_U and P_{D_j} such that

$$\mathbb{P}(U \neq D_j) \leq \sum_{x=1}^{\infty} d_{\text{TV}}(P_{U_x}, P_{D_{j,x}}). \quad (\text{G.12})$$

For each $x \geq 1$, let O_x be the maximal coupling distribution between P_{U_x} and $P_{D_{j,x}}$ i.e. for $(A, B) \sim O_x$, $\mathbb{P}(A \neq B) = d_{\text{TV}}(P_{U_x}, P_{D_{j,x}})$. Such O_x exists because both P_{U_x} and $P_{D_{j,x}}$ are Poisson (hence discrete) distributions. Furthermore, since O_x is itself a discrete distribution, the conditional distributions $D_{j,x} | U_x$ exists. Denote the natural zig-zag bijection from $\{\mathbb{N} \cup 0\}^2$ to \mathbb{N} to be L .²¹ Denote by F_x the cdf of the distribution of $L(A, B)$ for $(A, B) \sim O_x$. To generate samples from O_x , it suffices to generate samples from F_x and transform using the inverse of L . Consider the following coupling of P_U and P_{D_j} :

- Generate i.i.d uniform random variables V_1, V_2, \dots
- For $x \geq 1$, let $(U_x, D_{j,x}) = L^{-1}(F_x^{-1}(V_x))$.

²¹ $L(0,0) = 1, L(0,1) = 2, L(1,0) = 3, L(2,0) = 4, L(1,1) = 5, L(0,2) = 6$ and so on.

Marginally, each U_x (or $D_{j,x}$) is Poisson with the right mean, and across x , the U_x (or $D_{j,x}$) are independent of each other because we use i.i.d uniform r.v's. Alternatively, the conditional distribution of $D_j | U$ implied by this joint distribution is as follows:

- For $x \geq 1$, sample $U_x | D_{j,x}$ from the conditional distribution implied by the maximal coupling O_x .

If U is different from D_j , it must be that for at least one x , $U_x \neq D_{j,x}$. Therefore

$$\mathbb{P}(U \neq D_j) \leq \sum_{x=1}^{\infty} \mathbb{P}(U_x \neq D_{j,x}).$$

Since the coupling $(U_x, D_{j,x})$ attains the $d_{\text{TV}}(P_{U_x}, P_{D_{j,x}})$, we are done. From Lemma E.5, we know

$$\begin{aligned} & \sum_{x=1}^{\infty} d_{\text{TV}}(P_{U_x}, P_{D_{j,x}}) \\ & \leq \sum_{x=1}^{\infty} \left| M_{j,x} - \left(K - \sum_{i=1}^{j-1} \sum_{y=1}^{\infty} d_{i,y} \right) \tilde{h}(x | x_{1:(j-1)} = 0) \right| \\ & \leq \sum_{x=1}^{\infty} \left(|M_{j,x} - K \tilde{h}(x | x_{1:(j-1)} = 0)| + \sum_{i=1}^{j-1} \sum_{y=1}^{\infty} d_{i,y} \tilde{h}(x | x_{1:(j-1)} = 0) \right) \\ & \leq \sum_{x=1}^{\infty} |M_{j,x} - K \tilde{h}(x | x_{1:(j-1)} = 0)| + \left(\sum_{i=1}^{j-1} \sum_{y=1}^{\infty} d_{i,y} \right) \left(\sum_{x=1}^{\infty} \tilde{h}(x | x_{1:(j-1)} = 0) \right). \quad (\text{G.13}) \end{aligned}$$

The first term is upper bounded by Eq. (17). Regarding the second term, since we are in the typical set, $\sum_{i=1}^{j-1} \sum_{y=1}^{\infty} d_{i,y}$ is small and we also use Eq. (15). Therefore the overall bound on the second term is:

$$(\beta + 1) \max(C(K, C_1), C(N, C_1)) \frac{1}{K} \frac{C_1}{j - 1 + C_1}.$$

Combining the two bounds and Eq. (G.12) give the following bound on $\mathbb{P}(U \neq D_j)$:

$$\mathbb{P}(U \neq D_j) \leq \frac{1}{K} \frac{C_4 \ln j + C_5}{j - 1 + C_1} + (\beta + 1) \max(C(K, C_1), C(N, C_1)) \frac{1}{K} \frac{C_1}{j - 1 + C_1}. \quad (\text{G.14})$$

We now show how the combination of Eqs. (G.11) and (G.14) imply Eq. (G.10). From Eq. (G.14), there exists a coupling of P_U and P_{D_j} such that the difference probability is small. From Eq. (G.11), there exists a coupling of \tilde{P}_U and $P_{D'_j | D'_{1:(j-1)} = d_{1:(j-1)}}$ such that the difference probability is small. In both cases, we can sample from the conditional distribution based on U . $D_j | U$ exists because of the discussion after Eq. (G.12), while $D'_j | D'_{1:(j-1)} = d_{1:(j-1)}, U$ exists because of Lemma E.4. Therefore, we can glue the two couplings together, by first sampling U , and then sample from the appropriate conditional distributions. By taking expectations of the simple triangle inequality for the discrete metric i.e.

$$\mathbf{1}\{D_j \neq D'_j\} \leq \mathbf{1}\{D_j \neq U\} + \mathbf{1}\{D'_j \neq U\},$$

we reach Eq. (G.10).

We sum of the right hand side of Eq. (G.10) across j . This shows that $\sum_{j=1}^N B_j$ is at most

$$\begin{aligned} \frac{C_1^2}{K} \left(\sum_{j=1}^N \frac{1}{(j-1+C_1)^2} \right) &+ \frac{(\beta+1) \max(C(K, C_1), C(N, C_1))}{K} C(N, C_1) \\ &+ \frac{C_4 \ln N + C_5}{K} C(N, C_1). \end{aligned}$$

The first term is upper bounded by the trigamma function $\psi_1(\cdot)$:

$$\frac{C_1^2}{K} \sum_{j=1}^N \frac{1}{(j-1+C_1)^2} \leq \frac{C_1^2 \psi_1(C_1)}{K}.$$

This means, an upper bound on $\sum_{j=1}^N B_j$ is

$$\frac{C_1^2 \psi_1(C_1)}{K} + \frac{\beta+1}{K} C(N, C_1) [(C_1 + C_4) \ln N + C_1 \ln K + 2C_1 \ln(1 + 1/C_1) + C_5]. \quad (\text{G.15})$$

Because of Eqs. (G.8), (G.9) and (G.15), we can couple D and D' such that $\mathbb{P}(D \neq D') + \mathbb{P}(D \notin \mathcal{D}^*)$ is at most

$$\begin{aligned} &\frac{C_1^2 \psi_1(C_1) + \exp(2C_1(\psi(C_1) + 1))}{K} \\ &+ \frac{\beta+1}{K} C(N, C_1) [(C_1 + C_4) \ln N + C_1 \ln K + 2C_1 \ln(1 + 1/C_1) + C_5]. \end{aligned} \quad (\text{G.16})$$

Aggregating the results from Eqs. (G.7) and (G.16), we have that $d_{\text{TV}}(P_{N, \infty}, P_{N, K})$ is at most

$$\begin{aligned} &\frac{C_1^2 \psi_1(C_1) + \exp(2C_1(\psi(C_1) + 1))}{K} \\ &+ \frac{\beta+1}{K} C(N, C_1) [\max(C(K, C_1), C(N, C_1)) + (C_1 + C_4) \ln N] \\ &+ \frac{\beta+1}{K} C(N, C_1) [C_1 \ln K + 2C_1 \ln(1 + 1/C_1) + C_5]. \end{aligned}$$

We expand the sum of the last two term by upper bounding $\max(C(K, C_1), C(N, C_1))$ by $C(K, C_1) + C(N, C_1)$ and using the upper bound Lemma E.10. The end result is

$$\frac{\tilde{C}^{(0)} + \tilde{C}^{(1)} \ln K + \tilde{C}^{(2)} \ln N + \tilde{C}^{(3)} \ln N \ln K + \tilde{C}^{(4)} \ln^2 N}{K}$$

where $\tilde{C}^{(0)}$ is equal to

$$(\beta+1)C_1 \ln(1 + 1/C_1) [4C_1 \ln(1 + 1/C_1) + C_5] + C_1^2 \psi_1(C_1) + \exp(2C_1(\psi(C_1) + 1)),$$

and

$$\begin{aligned} \tilde{C}^{(1)} &= (\beta+1)2C_1^2 \ln(1 + 1/C_1), \\ \tilde{C}^{(2)} &= (\beta+1) [C_1(4C_1 \ln(1 + 1/C_1) + C_5) + (2C_1 + C_4)C_1 \ln(1 + 1/C_1)], \\ \tilde{C}^{(3)} &= (\beta+1)2C_1^2 \ln(1 + 1/C_1), \\ \tilde{C}^{(4)} &= (\beta+1)C_1(2C_1 + C_4). \end{aligned}$$

Since N is a natural number, $N \geq 1$ we can write $\ln N \leq (1/\ln 2) \ln^2 N$, to simplify the upper bound on total variation as

$$\frac{\tilde{C}^{(0)} + \left(\tilde{C}^{(4)} + \tilde{C}^{(2)}/\ln 2\right) \ln^2 N + \tilde{C}^{(3)} \ln N \ln K + \tilde{C}^{(1)} \ln K}{K}. \quad (\text{G.17})$$

Taking the sum of individual coefficients in front of $\ln^2 N$ (et cetera) between Eq. (G.17) and Eq. (G.2) yields the constants at the beginning of the proof. \square

In applications, the observational likelihood f and the ground measure H might be random rather than fixed quantities. For instance, in linear–Gaussian beta–Bernoulli processes without good prior information, probabilistic models put priors on the variances of the Gaussian features as well as the noise in observed data. In such cases, the AIFAs remain the same as the in Theorem B.2 (or Corollary 3.3) since the rate measure ν is still fixed. The above proof of Theorem 4.1 can be easily extended to the case where f and H are random, because the argument leading to Eq. (G.4) retains validity when f and H have the same distribution under the target and the approximate model. For completeness, we state the error bound in such cases where hyper-priors are used.

Corollary G.1 (Upper bound for hyper-priors). *Let \mathcal{H} be a prior distribution for ground measures H and \mathcal{F} be a prior distribution for observational likelihoods f . Suppose the target model is*

$$\begin{aligned} H &\sim \mathcal{H}(\cdot), \\ f &\sim \mathcal{F}(\cdot), \\ \Theta | H &\sim \text{CRM}(H, \nu), \\ X_n | \Theta &\stackrel{i.i.d.}{\sim} \text{LP}(\ell, \Theta), \quad n = 1, 2, \dots, N, \\ Y_n | f, X_n &\stackrel{indep}{\sim} f(\cdot | X_n), \quad n = 1, 2, \dots, N. \end{aligned}$$

The approximate model, with ν_K as in Theorem B.2 (or Corollary 3.3), is

$$\begin{aligned} H &\sim \mathcal{H}(\cdot), \\ f &\sim \mathcal{F}(\cdot), \\ \Theta_K | H &\sim \text{IFA}_K(H, \nu_K), \\ Z_n | \Theta_K &\stackrel{i.i.d.}{\sim} \text{LP}(\ell, \Theta_K), \quad n = 1, 2, \dots, N, \\ W_n | f, Z_n &\stackrel{indep}{\sim} f(\cdot | Z_n), \quad n = 1, 2, \dots, N. \end{aligned}$$

If Assumption 1 and Condition 1 hold, then there exist positive constants C', C'', C''' depending only on $\{C_i\}_{i=1}^5$ such that

$$d_{TV}(P_{Y_{1:N}}, P_{W_{1:N}}) \leq \frac{C' + C'' \ln^2 N + C''' \ln N \ln K}{K}.$$

The upper bound in Corollary G.1 is visually identical to Theorem 4.1, and has no dependence on the hyper-priors \mathcal{H} or \mathcal{F} .

G.2. Lower bound

Proof of Theorem 4.2. First we mention which probability kernel f results in the large total variation distance: the pathological f is the Dirac measure i.e., $f(\cdot | X) := \delta_X(\cdot)$. With this conditional likelihood $X_n = Y_n$ and $Z_n = W_n$, meaning:

$$d_{\text{TV}}(P_{N,\infty}^{\text{BP}}, P_{N,K}^{\text{BP}}) = d_{\text{TV}}(P_{X_{1:N}}, P_{Z_{1:N}}).$$

Now we discuss why the total variation is lower bounded by the function of N . Let \mathcal{A} be the event that there are at least $\frac{1}{2}\gamma C(N, \alpha)$ unique atom locations in among the latent states:

$$\mathcal{A} := \left\{ x_{1:N} : \#\text{unique atom locations} \geq \frac{1}{2}\gamma C(N, \alpha) \right\}.$$

The probabilities assigned to this event by the approximate and the target models are very different from each other. On the one hand, since $K < \frac{\gamma C(N, \alpha)}{2}$, under AIFA_K , \mathcal{A} has measure zero:

$$\mathbb{P}_{Z_{1:N}}(\mathcal{A}) = 0. \quad (\text{G.18})$$

On the other hand, under beta-Bernoulli, the number of unique atom locations drawn is a Poisson random variable with mean exactly $\gamma C(N, \alpha)$ — see Proposition C.1 and Proposition C.2. The complement of \mathcal{A} is a lower tail event. By Lemma E.3 with $\lambda = \gamma C(N, \alpha)$ and $x = \frac{1}{2}\gamma C(N, \alpha)$:

$$\mathbb{P}_{X_{1:N}}(\mathcal{A}) \geq 1 - \exp\left(-\frac{\gamma C(N, \alpha)}{8}\right). \quad (\text{G.19})$$

Because of Lemma E.10, we can lower bound $C(N, \alpha)$ by a multiple of $\ln N$:

$$\exp\left(-\frac{\gamma C(N, \alpha)}{8}\right) \leq \exp\left(-\frac{\gamma \alpha \ln N}{8} + \frac{\alpha \gamma (\psi(\alpha) + 1)}{8}\right) = \frac{\text{constant}}{N^{\gamma \alpha / 8}}.$$

We now combine Eqs. (G.18) and (G.19) and recall that total variation is the maximum over discrepancy in probabilistic masses. \square

The proof of Theorem 4.3 relies on the ability to compute a lower bound on the total variation distance between a binomial distribution and a Poisson distribution.

Proposition G.2 (Lower bound on total variation between binomial and Poisson). *For all K , it is true that*

$$d_{\text{TV}}\left(\text{Poisson}(\gamma), \text{Binom}\left(K, \frac{\gamma/K}{\gamma/K + 1}\right)\right) \geq C(\gamma)K \left(\frac{\gamma/K}{\gamma/K + 1}\right)^2,$$

where

$$C(\gamma) = \frac{1}{8} \frac{1}{\gamma + \exp(-1)(\gamma + 1) \max(12\gamma^2, 48\gamma, 28)}.$$

Proof of Proposition G.2. We adapt the proof of (Barbour and Hall, 1984, Theorem 2) to our setting. The Poisson(γ) distribution satisfies the functional equality:

$$\mathbb{E}[\gamma y(Z + 1) - Zy(Z)] = 0, \quad (\text{G.20})$$

where y is any real-valued function and $Z \sim \text{Poisson}(\gamma)$.

Denote $\gamma_K = \frac{\gamma}{\gamma/K+1}$. For $m \in \mathbb{N}$, let

$$x(m) = m \exp\left(-\frac{m^2}{\gamma_K \theta}\right),$$

where θ is a constant which will be specified later. $x(m)$ serves as a test function to lower bound the total variation distance between $\text{Poisson}(\gamma)$ and $\text{Binom}(K, \gamma_K/K)$. Let $X_i \sim \text{Ber}(\frac{\gamma_K}{K})$, independently across i from 1 to K , and $W = \sum_{i=1}^K X_i$. Then $W \sim \text{Binomial}(K, \gamma_K/K)$. The following identity is adapted from (Barbour and Hall, 1984, Equation 2.1):

$$\mathbb{E}[\gamma_K x(W+1) - Wx(W)] = \left(\frac{\gamma_K}{K}\right)^2 \sum_{i=1}^K \mathbb{E}[x(W_i+2) - x(W_i+1)], \quad (\text{G.21})$$

where $W_i = W - X_i$.

We first argue that the right hand side is not too small i.e. for any i ,

$$\mathbb{E}[x(W_i+2) - x(W_i+1)] \geq 1 - \frac{3\gamma_K^2 + 12\gamma_K + 7}{\theta\gamma_K}. \quad (\text{G.22})$$

Consider the derivative of $x(m)$:

$$\frac{d}{dm}x(m) = \exp\left(-\frac{m^2}{\gamma_K \theta}\right) \left(1 - \frac{2m^2}{\gamma_K \theta}\right) \geq 1 - \frac{3m^2}{\theta\gamma_K},$$

because of the easy-to-verify inequality $e^{-x}(1-2x) \geq 1-3x$ for $x \geq 0$. This means that

$$x(W_i+2) - x(W_i+1) \geq \int_{W_i+1}^{W_i+2} \left(1 - \frac{3m^2}{\theta\gamma_K}\right) dm = 1 - \frac{1}{\theta\gamma_K}(3W_i^2 + 9W_i + 7).$$

Taking expectations, noting that $\mathbb{E}(W_i) \leq \gamma_K$ and $\mathbb{E}(W_i^2) = \text{Var}(W_i) + [\mathbb{E}(W_i)]^2 \leq \sum_{j=1}^K \frac{\gamma_K}{K} + (\gamma_K)^2 = \gamma_K^2 + \gamma_K$ we have proven Eq. (G.22).

Now, because of positivity of x , and that $\gamma \geq \gamma_K$, we trivially have

$$\mathbb{E}[\gamma x(W+1) - Wx(W)] \geq \mathbb{E}[\gamma_K x(W+1) - Wx(W)]. \quad (\text{G.23})$$

Combining Eq. (G.21), Eq. (G.22) and Eq. (G.23) we have that

$$\mathbb{E}[\gamma x(W+1) - Wx(W)] \geq K \left(\frac{\gamma_K}{K}\right)^2 \left(1 - \frac{3\gamma_K^2 + 12\gamma_K + 7}{\theta\gamma_K}\right).$$

Recalling Eq. (G.20), for any coupling (W, Z) such that $W \sim \text{Binom}\left(K, \frac{\gamma/K}{\gamma/K+1}\right)$ and $Z \sim \text{Poisson}(\gamma)$:

$$\mathbb{E}[\gamma(x(W+1) - x(Z+1)) + Zx(Z) - Wx(W)] \geq \frac{\gamma_K^2}{K} \left(1 - \frac{3\gamma_K^2 + 12\gamma_K + 7}{\theta\gamma_K}\right).$$

Suppose (W, Z) is the maximal coupling attaining the total variation distance between P_W and P_Z i.e. $\mathbb{P}(W \neq Z) = d_{\text{TV}}(P_Y, P_Z)$. Clearly,

$$\begin{aligned} & \gamma(x(W+1) - x(Z+1)) + Zx(Z) - Wx(W) \\ & \leq \mathbf{1}\{W \neq Z\} \sup_{m_1, m_2} |(\gamma x(m_1+1) - m_1 x(m_1)) - (\gamma x(m_2+1) - m_2 x(m_2))| \\ & \leq 2\mathbf{1}\{W \neq Z\} \sup_m |(\gamma x(m+1) - mx(m))|. \end{aligned}$$

Taking expectations on both sides, we conclude that

$$2d_{\text{TV}}(P_W, P_Z) \times \sup_m |\gamma x(m+1) - mx(m)| \geq \frac{\gamma_K^2}{K} \left(1 - \frac{3\gamma_K^2 + 12\gamma_K + 7}{\theta\gamma_K}\right). \quad (\text{G.24})$$

It remains to upper bound $\sup_m |\gamma x(m+1) - mx(m)|$. Recall that the derivative of x is $\exp\left(-\frac{m^2}{\gamma_K\theta}\right) \left(1 - \frac{2m^2}{\gamma_K\theta}\right)$, taking values in $[-2e^{-3/2}, 1]$. This means for any m , $-2e^{-3/2} \leq x(m+1) - x(m) \leq 1$. Hence:

$$\begin{aligned} |\gamma x(m+1) - mx(m)| &= |\gamma(x(m+1) - x(m)) + (\gamma - m)x(m)| \\ &\leq \gamma + (m + \gamma)m \exp\left(-\frac{m^2}{\gamma_K\theta}\right) \\ &\leq \gamma + (\gamma + 1)m^2 \exp\left(-\frac{m^2}{\gamma_K\theta}\right) \\ &\leq \gamma + \theta\gamma_K(\gamma + 1) \exp(-1). \end{aligned} \quad (\text{G.25})$$

where the last inequality owes to the easy-to-verify $x \exp(-x) \leq \exp(-1)$. Combining Eq. (G.25) and Eq. (G.24) we have that

$$d_{\text{TV}}\left(\text{Binomial}\left(K, \frac{\gamma/K}{\gamma/K + 1}\right), \text{Poisson}(\gamma)\right) \geq \frac{1}{2} \frac{1 - \frac{3\gamma_K^2 + 12\gamma_K + 7}{\theta\gamma_K}}{\gamma + (\gamma + 1)\theta\gamma_K \exp(-1)} K \left(\frac{\gamma_K}{K}\right)^2.$$

Finally, we calibrate θ . By selecting $\theta = \max\left(12\gamma_K, \frac{28}{\gamma_K}, 48\right)$ we have that the numerator of the unwieldy fraction is at least $\frac{1}{4}$ and its denominator is at most $\gamma + \exp(-1)(\gamma + 1) \max(12\gamma^2, 48\gamma, 28)$, because $\gamma_K < \gamma$. This completes the proof. \square

Proof of Theorem 4.3. The constant C in the theorem statement is

$$C := \gamma^2 / (\gamma + \exp(-1)(\gamma + 1) \max(12\gamma^2, 48\gamma, 28)),$$

which is equal to $\gamma^2 C(\gamma)$, with $C(\gamma)$ from Proposition G.2.

First we mention which probability kernel f results in the large total variation distance. For any discrete measure $\sum_{i=1}^M \delta_{\psi_i}$, f is the Dirac measure sitting on M , the number of atoms.

$$f(\cdot | \sum_{i=1}^M \delta_{\psi_i}) := \delta_M(\cdot). \quad (\text{G.26})$$

Now we show that under such f , the total variation distance is lower bounded. From Lemma E.9, we know that

$$d_{\text{TV}}(P_{N,\infty}^{\text{BP}}, P_{N,K}^{\text{BP}}) = d_{\text{TV}}(P_{Y_{1:N}}, P_{W_{1:N}}) \geq d_{\text{TV}}(P_{Y_1}, P_{W_1}).$$

Hence it suffices to show:

$$d_{\text{TV}}(P_{Y_1}, P_{W_1}) \geq C(\gamma) \frac{\gamma^2}{K} \frac{1}{(1 + \gamma/K)^2}.$$

Recall the generative process defining P_{Y_1} and P_{W_1} . Y_1 is an observation from the target beta–Bernoulli model, and the functions h, \tilde{h} , and $M_{n,x}$ are given in Example 4.1. By Proposition C.1,

$$N_T \sim \text{Poisson}(\gamma), \quad \psi_k \stackrel{\text{i.i.d.}}{\sim} H, \quad X_1 = \sum_{i=1}^{N_T} \delta_{\psi_k}, \quad Y_1 \sim f(\cdot | X_1).$$

W_1 is an observation from the approximate model, so by Proposition C.2,

$$N_A \sim \text{Binom}\left(K, \frac{\gamma/K}{1 + \gamma/K}\right), \quad \phi_k \stackrel{\text{i.i.d.}}{\sim} H, \quad Z_1 = \sum_{i=1}^{N_A} \delta_{\phi_k}, \quad W_1 \sim f(\cdot | Z_1).$$

Because of the choice of f , $Y_1 = N_T$ and $W_1 = N_A$. Hence, by Proposition G.2,

$$\begin{aligned} d_{\text{TV}}(P_{Y_1}, P_{W_1}) &= d_{\text{TV}}(P_{N_T}, P_{N_A}) \\ &\geq C(\gamma) \frac{\gamma^2}{K} \frac{1}{(1 + \gamma/K)^2}. \end{aligned}$$

□

Appendix H: DPMM results

We consider Dirichlet process mixture models (Antoniak, 1974)

$$\begin{aligned} \Theta &\sim \text{DP}(\alpha, H), \\ X_n | \Theta &\stackrel{\text{i.i.d.}}{\sim} \Theta, \quad n = 1, 2, \dots, N, \\ Y_n | X_n &\stackrel{\text{indep}}{\sim} f(\cdot | X_n), \quad n = 1, 2, \dots, N. \end{aligned} \tag{H.1}$$

with corresponding approximation

$$\begin{aligned} \Theta_K &\sim \text{FSD}_K(\alpha, H), \\ Z_n | \Theta_K &\stackrel{\text{i.i.d.}}{\sim} \Theta_K, \quad n = 1, 2, \dots, N, \\ W_n | Z_n &\stackrel{\text{indep}}{\sim} f(\cdot | Z_n), \quad n = 1, 2, \dots, N. \end{aligned} \tag{H.2}$$

Let $P_{N,\infty}$ be the distribution of the observations $Y_{1:N}$. Let $P_{N,K}$ be the distribution of the observations $W_{1:N}$.

H.1. Upper bound

Upper bounds on the error made by FSD_K can be used to determine the sufficient K to approximate the target process for a given N and accuracy level. We upper bound $d_{\text{TV}}(P_{N,\infty}, P_{N,K})$ in Theorem H.1.

Theorem H.1 (Upper bound for DPMM). *For some constants C', C'', C''', C'''' that only depend on α ,*

$$d_{\text{TV}}(P_{N,\infty}, P_{N,K}) \leq \frac{C' + C'' \ln^2 N + C''' \ln N \ln K + C'''' \ln K}{K}.$$

The proof and explicit values of the constants are given in Appendix I.1. Theorem H.1 is similar to Theorem 4.1, although the exact values of the constants C', C'', C''', C'''' are different. The $O(\ln^2 N)$ growth of the bound for fixed N can likely be reduced to $O(\ln N)$, the inherent growth rate of DP mixture models (Arratia, Barbour and Tavaré, 2003, Section 5.2). The $O(\ln K/K)$ rate of decrease to zero is tight because of a $1/K$ lower bound on the approximation error. Theorem H.1 is an improvement over the existing theory for FSD_K , in the sense that Ishwaran and Zarepour (2002, Theorem 4) provide an upper bound on $d_{TV}(P_{N,\infty}, P_{N,K})$ that lacks an explicit dependence on K or N — that bound cannot be inverted to determine the sufficient K to approximate the target to a given accuracy, while it is simple to determine using Theorem H.1.

H.2. Lower bounds

As Theorem H.1 is only an upper bound, we now investigate the tightness of the inequality in terms of N and K . We first look at the dependence of the error bound in terms of $\ln N$. Theorem H.2 shows that finite approximations cannot be accurate if the approximation level is too small compared to the growth rate $\ln N$.

Theorem H.2 ($\ln N$ is necessary). *There exists a probability kernel $f(\cdot)$, independent of K, N , such that for any $N \geq 2$, if $K \leq \frac{1}{2}C(N, \alpha)$, then*

$$d_{TV}(P_{N,\infty}, P_{N,K}) \geq 1 - \frac{C'}{N^{\alpha/8}}$$

where C' is a constant only dependent on α .

See Appendix I.2 for the proof. Theorem H.2 implies that as N grows, if the approximation level K fails to surpass the $C(N, \alpha)/2$ threshold, then the total variation between the approximate and the target model remains bounded from zero — in fact, the error tends to one. Recall that $C(N, \alpha) = \Omega(\ln N)$, so the necessary approximation level is $\Omega(\ln N)$. Theorem H.2 is the analog of Theorem 4.2.

We also investigate the tightness of Theorem H.1 in terms of K . In Theorem H.3, our lower bound indicates that the $1/K$ factor in Theorem H.1 is tight (up to log factors).

Theorem H.3 ($1/K$ lower bound). *There exists a probability kernel $f(\cdot)$, independent of K, N , such that for any $N \geq 2$,*

$$d_{TV}(P_{N,\infty}, P_{N,K}) \geq \frac{\alpha}{1 + \alpha} \frac{1}{K}.$$

See Appendix I.2 for the proof. While Theorem H.1 implies that the normalized AIFA with $K = O(\text{poly}(\ln N)/\epsilon)$ atoms suffices in approximating the DP mixture model to less than ϵ error, Theorem H.3 implies that a normalized AIFA with $K = \Omega(1/\epsilon)$ atoms is *necessary* in the worst case. This worst-case behavior is analogous to Theorem 4.3 for DP-based models.

The $1/\epsilon$ dependence means that AIFAs are worse than TFAs in theory. It is known that small TFA models are already excellent approximations of the DP. Definition 4.5 is a very well-known finite approximation whose error is upper bounded in Proposition H.4.

Proposition H.4. (Ishwaran and James, 2001, Theorem 2) *Let $\Xi_K \sim \text{TSB}_K(\alpha, H)$, $R_n | \Xi_K \stackrel{i.i.d.}{\sim} \Xi_K, T_n | R_n \stackrel{indep}{\sim} f(\cdot | R_n)$ with N observations. Let $Q_{N,K}$ be the distribution of the observations $T_{1:N}$. Then: $d_{TV}(P_{N,\infty}, Q_{N,K}) \leq 2N \exp(-\frac{K-1}{\alpha})$.*

Proposition H.4 implies that a TFA with $K = O(\ln(N/\epsilon))$ atoms suffices in approximating the DP mixture model to less than ϵ error. Modulo log factors, comparing the necessary $1/\epsilon$ level for AIFA and the sufficient $\ln(1/\epsilon)$ level for TFA, we conclude that the necessary size for normalized IFA is exponentially larger than the sufficient size for TFA, in the worst case.

Appendix I: Proofs of DP bounds

Our technique to analyze the error made by FSD_K follows a similar vein to the technique in Appendix G. We compare the joint distribution of the latents $X_{1:N}$ and $Z_{1:N}$ (with the underlying Θ or Θ_K marginalized out) using the conditional distributions $X_n | X_{1:(n-1)}$ and $Z_n | Z_{1:(n-1)}$. Before going into the proofs, we give the form of the conditionals.

The conditional $X_{1:N} | X_{1:(n-1)}$ is the well-known Blackwell-MacQueen prediction rule.

Proposition I.1. *Blackwell and MacQueen (1973)* For $n = 1$, $X_1 \sim H$. For $n \geq 2$,

$$X_n | X_{n-1}, X_{n-2}, \dots, X_1 \sim \frac{\alpha}{n-1+\alpha} H + \sum_j \frac{n_j}{n-1+\alpha} \delta_{\psi_j},$$

where $\{\psi_j\}$ is the set of unique values among $X_{n-1}, X_{n-2}, \dots, X_1$ and n_j is the cardinality of the set $\{i : 1 \leq i \leq n-1, X_i = \psi_j\}$.

The conditionals $Z_n | Z_{1:(n-1)}$ are related to the Blackwell-MacQueen prediction rule.

Proposition I.2. *Pitman (1996)* For $n = 1$, $Z_1 \sim H$. For $n \geq 2$, let $\{\psi_j\}_{j=1}^{J_n}$ be the set of unique values among $Z_{n-1}, Z_{n-2}, \dots, Z_1$ and n_j is the cardinality of the set $\{i : 1 \leq i \leq n-1, Z_i = \psi_j\}$. If $J_n < K$:

$$Z_n | Z_{n-1}, Z_{n-2}, \dots, Z_1 \sim \frac{(K - J_n)\alpha/K}{n-1+\alpha} H + \sum_{j=1}^{J_n} \frac{n_j + \alpha/K}{n-1+\alpha} \delta_{\psi_j},$$

Otherwise, if $J_n = K$, there is zero probability of drawing a fresh component from H i.e. Z_n comes only from $\{\psi_j\}_{j=1}^{J_n}$:

$$Z_n | Z_{n-1}, Z_{n-2}, \dots, Z_1 \sim \sum_{j=1}^{J_n} \frac{n_j + \alpha/K}{n-1+\alpha} \delta_{\psi_j}.$$

$J_n \leq K$ is an invariant of these of prediction rules: once $J_n = K$, all subsequent J_m for $m \geq n$ is also equal to K .

I.1. Upper bounds

Proof of Theorem H.1. The constants C', C'', C''', C'''' are as follows

$$\begin{aligned} C' &= \exp(\alpha(\psi(\alpha) + 1)) + 2\alpha^2 \ln^2(1 + 1/\alpha), \\ C'' &= \alpha^2 + \frac{3\alpha^2 \ln(1 + 1/\alpha)}{\ln 2}, \\ C''' &= \alpha^2, \\ C'''' &= \alpha^2 \ln(1 + 1/\alpha). \end{aligned} \tag{I.1}$$

The reasoning for these constants will be clear by the end of the proof.

To begin, observe that the conditional distributions of the observations given the latent variables are the same across target and approximate models: $P_{Y_{1:N}|X_{1:N}}$ is the same as $P_{W_{1:N}|Z_{1:N}}$ if $X_{1:N} = Z_{1:N}$. Therefore, using Lemma E.8, we want to show that there exists a coupling of $P_{X_{1:N}}$ and $P_{Z_{1:N}}$ that has small difference probability.

First, we construct a coupling of $P_{X_{1:N}}$ and $P_{Z_{1:N}}$ such that, for any $n \geq 1$, for any $x_{1:(n-1)}$ such that J_n is the number of unique atom locations among $x_{1:(n-1)}$ is at most K ,

$$\mathbb{P}(X_n \neq Z_n \mid X_{1:(n-1)} = Z_{1:(n-1)} = x_{1:(n-1)}) \leq \frac{\alpha}{K} \frac{J_n}{n-1+\alpha}. \quad (\text{I.2})$$

The case where $n = 1$ reads that $\mathbb{P}(X_1 \neq Z_1) = 0$. Such a coupling exists because the total variation distance between the prediction rules $X_n \mid X_{1:(n-1)}$ and $Z_n \mid Z_{1:(n-1)}$ is small. Let $\{\psi_j\}_{j=1}^{J_n}$ be the unique atom locations in $x_{1:(n-1)}$ and n_j be the number of latents x_i that manifest atom location ψ_j . The distribution $X_n \mid X_{1:(n-1)}$ can be sampled from in two steps:

- Sample I_1 from the categorical distribution over $J_n + 1$ elements where, for $1 \leq j \leq J_n$, $\mathbb{P}(I_1 = j) = n_j / (n - 1 + \alpha)$ and $\mathbb{P}(I_1 = J_n + 1) = \alpha / (n - 1 + \alpha)$.
- If $I_1 = j$ for $1 \leq j \leq J_n$, set $X_n = \delta_{\psi_j}$. If $I_1 = J_n + 1$, draw a fresh atom from H , label ψ_{J_n+1} and set $X_n = \delta_{\psi_{J_n+1}}$.

Similarly, we can generate $Z_n \mid Z_{1:(n-1)}$ in two steps:

- Sample I_2 from the categorical distribution over $J_n + 1$ elements where, for $1 \leq j \leq J_n$, $\mathbb{P}(I_2 = j) = \frac{n_j + \alpha/K}{n-1+\alpha}$ and $\mathbb{P}(I_2 = J_n + 1) = \frac{\alpha(1-J_n/K)}{n-1+\alpha}$.
- If $I_2 = j$ for $1 \leq j \leq J_n$, set $Z_n = \delta_{\psi_j}$. If $I_2 = J_n + 1$, draw a fresh atom from H , label ψ_{J_n+1} and set $Z_n = \delta_{\psi_{J_n+1}}$.

Still conditioning on $X_{1:(n-1)}$ and $Z_{1:(n-1)}$, we observe that the distribution of $X_n \mid I_1$ is the same as $Z_n \mid I_2$. Hence, using the propagation argument from Lemma E.8, it suffices to couple I_1 and I_2 so that

$$\mathbb{P}(I_1 \neq I_2 \mid X_{1:(n-1)} = Z_{1:(n-1)} = x_{1:(n-1)})$$

is small. Since I_1 and I_2 are categorical distributions, the minimum of the difference probability is the total variation distance between the two distributions, which equals 1/2 the L_1 distance between marginals

$$\sum_{j=1}^{J_n} \left| \frac{n_j + \alpha/K}{n-1+\alpha} - \frac{n_j}{n-1+\alpha} \right| + \left| \frac{\alpha}{n-1+\alpha} - \frac{\alpha(1-J_n/K)}{n-1+\alpha} \right| = 2 \frac{\alpha}{K} \frac{J_n}{n-1+\alpha}.$$

Dividing the last equation by 2 gives Eq. (I.2). The joint coupling of $P_{X_{1:N}}$ and $P_{Z_{1:N}}$ is the natural gluing of the couplings $P_{X_n \mid X_{1:(n-1)}}$ and $P_{Z_n \mid Z_{1:(n-1)}}$.

We now show that for the coupling satisfying Eq. (I.2), the overall probability of difference $\mathbb{P}(X_{1:N} \neq Z_{1:N})$ is small. Recall the growth function from Eq. (18). We will use the notation of a *typical* set in the rest of the proof:

$$\mathcal{D}_n := \{x_{1:(n-1)} : J_n \leq (1 + \delta) \max(C(N, \alpha), C(K, \alpha))\}.$$

In other words, the number of unique values among the $x_{1:(n-1)}$ is small. The constant δ satisfies $\frac{\delta^2}{2+\delta} \alpha = 2$: such δ always exists and is unique. The following decomposition is used

to investigate the difference probability on the typical set:

$$\begin{aligned}\mathbb{P}(X_{1:N} \neq Z_{1:N}) &= \mathbb{P}((X_{1:(N-1)}, X_N) \neq (Z_{1:(N-1)}, Z_N)) \\ &= \mathbb{P}(X_{1:(N-1)} \neq Z_{1:(N-1)}) + \mathbb{P}(X_N \neq Z_N, X_{1:(N-1)} = Z_{1:(N-1)}).\end{aligned}\quad (\text{I.3})$$

The second term can be further expanded:

$$\begin{aligned}\mathbb{P}(X_N \neq Z_N, X_{1:(N-1)} = Z_{1:(N-1)}, X_{1:(N-1)} \in \mathcal{D}_N) \\ + \mathbb{P}(X_N \neq Z_N, X_{1:(N-1)} = Z_{1:(N-1)}, X_{1:(N-1)} \notin \mathcal{D}_N).\end{aligned}$$

The former term is at most

$$\mathbb{P}(X_N \neq Z_N \mid X_{1:(N-1)} = Z_{1:(N-1)}, X_{1:(N-1)} \in \mathcal{D}_N),$$

while the latter term is at most

$$\mathbb{P}(X_{1:(N-1)} \notin \mathcal{D}_N).$$

To recap, we can bound $\mathbb{P}(X_{1:N} \neq Z_{1:N})$ by bounding three quantities:

1. The difference probability of a shorter process $\mathbb{P}(X_{1:(N-1)} \neq Z_{1:(N-1)})$.
2. The difference probability of the prediction rule on typical sets $\mathbb{P}(X_N \neq Z_N \mid X_{1:(N-1)} = Z_{1:(N-1)}, X_{1:(N-1)} \in \mathcal{D}_N)$.
3. The probability of the atypical set $\mathbb{P}(X_{1:(N-1)} \notin \mathcal{D}_N)$.

By recursively applying the expansion initiated in Eq. (I.3) to $\mathbb{P}(X_{1:(N-1)} \neq Z_{1:(N-1)})$, we actually only need to bound difference probability of the different prediction rules on typical sets and the atypical set probabilities.

Regarding difference probability of the different prediction rules, being in the typical set allows us to control J_n in Eq. (I.2). Summation across $n = 1$ through N gives the overall bound of

$$\frac{\alpha}{K}(1 + \delta) \max(C(N, \alpha), C(K, \alpha))C(N, \alpha).\quad (\text{I.4})$$

Regarding the atypical set probabilities, because J_{n-1} is stochastically dominated by J_n i.e., the number of unique values at time n is at least the number at time $n - 1$, all the atypical set probabilities are upper bounded by the last one i.e. $\mathbb{P}(X_{1:(N-1)} \notin \mathcal{D}_N)$. When $N > 1$, J_N is the sum of independent Poisson trials, with an overall mean equaling exactly $C(N - 1, \alpha)$ and J_1 is defined to be 0. Therefore, the atypical event has small probability because of Lemma E.1:

$$\begin{aligned}\mathbb{P}(J_N > (1 + \delta) \max(C(N - 1, \alpha), C(K, \alpha))) &\leq \mathbb{P}(J_N > (1 + \delta) \max(C(N, \alpha), C(K, \alpha))) \\ &\leq \exp\left(-\frac{\delta^2}{2 + \delta} \max(C(N, \alpha), C(K, \alpha))\right).\end{aligned}$$

Even accounting for all N atypical events through union bound, the total probability is still small small:

$$\exp\left(-\left(\frac{\delta^2}{2 + \delta} \max(C(N, \alpha), C(K, \alpha)) - \ln N\right)\right).$$

By Lemma E.10, $\max(C(N, \alpha), C(K, \alpha)) \geq \alpha \max(\ln N, \ln K - \alpha(\psi(\alpha) + 1))$. we have

$$\frac{\delta^2}{2 + \delta} \max(C(N, \alpha), C(K, \alpha)) - \ln N \geq \ln K - \alpha(\psi(\alpha) + 1),$$

meaning the overall atypical probabilities is at most

$$\frac{\exp(\alpha(\psi(\alpha) + 1))}{K}. \quad (\text{I.5})$$

The overall total variation bound combines Eqs. (I.4) and (I.5). We first upper bound $C(N, \alpha)$ using Lemma E.10 and upper bound $\max(C(N, \alpha), C(K, \alpha))$ by the sum of the two constituent terms. We also upper bound $\ln N \leq \ln^2 N / \ln 2$ to remove the dependence on the sole $\ln N$ factor. After the algebraic manipulations, we arrive at the constants in Eq. (I.1)s. \square

Proof of Theorem 4.6. The constants C', C'', C''', C'''' are as follows:

$$\begin{aligned} C' &= \exp(\omega(\psi(\omega) + 1)) + 2\omega^2 \ln^2(1 + 1/\omega), \\ C'' &= \omega^2 + \frac{3\omega^2 \ln(1 + 1/\omega)}{\ln 2}, \\ C''' &= \omega^2, \\ C'''' &= \omega^2 \ln(1 + 1/\omega). \end{aligned}$$

The main idea is reducing to the Dirichlet process mixture model. We do this in two steps.

First, the conditional distribution of the observations $W | H_{1:D}$ of the target model is the same as the conditional distribution $Z | F_{1:D}$ of the approximate model if $H_{1:D} = F_{1:D}$. Second, there exists latent variables Λ and Φ such that the conditional distribution of $H_{1:D} | \Lambda$ and the conditional $F_{1:D} | \Phi$ are the same when $\Lambda = \Phi$. Recall the construction of the F_d in terms of atom locations $\phi_{d,j}$ and stick-breaking weights $\gamma_{d,j}$:

$$\begin{aligned} G_K &\sim \text{FSD}_K(\omega, H), \\ \phi_{dj} | G_K &\stackrel{\text{i.i.d.}}{\sim} G_K(\cdot) && \text{across } d, j, \\ \gamma_{dj} &\stackrel{\text{i.i.d.}}{\sim} \text{Beta}(1, \alpha) && \text{across } d, j \text{ (except } \gamma_{dT} = 1), \\ F_d | \phi_{d,\cdot}, \gamma_{d,\cdot} &= \sum_{i=1}^T \left(\gamma_{di} \prod_{j<i} (1 - \gamma_{dj}) \right) \delta_{\phi_{dj}}. \end{aligned}$$

Similarly H_d is also constructed in terms of atom locations $\lambda_{d,j}$ and stick-breaking weights $\eta_{d,j}$:

$$\begin{aligned} G &\sim \text{DP}(\omega, H), \\ \lambda_{dj} | G &\stackrel{\text{i.i.d.}}{\sim} G(\cdot) && \text{across } d, j, \\ \eta_{dj} &\stackrel{\text{i.i.d.}}{\sim} \text{Beta}(1, \alpha) && \text{across } d, j \text{ (except } \eta_{dT} = 1), \\ H_d | \lambda_{d,\cdot}, \eta_{d,\cdot} &= \sum_{i=1}^T \left(\eta_{di} \prod_{j<i} (1 - \eta_{dj}) \right) \delta_{\lambda_{dj}}. \end{aligned}$$

Therefore, if we set $\Lambda = \{\lambda_{dj}\}_{d,j}$ and $\Phi = \{\phi_{dj}\}_{d,j}$, then $H_{1:D} | \Lambda$ is the same as the conditional $F_{1:D} | \Phi$ if $\Lambda = \Phi$.

Overall, this means that $W | \Lambda$ is the same as $Z | \Phi$. Again by Lemma E.8, we only need to demonstrate a coupling between P_Λ and P_Φ such that the difference probability is small.

From the proof of Theorem 4.1 in Appendix I.1, we already know how to couple P_Λ and P_Φ . On the one hand, since λ_{dj} are conditionally iid given G across d, j , the joint distribution of λ_{dj} is from a DPMM (probability kernel f being Dirac $f(\cdot | x) = \delta_x(\cdot)$) where the underlying DP has concentration ω . On the other hand, since ϕ_{dj} are conditionally iid given G_K across d, j , the joint distribution ϕ_{dj} comes from the finite mixture with FSD $_K$. Each observational process has cardinality DT . Therefore, we can couple P_Λ and P_Φ such that

$$\mathbb{P}(\Lambda \neq \Phi) \leq \frac{C' + C'' \ln^2(DT) + C''' \ln(DT) \ln K + C'''' \ln K}{K},$$

where the constants have been given at the beginning of this proof. \square

I.2. Lower bounds

Proof of Theorem H.2. First we mention which probability kernel f results in the large total variation distance: the pathological f is the Dirac measure i.e., $f(\cdot | x) = \delta_x(\cdot)$. With this conditional likelihood $X_n = Y_n$ and $Z_n = W_n$, meaning:

$$d_{\text{TV}}(P_{N,\infty}, P_{N,K}) = d_{\text{TV}}(P_{X_{1:N}}, P_{Z_{1:N}}).$$

Now we discuss why the total variation is lower bounded by the function of N . Let \mathcal{A} be the event that there are at least $\frac{1}{2}C(N, \alpha)$ unique components in among the latent states:

$$\mathcal{A} := \left\{ x_{1:N} : \#\text{unique values} \geq \frac{1}{2}C(N, \alpha) \right\}.$$

The probabilities assigned to this event by the approximate and the target models are very different from each other. On the one hand, since $K < \frac{C(N, \alpha)}{2}$, under FSD $_K$, \mathcal{A} has measure zero:

$$\mathbb{P}_{Z_{1:N}}(\mathcal{A}) = 0. \quad (\text{I.6})$$

On the other hand, under DP, the number of unique atoms drawn is the sum of Poisson trials with expectation exactly $C(N, \alpha)$. The complement of \mathcal{A} is a lower tail event. Hence by Lemma E.2 with $\delta = 1/2, \mu = C(N, \alpha)$, we have:

$$\mathbb{P}_{X_{1:N}}(\mathcal{A}) \geq 1 - \exp\left(-\frac{C(N, \alpha)}{8}\right) \quad (\text{I.7})$$

Because of Lemma E.10, we can lower bound $C(N, \alpha)$ by a multiple of $\ln N$:

$$\exp\left(-\frac{C(N, \alpha)}{8}\right) \leq \exp\left(-\frac{\alpha \ln N}{8} + \frac{\alpha(\psi(\alpha) + 1)}{8}\right) = \frac{\text{constant}}{N^{\alpha/8}}.$$

We now combine Eqs. (I.6) and (I.7) and recall that total variation is the maximum over probability discrepancies. \square

Proof of Theorem H.3. First we mention which probability kernel f results in the large total variation distance: the pathological f is the Dirac measure i.e., $f(\cdot | x) = \delta_x(\cdot)$.

Now we show that under such f , the total variation distance is lower bounded. Observe that it suffices to understand the total variation between P_{Y_1, Y_2} and P_{W_1, W_2} , because Lemma E.9 already implies

$$d_{\text{TV}}(P_{N, \infty}, P_{N, K}) \geq d_{\text{TV}}(P_{Y_1, Y_2}, P_{W_1, W_2}).$$

Since f is Dirac, $X_n = Y_n$ and $Z_n = W_n$ and we have:

$$d_{\text{TV}}(P_{Y_1, Y_2}, P_{W_1, W_2}) = d_{\text{TV}}(P_{X_1, X_2}, P_{Z_1, Z_2}).$$

Consider the event that the two latent states are equal. Under the target model,

$$\mathbb{P}(X_2 = X_1) = \frac{1}{1 + \alpha},$$

while under the approximate one,

$$\mathbb{P}(Z_2 = Z_1) = \frac{1 + \alpha/K}{1 + \alpha}.$$

They are simple consequences of the prediction rules in Propositions I.1 and I.2. Therefore, there exists a measurable event where the probability mass assigned by the target and approximate models differ by

$$\frac{1 + \alpha/K}{1 + \alpha} - \frac{1}{1 + \alpha} = \frac{\alpha}{1 + \alpha} \frac{1}{K}, \quad (\text{I.8})$$

meaning $d_{\text{TV}}(P_{X_1, X_2}, P_{Z_1, Z_2}) \geq \frac{\alpha}{1 + \alpha} \frac{1}{K}$. □

Appendix J: More ease-of-use results

J.1. Conceptual results (continued.)

We begin by stating the log density of the optimal q_ρ^* under general priors.

Proposition J.1 (Optimal distribution over atom rates). *Define the normalization constant $C := \int_\rho \exp\left(\ln \mathbb{P}(\rho) + \sum_{n,k} \mathbb{E}_{x_{n,k} \sim q_x} \ln \mathbb{P}(x_{n,k} | \rho_k)\right) d\rho$ where $x_{n,k} \sim q_x$ denote the marginal distribution of $x_{n,k}$ under $q_x(x)$ (which is a distribution over the whole set $(x_{n,k})_{n,k}$). Then*

$$q_\rho^*(\rho) = -\ln C + \ln \mathbb{P}(\rho) + \sum_{n,k} \mathbb{E}_{x_{n,k} \sim q_x} \ln \ell(x_{n,k} | \rho_k). \quad (\text{J.1})$$

The proof of Proposition J.1 is given in Appendix J.2.

Knowing the log density Eq. (J.1) does not mean that drawing inference is easy. By drawing inference, we mean computing posterior expectations of important integrands. Polynomials (such as ρ_k) are natural integrands. In addition, we also need to compute quantities like $\mathbb{E}_{\rho_k \sim q_\rho} \{\ln \ell(x_{n,k} | \rho_k)\}$ to derive the optimal distribution for $q_x(x)$.

Proposition J.2. *Suppose that the variational distribution $q_x(x)$ factorizes as $q_x(x) = \prod_{n,k} f_{n,k}(x_{n,k})$. For a particular n, k , let $f_{n,k}^*$ be the optimal distribution over (n, k) trait count with all other variational distributions being fixed i.e.*

$$f_{n,k}^* := \arg \min_{f_{n,k}} KL \left(q_\rho q_\psi f_{n,k} \prod_{(n',k') \neq (n,k)} f_{n',k'} \parallel \bar{P} \right),$$

where \bar{P} denotes the posterior $\mathbb{P}(\cdot, \cdot, \cdot | y)$. Then, the p.m.f. of $f_{n,k}^*$ at $x_{n,k}$ is equal to

$$-\ln C + \mathbb{E}_{\rho_k \sim q_\rho} \ln \ell(x_{n,k} | \rho_k) + \mathbb{E}_{\psi \sim q_\psi, x_{n,-k} \sim f_{n,-k}} \ln \mathbb{P}(y_n | x_{n,\cdot}, \psi).$$

for some positive constant C .

See Appendix J.2 for the proof of this proposition.

Under TFAs such as Example 5.1, since we cannot identify the log density in Eq. (J.1) with a well-known distribution, we do not have formulas for expectations. For Example 5.1, strategies to make computing expectations more tractable include introducing auxiliary round indicator variables r_k , replacing the product $\prod_{l=1}^{i-1} (1 - V_{i,j}^{(l)})$ with a more succinct representation and fixing the functional form q_ρ rather than using optimality conditions (Paisley, Carin and Blei, 2011, Section 3.2). However, Paisley, Carin and Blei (2011, Section 3.3) still runs into intractability issues when evaluating $\mathbb{E}_{\rho_k \sim q_\rho} \{\ln \ell(x_{n,k} | \rho_k)\}$ in the beta-Bernoulli process, and additional approximations such as Taylor series expansion are needed.

In our second TFA example, the complete conditional of the atom sizes can be sampled without auxiliary variables, but important expectations are not analytically tractable.

Example J.1 (Bondesson approximation (Doshi-Velez et al., 2009; Teh, Görür and Ghahramani, 2007)). When $\alpha = 1$, the Bondesson approximation in Example 4.3 becomes

$$\Theta_K = \sum_{i=1}^K \rho_i \delta_{\psi_i}, \quad \rho_i = \prod_{j=1}^i p_j, \quad p_j \stackrel{\text{i.i.d.}}{\sim} \text{Beta}(\gamma, 1), \quad \psi_i \stackrel{\text{i.i.d.}}{\sim} H. \quad (\text{J.2})$$

The atom sizes are dependent because they jointly depend on p_1, \dots, p_K , but the complete conditional of atom sizes $\mathbb{P}(\rho | x)$ admits a density proportional to

$$\mathbf{1}\{0 \leq \rho_K \leq \rho_{K-1} \leq \dots \leq \rho_1 \leq 1\} \prod_{j=1}^K \rho_j^{\mathbf{1}\{j=K\} + \sum_{n=1}^N x_{n,j} - 1} (1 - \rho_j)^{N - \sum_{n=1}^N x_{n,j}}.$$

The conditional distributions $\mathbb{P}(\rho_i | \rho_{-i}, x)$ are truncated betas, so adaptive rejection sampling (Gilks and Wild, 1992) can be used as a sub-routine to sample each $\mathbb{P}(\rho_i | \rho_{-i}, x)$ and then sweep over all atom sizes. However, for this exponential family, expectations of the sufficient statistics are not tractable. The optimal q_ρ^* in the sense of Eq. (22) has a density proportional to

$$\mathbf{1}\{0 \leq \rho_K \leq \rho_{K-1} \leq \dots \leq \rho_1 \leq 1\} \prod_{j=1}^K \rho_j^{\mathbf{1}\{j=K\} + \sum_{n=1}^N \mathbb{E}_{q_x} x_{n,j} - 1} (1 - \rho_j)^{N - \sum_{n=1}^N \mathbb{E}_{q_x} x_{n,j}}.$$

We do not know closed-form formulas for $\mathbb{E}\{\ln(\rho_i)\}$ or $\mathbb{E}\{\ln(1 - \rho_i)\}$. Rather than using the q_ρ^* which comes from optimality arguments, Doshi-Velez et al. (2009) fixes the functional form of the variational distribution. Even then, further approximations such as Taylor series expansion are necessary to approximate $\mathbb{E}\{\ln(\rho_i)\}$ or $\mathbb{E}\{\ln(1 - \rho_i)\}$.

Other series-based approximations, like thinning or rejection sampling (Campbell et al., 2019), are characterized by even less tractable dependencies between atom sizes in both the prior and the conditional $\mathbb{P}(\rho | x)$.

J.2. Proofs

Proof of Proposition 5.1. Because of the Markov blanket, conditioning on x, ψ, y is the same as conditioning on x :

$$\mathbb{P}(\rho | x, \psi, y) = \mathbb{P}(\rho | x).$$

Conditioned on the atom rates, the trait counts are independent across the atoms. In the prior over atom rates, the atom rates are independent across the atoms. These facts mean that the posterior also factorizes across the atoms

$$\mathbb{P}(\rho | x) = \prod_{k=1}^K \mathbb{P}(\rho_k | x_{.,k})$$

We look at each factor $\mathbb{P}(\rho_k | x_{.,k})$. This is the posterior for ρ_k after observing N observations $(x_{n,k})_{n=1}^N$. Since the AIFA prior over ρ_k is the conjugate prior of the trait count likelihood, the posterior is in the same exponential family, with updated parameters based on the sufficient statistics and the log partition function. \square

Proof of Proposition J.1. Minimizing the KL divergence is equivalent to maximizing the evidence lower bound (ELBO):

$$\text{ELBO}(q) := \mathbb{E}_{(\rho, \psi, x) \sim q} \ln \mathbb{P}(y, \rho, \psi, x) - \mathbb{E}_{(\rho, \psi, x) \sim q} \ln q(\rho, \psi, x). \quad (\text{J.3})$$

The log joint probability $\mathbb{P}(y, \rho, \psi, x)$, regardless of the prior over ρ , decomposes as

$$\begin{aligned} \ln \mathbb{P}(y, \rho, \psi, x) &= \ln \mathbb{P}(\rho) + \sum_k \ln \mathbb{P}(\psi_k) \\ &\quad + \sum_{n,k} \ln \mathbb{P}(x_{n,k} | \rho_k) + \sum_n \ln \mathbb{P}(y_n | x_{n.,}, \psi). \end{aligned} \quad (\text{J.4})$$

Recall that the variational distribution factorizes like as $q(\rho, \psi, x) = q_\rho(\rho)q_\psi(\psi)q_x(x)$. Therefore, for fixed $q_\psi(\psi)$ and $q_x(x)$, the ELBO from Eq. (J.3) depends on $q_\rho(\rho)$ only through

$$f(q_\rho) := \mathbb{E}_{\rho \sim q_\rho} \ln \mathbb{P}(\rho) + \sum_{n,k} \mathbb{E}_{x_{n,k} \sim q_x, \rho_k \sim q_\rho} \ln \mathbb{P}(x_{n,k} | \rho_k) - \mathbb{E}_{\rho \sim q_\rho} \ln q_\rho(\rho).$$

Here, the notation $\rho_k \sim q_\rho$ means the marginal distribution of ρ_k under q_ρ . Using Fubin's theorem, we rewrite the last integral as

$$f(q_\rho) = -\mathbb{E}_{\rho \sim q_\rho} \ln \frac{q_\rho(\rho)}{\mathbb{P}(\rho) \times \exp(\sum_{n,k} \mathbb{E}_{x_{n,k} \sim q_x} \ln \mathbb{P}(x_{n,k} | \rho_k))}$$

The denominator $\mathbb{P}(\rho) \times \exp(\sum_{n,k} \mathbb{E}_{x_{n,k} \sim q_x} \ln \mathbb{P}(x_{n,k} | \rho_k))$ is exactly equal to $Cq_0(\rho)$ where $\ln q_0(\rho) = -\ln C + \ln \mathbb{P}(\rho) + \sum_{n,k} \mathbb{E}_{x_{n,k} \sim q_x} \ln \ell(x_{n,k} | \rho_k)$. Therefore

$$f(q_\rho) = -\text{KL}(q_\rho || q_0) + \ln C.$$

This means that the unique maximizer of $f(q_\rho)$ is $q_\rho = q_0$ i.e. the log density of q_ρ^* is as given in Eq. (J.1). \square

Proof of Corollary 5.2. We specialize the formula in Eq. (J.1) to the AIFA prior.

Recall the exponential-family form of $\ell(x_{n,k} \mid \rho_k)$:

$$\ell(x_{n,k} \mid \rho_k) = \ln \kappa(x_{n,k}) + \phi(x_{n,k}) \ln \rho_k + \langle \mu(\rho_k), t(x_{n,k}) \rangle - A(\rho_k). \quad (\text{J.5})$$

Next, observe that $\mathbb{E}_{x_{n,k} \sim q_x} \ln \ell(x_{n,k} \mid \rho_k)$ is equal to

$$\mathbb{E}_{x_{n,k} \sim q_x} \ln \kappa(x_{n,k}) + \mathbb{E}_{x_{n,k} \sim q_x} \phi(x_{n,k}) \times \ln \rho_k + \langle \mu(\rho_k), \mathbb{E}_{x_{n,k} \sim q_x} t(x_{n,k}) \rangle - A(\rho_k). \quad (\text{J.6})$$

Recall that AIFA prior over ρ_k is the conjugate prior for the likelihood in Eq. (J.5):

$$\ln \mathbb{P}(\rho_k) = (c/K - 1) \ln \rho_k + \left\langle \begin{bmatrix} \psi \\ \lambda \end{bmatrix}, \begin{bmatrix} \mu(\rho_k) \\ -A(\rho_k) \end{bmatrix} \right\rangle - \ln Z(c/K - 1, \begin{bmatrix} \psi \\ \lambda \end{bmatrix}), \quad (\text{J.7})$$

and the prior factorizes across atoms:

$$\ln \mathbb{P}(\rho) = \sum_k \ln \mathbb{P}(\rho_k)$$

Putting Eq. (J.6) and Eq. (J.7) together, We have

$$\ln \mathbb{P}(\rho) + \sum_{n,k} \mathbb{E}_{x_{n,k} \sim q_x} \ln \ell(x_{n,k} \mid \rho_k) = \sum_k T_k(\rho_k)$$

where $T_k(\rho_k)$ is equal to

$$(c/K + \sum_n \mathbb{E}_{x_{n,k} \sim q_x} \phi(x_{n,k}) - 1) \ln \rho_k + \left\langle \begin{bmatrix} \psi + \sum_n \mathbb{E}_{x_{n,k} \sim q_x} t(x_{n,k}) \\ \lambda + N \end{bmatrix}, \begin{bmatrix} \mu(\rho_k) \\ -A(\rho_k) \end{bmatrix} \right\rangle$$

Accounting for the normalization constant Z_k for each dimension k , we arrive at Eq. (23). \square

Proof of Proposition J.2. The argument is the same as Appendix J.2. In the overall ELBO, the only terms that depend on $f_{n,k}$ is

$$\begin{aligned} & \mathbb{E}_{x_{n,k} \sim f_{n,k}, \rho_k \sim q_\rho} \ln \ell(x_{n,k} \mid \rho_k) + \mathbb{E}_{x_{n,k} \sim f_{n,k}, x_{n,-k} \sim f_{n,-k}, \psi \sim q_\psi} \ln \mathbb{P}(y_n \mid x_{n,\cdot}, \psi) \\ & - \mathbb{E}_{x_{n,k} \sim f_{n,k}} \ln f_{n,k}(x_{n,k}). \end{aligned}$$

We use Fubini to express the last integral as a negative KL-like quantity, and use optimality of KL arguments to derive the p.m.f. of the minimizer. \square

Appendix K: Experimental setup

In this section, the notation for atom sizes, atom locations, latent trait counts and observed data follow that of Section 5 i.e. $(\rho_k)_{k=1}^K$ denotes the collection of atom sizes, $(\psi_k)_{k=1}^K$ denotes the collection of atom locations, $(x_{n,k})_{k=1, n=1}^{K,N}$ denotes the latent trait counts of each observation, and $(y_n)_{n=1}^N$ denotes the observed data.

K.1. Image denoising using the beta–Bernoulli process

Data. We obtain the “clean” house image from <http://sipi.usc.edu/database/>. We downscale the original 512×512 image to 256×256 and convert colors to gray scale. We add iid Gaussian noise to the pixels of the clean image, resulting in the noisy input image. We follow Zhou et al. (2009) in extracting the patches. We use patches of size 8×8 , and flatten each observed patch y_i into a vector in \mathbb{R}^{64} .

Finite approximations. We use finite approximations that target the beta–Bernoulli process with BP(1, 1, 0) i.e. $\gamma = 1, \alpha = 1, d = 0$. Zhou et al. (2009) remark that the denoising performance is not sensitive to the choice of γ and α . Therefore, we pick $\gamma = \alpha = 1$ for computational convenience, since the beta process with $\alpha = 1$ has the simple TFA in Example J.1. To be explicit, the TFA for the given beta–Bernoulli process is

$$\begin{aligned} v_j &\stackrel{\text{i.i.d.}}{\sim} \text{Beta}(1, 1), \quad i = 1, 2, \dots, K, \\ \rho_i &= \prod_{j=1}^i v_j, \quad i = 1, 2, \dots, K, \\ x_{n,i} | \rho_i &\stackrel{\text{indep}}{\sim} \text{Ber}(\rho_i), \quad \text{across } n, i. \end{aligned} \tag{K.1}$$

while the corresponding AIFA is

$$\begin{aligned} \rho_i &\stackrel{\text{i.i.d.}}{\sim} \text{Beta}\left(\frac{1}{K}, 1\right), \quad i = 1, 2, \dots, K, \\ x_{n,i} | \rho_i &\stackrel{\text{indep}}{\sim} \text{Ber}(\rho_i), \quad \text{across } n, i. \end{aligned} \tag{K.2}$$

We report the performance for K 's between 10 and 100 with spacing 10.

Ground measure and observational likelihood. Following Zhou et al. (2009), we fix the ground measure but put a hyper-prior (in the sense of Corollary G.1) on the observational likelihood. The ground measure is a fixed Gaussian distribution:

$$\psi_i \stackrel{\text{i.i.d.}}{\sim} \mathcal{N}\left(0, \frac{1}{64} \mathbf{I}_{64}\right), \quad i = 1, 2, \dots, K. \tag{K.3}$$

The observational likelihood involves two Gaussian distributions with random variances:

$$\begin{aligned} \gamma_w &\sim \text{Gamma}(10^{-6}, 10^{-6}), \\ \gamma_e &\sim \text{Gamma}(10^{-6}, 10^{-6}), \\ w_{n,i} | \gamma_w &\stackrel{\text{i.i.d.}}{\sim} \mathcal{N}(0, \gamma_w^{-1}), \quad \text{across } i, n, \\ y_n | x_{n,\cdot}, w_{n,\cdot}, \psi, \gamma_e &\stackrel{\text{indep}}{\sim} \mathcal{N}\left(\sum_{i=1}^K x_{n,i} w_{n,i} \psi_i, \gamma_e^{-1} \mathbf{I}_{64}\right), \quad \text{across } n. \end{aligned} \tag{K.4}$$

We use the (shape,rate) parametrization of the gamma distribution. The weights $w_{n,i}$ enable an observation to manifest a non-integer (and potentially negative) scaled version of the i -th basis element. The precision γ_w determines the scale of these weights. The precision γ_e determines the noise variance of the observations. We are uninformative about the precisions by choosing the $\text{Gamma}(10^{-6}, 10^{-6})$ priors.

In sum, the full finite models combine either Eqs. (K.2), (K.3) and (K.4) (for AIFA) or Eqs. (K.1), (K.3) and (K.4) (for TFA).

Approximate inference. We use Gibbs sampling to traverse the posterior over all the latent variables — the ones that are most important for denoising are x, w, ψ . The chosen ground measure and observational likelihood have the right conditional conjugacies so that blocked Gibbs sampling is conceptually simple for most of the latent variables. The only

difference between AIFA and TFA is the step to sample the feature proportions ρ : TFA updates are much more involved compared to AIFA (see Section 5). The order in which Gibbs sampler scans through the blocks of variables does not affect the denoising quality. To generate the PSNR in Fig. 2a, after finishing the gradual introduction of all patches, we run 150 Gibbs sweeps. We use the final state of the latent variables at the end of these Gibbs sweep as the warm-start configurations in Figs. 2b and 2c.

Evaluation metric. We discuss how iterates from Gibbs sampling define output images. Each configuration of x, w, ψ defines each patch’s “noiseless” value:

$$\tilde{y}_n = \sum_{i=1}^K x_{n,i} w_{n,i} \psi_i.$$

Each pixel in the overall image is covered by a small number of patches. The “noiseless” value of each pixel is the average of the pixel value suggested by the various patches that cover that pixel. We aggregate the output images across Gibbs sweeps by a simple weighted averaging mechanism. We report the PSNR of the output image with the original image following the formulas from Hore and Ziou (2010).

K.2. Topic modelling with the modified HDP

Data. We download and pre-process into bags-of-words about one million random Wikipedia documents, following Hoffman, Bach and Blei (2010).

Finite models. We fix the ground measure to be a Dirichlet distribution and the observational likelihood to be a categorical distribution i.e. no hyper-priors. The AIFA is

$$\begin{aligned} G_0 &\sim \text{FSD}_K(\omega, \text{Dir}(\eta \mathbf{1}_V)), \\ G_d | G_0 &\stackrel{\text{i.i.d.}}{\sim} \text{TSB}_T(\alpha, G_0), && \text{across } d, \\ \beta_{dn} | G_d &\stackrel{\text{indep}}{\sim} G_d(\cdot), && \text{across } d, n, \\ w_{dn} | \beta_{dn} &\stackrel{\text{indep}}{\sim} \text{Categorical}(\beta_{dn}), && \text{across } d, n. \end{aligned}$$

while the TFA is

$$\begin{aligned} G_0 &\sim \text{TSB}_K(\omega, \text{Dir}(\eta \mathbf{1}_V)), \\ G_d | G_0 &\stackrel{\text{i.i.d.}}{\sim} \text{TSB}_T(\alpha, G_0), && \text{across } d, \\ \beta_{dn} | G_d &\stackrel{\text{indep}}{\sim} G_d(\cdot), && \text{across } d, n, \\ w_{dn} | \beta_{dn} &\stackrel{\text{indep}}{\sim} \text{Categorical}(\beta_{dn}), && \text{across } d, n. \end{aligned}$$

We set the hyperparameters η, α, ω , and T following Wang, Paisley and Blei (2011), in that $\eta = 0.01, \alpha = 1.0, \omega = 1.0, T = 20$. We report the performance for K ’s between 20 and 300 with spacing 40.

Approximate inference. We approximate the posterior in each model using stochastic variational inference (Hoffman et al., 2013). Both models have conditional conjugacies that enable the use of exponential family variational distributions and closed-form expectation

equations for all update types. The batch size is 500. We use the learning rate $(t + \tau)^{-\kappa}$, where t is the number of data mini-batches. For cold-start experiments, we set $\tau = 1.0$ and $\kappa = 0.9$. To generate the results of Fig. 3a, we process 4000 mini-batches of documents. We obtain the warm-start initializations in Figs. 3b and 3c by processing 512 mini-batches of documents. When training from warm-start initialization, to reflect the fact that the initial topics are the results of a training period, we change $\tau = 512$, but use the same κ as cold start.

Evaluation metrics. We compute held-out log-likelihood following Hoffman et al. (2013). Each test document d' is separated into two parts w_{ho} and w_{obs} ²², with no common words between the two. In our experiments, we set 75% of words to be observed, the remaining 25% unseen. The predictive distribution of each word w_{new} in the w_{ho} is exactly equal to:

$$p(w_{new} | \mathcal{D}, w_{obs}) = \int_{\theta_{d'}, \beta} p(w_{new} | \theta_{d'}, \beta) p(\theta_{d'}, \beta | \mathcal{D}, w_{obs}) d\theta_{d'} d\beta.$$

This is an intractable computation as the posterior $p(\theta_{d'}, \beta | \mathcal{D}, w_{obs})$ is not analytical. We approximate it with a factorized distribution:

$$p(\theta_{d'}, \beta | \mathcal{D}, w_{obs}) \approx q(\beta | \mathcal{D}) q(\theta_{d'}),$$

where $q(\beta | \mathcal{D})$ is fixed to be the variational approximation found during training and $q(\theta_{d'})$ minimizes the KL between the variational distribution and the posterior. Operationally, we do an E-step for the document d' based on the variational distribution of β and the observed words w_{obs} , and discard the distribution over $z_{d', \cdot}$, the per-word topic assignments because of the mean-field assumption. Using those approximations, the predictive approximation is approximately:

$$p(w_{new} | \mathcal{D}, w_{obs}) \approx \tilde{p}(w_{new} | \mathcal{D}, w_{obs}) = \sum_{k=1}^K \mathbb{E}_q(\theta_{d'}(k)) \mathbb{E}_q(\beta_k(w_{new})),$$

and the final number we report for document d' is:

$$\frac{1}{|w_{ho}|} \sum_{w \in w_{ho}} \ln \tilde{p}(w | \mathcal{D}, w_{obs}).$$

K.3. Comparing IFAs

Data. For the AIFA versus BFRY IFA comparison i.e. Fig. 4a, we generate synthetic data $\{y_n\}_{n=1}^{2000}$ from a power-law beta-Bernoulli process $\text{BP}(2, 0, 0.6)$.

$$\begin{aligned} \sum_{i=1}^{\infty} \theta_i \psi_i &\sim \text{BP}(2, 0, 0.6; \mathcal{N}(0, 5I_5)), \\ x_{n,i} | \theta_i &\stackrel{\text{indep}}{\sim} \text{Ber}(\theta_i), && \text{across } n, i, \\ y_n | x_{n,\cdot}, \psi &\stackrel{\text{indep}}{\sim} \mathcal{N}\left(\sum_i x_{n,i} \psi_i, I_5\right), && \text{across } n. \end{aligned}$$

²²How each document is separated into these two parts can have an impact on the range of test log-likelihood values encountered. For instance, if the first (in order of appearance in the document) $x\%$ of words were the observed words and the last $(100 - x)\%$ words were unseen, then the test log-likelihood is low, presumably since predicting future words using only past words and without any filtering is challenging. Randomly assigning words to be observed and unseen gives better test log-likelihood.

For the AIFA vs GenPar IFA comparison i.e. Fig. 4b, we use the same generative process except the beta process is $\text{BP}(2, 1.0, 0.6)$. We marginalize out the feature proportions θ_i and sample the assignment matrix $X = \{x_{n,i}\}$ from the power-law Indian buffet process (Teh and Görür, 2009). The feature means are Gaussian distributed, with prior mean 0 and prior covariance $5I_5$. Conditioned on the feature combination, the observations are Gaussian with noise variance I_5 . Since the data is exchangeable, without loss of generality, we use $y_{1:1500}$ for training and $y_{1501:2000}$ for evaluation.

Finite approximations. We use finite approximations that have exact knowledge of the beta process hyperparameters. For instance, for the AIFA versus BFRY IFA comparison, we use K -atom AIFA prior with densities

$$\nu_{\text{AIFA}}(d\theta) := \frac{\mathbf{1}\{0 \leq \theta \leq 1\}}{Z_K} \theta^{-1+c/K-0.6S(\theta-1/K)} (1-\theta)^{-0.4} d\theta, \quad (\text{K.5})$$

where $c := \frac{2}{B(0.6, 0.4)}$ and $S(\theta) = \begin{cases} \exp\left(\frac{-1}{1-K^2(\theta-1/K)^2} + 1\right) & \text{if } \theta \in (0, 1/K) \\ \mathbf{1}\{\theta > 0\} & \text{otherwise.} \end{cases}$, and Z_K is the suitable normalization constant.

In all, the approximation to the beta–Bernoulli part of the generative process is

$$\begin{aligned} \rho_i &\stackrel{\text{i.i.d.}}{\sim} \tilde{\nu}(\cdot) && \text{for } i \in [K], \\ x_{n,i} \mid \rho_i &\stackrel{\text{indep}}{\sim} \text{Ber}(\rho_i) && \text{across } n, i, \end{aligned} \quad (\text{K.6})$$

where $\tilde{\nu}(\cdot)$ is either ν_{AIFA} , ν_{BFRY} or ν_{GenPar} . We report the performance for K from 2 to 100.

Ground measure and observational likelihood. We use hyper-priors in the sense of Corollary G.1. The ground measure is random because the we do not fix the variance of the feature means.

$$\begin{aligned} \sigma_g &\sim \text{Gamma}(5, 5), \\ \psi_i &\stackrel{\text{i.i.d.}}{\sim} \mathcal{N}(0, \sigma_g^2 I_5) \text{ for } i \in [K]. \end{aligned} \quad (\text{K.7})$$

The observational likelihood is also random because we do not fix the noise variance of the observed data.

$$\begin{aligned} \sigma_c &\sim \text{Gamma}(5, 5), \\ y_n \mid x_{n,\cdot}, \psi, \sigma_c &\stackrel{\text{indep}}{\sim} \mathcal{N}\left(\sum_i x_{n,i} \psi_i, \sigma_c^2 I_5\right). \end{aligned} \quad (\text{K.8})$$

In Eqs. (K.7) and (K.8), we use the (shape, rate) parametrization of the gamma distribution. The full finite models are described by Eqs. (K.6), (K.7) and (K.8).²³

Approximate inference. We use mean-field variational inference to approximate the posterior. We pick the variational distribution $q(\sigma_c, \sigma_g, \rho, \psi, x)$ with the following factorization structure:

$$q(\sigma_c) q(\sigma_g) \prod_i q(\rho_i) \prod_i q(\psi_i) \prod_{i,n} q(x_{n,i}).$$

²³During inference, we add a small tolerance of 10^{-3} to the standard deviations $\sigma_c, \sigma_g, \zeta_i$ in the model to avoid singular covariance matrices, although this is not strictly necessary if we clip gradients.

Each variation distribution is the natural exponential family. Specifically, we have $q(\sigma_c) = \text{Gamma}(\nu_c(0), \nu_c(1))$, $q(\sigma_g) = \text{Gamma}(\nu_g(0), \nu_g(1))$, $q(\psi_i) = \mathcal{N}(\tau_i, \zeta_i)$, $q(\rho_i) = \text{Beta}(\kappa_i(0), \kappa_i(1))$, $q(x_{n,i}) = \text{Ber}(\phi_{n,i})$. We set the initial variational parameters using the latent features, feature assignment matrix, and the variances of the features prior and the observations around the feature combination. We use the ADAM optimizer in Pyro (learning rate 0.001, $\beta_1 = 0.9$, clipping gradients if their norms exceed 40) to minimize the KL divergence between the approximation and exact posterior. We sub-sample 50 data points at a time to form the objective for stochastic variational inference. We terminate training after processing 5,000 mini-batches of data.

Evaluation metrics. We use the following definition of predictive likelihood:

$$\sum_{i=1}^m \ln \mathbb{P}(y_{n+i} | y_{1:n}), \quad (\text{K.9})$$

where $y_{1:n}$ are the training data and $\{y_{n+i}\}_{i=1}^m$ are the held-out data points.

We estimate $\mathbb{P}(y_{n+i} | y_{1:n})$ using Monte Carlo samples, since the predictive likelihood is an integral of the posterior over training data:

$$\mathbb{P}(y_{n+i} | y_{1:n}) = \int_{x_{n+i}, \sigma, \psi, \rho} \mathbb{P}(y_{n+i} | x_{n+i}, \psi, \sigma) \mathbb{P}(x_{n+i}, \psi, \sigma, \rho | y_{1:n}),$$

where x_{n+i} is the assignment vector of the $n+i$ test point. Define the S Monte Carlo samples of the variational approximation to the posterior as $(x_{(n+1):(n+m)}^s, \rho^s, \psi^s, \sigma^s)_{s=1}^S$. We jointly estimate $\mathbb{P}(y_{n+i} | y_{1:n})$ across test points y_{n+i} using the S Monte Carlo samples:

$$\mathbb{P}(y_{n+i} | y_{1:n}) \approx \frac{1}{S} \sum_{s=1}^S \mathbb{P}(y_{n+i} | x_{n+i}^s, \psi^s, \sigma^s).$$

We use $S = 1,000$ samples from the (approximate) posterior to estimate the average log test-likelihood in Eq. (K.9).

K.4. Beta process hyperparameter estimation

Data. In this experiment, the number of observations, or the number of rows in the feature matrix, is $N = 1000$. For discount estimation, we generate 50 matrices from the corresponding IBP (Teh and Görür, 2009) with for mass $\gamma = 3.0$, concentration $\alpha = 1.0$ and discount varying from 0 through 0.5. For mass estimation, we generate 50 matrices from the IBP with concentration $\alpha = 1.0$, discount $d = 0.25$ and mass varying from 1.0 through 5.0. For the concentration estimation, we generate 50 matrices from the IBP with mass $\alpha = 3.0$, discount $d = 0.25$ and concentration varying from 0 through 5.0.

AIFA marginal likelihood. The K -atom AIFA rates define a generative process over feature matrices with N rows and K columns:

$$\begin{aligned} \theta_k &\stackrel{\text{i.i.d.}}{\sim} \text{AIFA}_K && \text{across } k, \\ x_{n,k} | \theta_k &\stackrel{\text{indep}}{\sim} \text{Ber}(\theta_k) && \text{across } n, k. \end{aligned}$$

$x_{n,k}$ is the entry in the n th row and k th column of the feature matrix. Treating the beta process hyperparameters γ, α, d as unknowns, we compute the probability of observing a particular feature matrix $\{x_{n,k}\}$ (integrating out the AIFA rates) as a function of γ, α, d . By symmetry and independence among the columns $x_{.,k}$, it suffices to compute the probability of observing just one column, say $\{x_{n,1}\}_{n=1}^N$. Conditioned on θ_1 , the probability of observing $\{x_{n,1}\}_{n=1}^N$ is exactly

$$\prod_{n=1}^N \theta_1^{x_{n,1}} (1 - \theta_1)^{1-x_{n,1}}$$

We integrate out θ_1 to compute the marginal likelihood. Recall that $c(\gamma, \alpha, d) = \gamma/B(\alpha + d, 1 - d)$ for the beta process AIFA. The marginal likelihood of observing the first column $\{x_{n,1}\}_{n=1}^N$ is

$$\begin{aligned} \mathbb{E}_{\theta \sim \text{AIFA}_K} \left[\prod_{n=1}^N \theta_1^{x_{n,1}} (1 - \theta_1)^{1-x_{n,1}} \right] \\ = \frac{\int_0^1 \theta^{-1+c(\gamma, \alpha, d)/K + \sum_n x_{n,1} - dS_{1/K}(\theta-1/K)} (1 - \theta)^{\alpha+d+N-\sum_n x_{n,1}-1} d\theta}{\int_0^1 \theta^{-1+c(\gamma, \alpha, d)/K - dS_{1/K}(\theta-1/K)} (1 - \theta)^{\alpha+d-1} d\theta}. \end{aligned}$$

In all, if we denote

$$Z_K(\gamma, \alpha, d; x, y) := \int_0^1 \theta^{-1+c(\gamma, \alpha, d)/K + x - dS_{1/K}(\theta-1/K)} (1 - \theta)^{\alpha+d+(y-x)-1} d\theta,$$

then the marginal probability of observing a particular binary matrix $\{x_{n,k}\}$, as a function of γ, α, d , is

$$\prod_{k=1}^K \frac{Z_K(\gamma, \alpha, d; \sum_n x_{n,k}, N)}{Z_K(\gamma, \alpha, d; 0, 0)}. \quad (\text{K.10})$$

For feature matrices coming from an IBP, the number of columns \widehat{K} is random, and usually (much) smaller than the number of atoms in the approximation. In this section, the approximation level is $K = 100,000$: the distribution of the number of active features in the finite model (for $d \in [0, 0.5]$) has no noticeable change between $K = 100,000$ and $K > 100,000$. The fact that $K - \widehat{K}$ columns are missing is the same as $K - \widehat{K}$ columns being identically zero; hence, when evaluating the marginal probability of matrices that have less than K columns, we simply pad the missing columns with zeros.

It remains to show how to compute Eq. (K.10) using numerical methods. The bottleneck is computing $Z_K(\gamma, \alpha, d; x, y)$. We split the integral into two disjoint domains. The first domain is $(0, 1/K)$: on this domain, the integral is an incomplete beta integral, which is implemented in libraries such as Virtanen et al. (2020). The second domain is $[1/K, 1]$. On this domain, we first compute m^* , the maximum value of the integrand $\theta^{-1+c(\gamma, \alpha, d)/K + x - dS_{1/K}(\theta-1/K)} (1 - \theta)^{\alpha+d+(y-x)-1}$. We then use numerical integration to integrate $\theta^{-1+c(\gamma, \alpha, d)/K + x - dS_{1/K}(\theta-1/K)} (1 - \theta)^{\alpha+d+(y-x)-1} / m^*$. We divide by m^* to avoid the integrand getting too small, which happens if x or y are large. The last integrand is well-behaved (bounded and smooth), and we expect numerical integration to be accurate.

Marginal likelihood under BFRY IFA (or GenPar IFA) are challenging to estimate. In theory, for the BFRY IFA, it is also possible to express the marginal likelihood

(as a function of γ, α, d) for an observed feature matrix $x_{n,k}$ under the BFRY IFA prior as a ratio between normalization constants. However, we run into numerical issues (divergence errors) computing the BFRY IFA normalization constants that are not present in computing the AIFA normalization constants. For completeness, the BFRY IFA normalization constants are of the kind

$$Z_{\text{BFRY}}(\gamma, d; x, y) = \int_0^1 \frac{\gamma/K}{B(d, 1-d)} \theta^{x-d-1} (1-\theta)^{y-x+d-1} \left[1 - \exp\left(-\left(Kd/\gamma\right)^{1/d} \frac{\theta}{1-\theta}\right) \right]. \quad (\text{K.11})$$

Whether this integral has a closed-form solution is unknown: the closed-form marginal likelihoods from Lee, James and Choi (2016) apply to clustering models from normalized CRMs rather than feature-allocation models from unnormalized CRMs. Numerical integration struggles with Equation (K.11) for $x = 0$. $(Kd/\gamma)^{1/d}$ is typically very large: when $\gamma = 1, d = 0.1$, even $K = 100$ leads to $(Kd/\gamma)^{1/d}$ being on the order of 10^{20} . As a result, under standard floating point precision, $1 - \exp\left(-\left(Kd/\gamma\right)^{1/d} \frac{\theta}{1-\theta}\right)$ evaluates to 1 on all points of the quadrature grid: this leads to divergent behavior, as the factor θ^{-d-1} by itself grows too fast near 0.

We resort to Monte Carlo to estimate the normalization constant. In each Monte Carlo batch, we draw K random variables $\theta_1, \theta_2, \dots, \theta_K$ from the BFRY density Eq. (4), and estimate the log of $Z_{\text{BFRY}}(\gamma, d; x, y)$ with

$$\text{logsumexp} \left\{ \left[(x-d-1) \ln \theta_k + (y-x+d-1) \ln(1-\theta_k) - \ln K \right] \right\}_{k=1}^K.$$

In the left panel of Fig. 5b, we first generate an feature matrix from IBP with mass 3.0, concentration 0.0 and discount 0.25. We then plot the estimate of the marginal likelihood under BFRY IFA for this feature matrix as a function of d for mass fixed at 3.0 and discount fixed at 0.0.

GenPar IFA faces similar problems as BFRY IFA. We are not aware of a closed-form formula for the marginal likelihood. Namely, we are not able to show that Eq. (5) is a conjugate prior for the Bernoulli likelihood: when we observe an observation $X = 1$ from the model $X \sim \text{Ber}(\theta), \theta \sim \nu_{\text{GenPar}}$, the posterior density for θ is proportional to

$$\frac{\theta^{-d}(1-\theta)^{\alpha+d-1}}{B(1-d, \alpha+d)} \left(1 - \frac{1}{\left(\theta \left[\left(1 + \frac{Kd}{\gamma\alpha} \right)^{1/d} - 1 \right] + 1 \right)^\alpha} \right) \mathbf{1}\{0 \leq \theta \leq 1\}.$$

This new density is not in the same family as the original generalized Pareto variate. Default schemes to numerically integrate $\mathbb{P}(0 | \theta_k)$ against the generalized Pareto prior for θ_k fail because of overflow issues associated with the magnitude of the term $\left(1 + \frac{Kd}{\gamma\alpha} \right)^{1/d}$. In the left panel of Fig. 5b, we first generate an feature matrix from IBP with mass 3.0, concentration 1.0 and discount 0.25. We then plot the estimate of the marginal likelihood under BFRY IFA for this feature matrix as a function of d for mass fixed at 3.0 and discount fixed at 0.0.

Optimization. For AIFA i.e. left panel of Fig. 5a, to estimate the beta process hyperparameters given an observed feature matrix, we maximize the marginal probability in Eq. (K.10) with respect to γ, α, d , by doing a grid search with a fine resolution. The base grid

for the triplet γ, α, d is the Cartesian product of three lists: [1.0, 2.0, 3.0, 4.0, 5.0], [0.5, 1.0, 1.5, 2.0, 2.5], [0.0, 0.1, 0.2, 0.3]. We refine the base grid around the true hyperparameters. For example, in the discount estimation experiment, a true configuration is (3.0, 1.0, 0.4). The refinement here is the Cartesian product of three lists [2.6, 2.8, 3.0, 3.2, 3.4], [0.8, 0.9, 1.0, 1.1, 1.2], [0.36, 0.38, 0.4, 0.42, 0.44]. We append the refinement to the base grid by looping through all the configurations. We propose the best hyperparameters by evaluating the marginal likelihood (Eq. (K.10)) at all points on the grid, and reporting the maximizer.

For the nonparametric process i.e. right panel of Fig. 5a, the probability of observing a particular feature matrix under the IBP prior over N rows is given in Broderick, Pitman and Jordan (2013, Equation 7). We maximize this function with respect to γ, α, d using differential evolution techniques (Storn and Price, 1997; Virtanen et al., 2020).

K.5. Dispersion estimation

Generative model. The probabilistic model is

$$\begin{aligned} \lambda_k &\stackrel{\text{i.i.d.}}{\sim} \text{XGamma}(\alpha/K, c, \tau, T) && \text{across } k, \\ \phi_k &\stackrel{\text{i.i.d.}}{\sim} \text{Dir}(a_\phi \mathbf{1}_V) && \text{across } k, \\ z_{n,k} &| \lambda_k \stackrel{\text{indep}}{\sim} \text{CMP}(\lambda_k, \tau) && \text{across } k, n, \\ x_{n,v} &| z_{n,:}, \phi \stackrel{\text{indep}}{\sim} \text{Poisson}\left(\sum_k z_{n,k} \phi_{k,v}\right), && \text{across } v, n. \end{aligned} \tag{K.12}$$

Recall the definition of the Xgamma variate from Eq. (A.1). The observed data is the count matrix $x_{n,v}$, the number of times document n manifests vocab word v . The hyperparameters are α, c, τ, T and a_ϕ . To draw data for Eq. (K.12), we need to sample from XGamma and CMP, two distributions that are not implemented in standard numerical libraries. The only bottleneck in drawing $\text{CMP}(\theta, \tau)$ is computing $Z_\tau(\theta)$. We approximate the infinite sum $\sum_{y=0}^{\infty} \frac{\theta^y}{(y!)^\tau}$ with a truncation $\sum_{y=0}^L \frac{\theta^y}{(y!)^\tau}$, using the bounds from Minka et al. to make sure the contribution of the left-out terms is small. To draw from XGamma, whose unnormalized density has a contribution from $Z_\tau^{-c}(\theta)$, we use the above approximation of $Z_\tau(\theta)$ and slice sampling on the approximation of the unnormalized density.

When generating synthetic data, we draw $N = 600$ documents, over a vocabulary of size 100, from a model with $K = 500$. The under-dispersed case and the over-dispersed case have the same following hyperparameters: $\alpha = 20, c = 1, T = 1000, a_\phi = 0.01$. For underdispersion, $\tau = 1.5$, while for overdispersion, $\tau = 0.7$. Our primary goal of inference is estimating the topics and the shape τ . As such, during posterior inference, we fix the hyperparameters α, c, T , and a_ϕ at the data-generating values, and sample the remaining latent variables (λ, ϕ, z) and shape τ . We put a uniform $(0, 100]$ prior on the shape τ : τ is always positive, and there is no noticeable difference in amount of dispersion (ratio of variance over mean) between $\tau = 100$ and $\tau > 100$. Furthermore, during sampling, the values of τ are much smaller than 100, indicating that inference would have remained the same for different choices of the uniform’s upper limit.

Gibbs sampling. During sampling, following Zhou et al. (2012, Section 4), we augment the original model by introducing three additional families of latent variables: s, u and q . Conditioned on z and ϕ , the *pseudocount* $s_{n,k,v}$ is distributed as Poisson

$$s_{n,k,v} | z, \phi \stackrel{\text{indep}}{\sim} \text{Poisson}(z_{n,k} \phi_{k,v}), \quad \text{across } n, k, v,$$

and the $s_{n,k,v}$ add up to be $x_{n,v}$ in the following way

$$x_{n,v} = \sum_k s_{n,k,v}.$$

Summing up the pseudocounts across words, we have

$$u_{n,k} := \sum_v s_{n,k,v}.$$

It is true that

$$\begin{aligned} u_{n,k} | z_{n,k} &\stackrel{\text{indep}}{\sim} \text{Poisson}(z_{n,k}), & \text{across } n, k, \\ \{s_{n,k,v}\}_{v=1}^V | u_{n,k}, \phi_k &\stackrel{\text{indep}}{\sim} \text{Multi}(u_{n,k}; \phi_k), & \text{across } n, k. \end{aligned} \quad (\text{K.13})$$

Summing up the pseudocounts across documents, we have

$$q_{k,v} := \sum_n s_{n,k,v}.$$

We use a blocked Gibbs sampling strategy. The variable blocks variables are ϕ , λ , s (which determines u and q), z , τ . First, we compute the Gibbs conditional of the *topics* ϕ . Since u is determined by s (Eq. (K.13)), conditioned on s , ϕ is independent of the remaining latent variables:

$$\mathbb{P}(\phi | x, \lambda, s, z, \tau) = \mathbb{P}(\phi | s) \propto \mathbb{P}(\phi) \mathbb{P}(s | u, \phi) = \prod_{k=1}^K \text{Dir}(\phi_k \mathbf{1}_V | [a_\phi + q_{k,v}]_{v=1}^V).$$

We compute the Gibbs conditionals of the *rates* λ . Conditioned on the trait counts z and shape τ , λ is independent of the remaining latent variables:

$$\begin{aligned} \mathbb{P}(\lambda | x, \phi, s, z, \tau) &= \mathbb{P}(\lambda | z, \tau) = \prod_{k=1}^K \mathbb{P}(\lambda_k | z_{\cdot,k}, \tau) \\ &= \prod_{k=1}^K \text{XGamma} \left(\lambda_k \mid \frac{\alpha}{K} + \sum_n z_{n,k}, c + N, \tau, T \right). \end{aligned}$$

We use the scheme discussed after Eq. (K.12) to sample these XGamma variates. The Gibbs conditionals of the *trait counts* z are

$$\begin{aligned} \mathbb{P}(z | x, \phi, \lambda, s, \tau) &= \mathbb{P}(z | \lambda, s, \tau) = \prod_{n,k} \mathbb{P}(z_{n,k} | \lambda_k, u_{n,k}, \tau) \\ &\propto \prod_{n,k} \text{Poisson}(u_{n,k} | z_{n,k}) \text{CMP}(z_{n,k} | \lambda_k, \tau). \end{aligned}$$

To draw from the distribution whose p.m.f. at $z \in \mathbb{N} \cup \{0\}$ is proportional to $\text{Poisson}(u_{n,k} | z) \text{CMP}(z | \lambda_k, \tau)$, the only bottleneck is computing the normalization constant

$$\sum_{z=0}^{\infty} \exp(-z) \frac{z^{u_{n,k}}}{u_{n,k}!} Z_\tau^{-1}(\lambda_k) \frac{\lambda_k^z}{(z!)^\tau}$$

The multiplicative factors that don't depend on z can be taken out of the sum: we only need to compute $\sum_{z=0}^{\infty} \frac{(\lambda_k/e)^z z^{u_{n,k}}}{(z!)^\tau}$. Similar to the computation of $Z_\tau(\theta)$, we approximate the above infinite sum with a finite truncation, making sure the left-out terms have a small contribution. The Gibbs conditionals of the *pseudocounts* s are

$$\begin{aligned} \mathbb{P}(s \mid x, \phi, \lambda, z, \tau) &= \mathbb{P}(s \mid x, \phi, z) \\ &= \prod_{n,v} \text{Multi}(\{s_{n,k,v}\}_{k=1}^K \mid x_{n,v}; [z_{n,k}\phi_{k,v} / \sum_{k'} z_{n,k'}\phi_{k',v}]). \end{aligned}$$

Finally, the Gibbs conditionals of the *shape* τ are

$$\mathbb{P}(\tau \mid x, \phi, \lambda, s, z) = \mathbb{P}(\tau \mid z, \lambda) \propto \mathbb{P}(z \mid \tau, \lambda) \mathbb{P}(\lambda \mid \tau) \mathbb{P}(\tau).$$

In implementations, we omit the contribution from $\mathbb{P}(\lambda \mid \tau)$, since it contributes a very small amount (less than 0.1%) to the overall value of $\ln \mathbb{P}(z \mid \tau, \lambda) + \ln \mathbb{P}(\lambda \mid \tau) + \ln \mathbb{P}(\tau)$, but takes up more time to evaluate than the other two components. In other words, the unnormalized log density of τ conditioned on the other variables is just

$$\ln \mathbb{P}(z \mid \tau, \lambda) + \ln \mathbb{P}(\tau) = \sum_{n,k} \ln \text{CMP}(z_{n,k} \mid \lambda_k, \tau) + \ln \mathbf{1}\{\tau \in (0, 100]\}.$$

We use slice sampling to draw from this distribution.

MCMC results. We run 40 chains, each for 50,000 iterations. By discarding the first 25,000 iterations, all chains have \hat{R} diagnostic (Gelman and Rubin, 1992) smaller than 1.01. To combat the serial correlation, we thin samples after burn-in, selecting only one draw after 2,000 iterations. The effective number of samples remaining after burn-in and thinning is about 1,000.

Appendix L: Additional experiments

L.1. Denoising other images

Similar to the house image, the clean plane image was obtained from <http://sipi.usc.edu/database/>. The clean, the corrupted, and the example denoised images from AIFA/TFA for plane images are given in Fig. L.1. In Figs. L.2b and L.2c, the approximation level is $K = 60$.

Similar to the house image, the clean truck image was obtained from <http://sipi.usc.edu/database/>. The clean, the corrupted, and the example denoised images from AIFA/TFA for truck images are given in Fig. L.3. In Figs. L.4b and L.4c, the approximation level is $K = 60$.

L.2. Effect of AIFA tuning hyperparameters

We investigate the impact of a and b_K , which are two tunable parameters in the more general definition of AIFA from Theorem B.2. Other than the setting of a and b_K , the experimental set up is the same as Appendix K.3.

From Fig. L.5, we see that the setting of a and b_K do not have a big impact on the performance of the IFA from Theorem B.2. We report results for a combination of $a \in \{0.1, 1\}$ and $b_K = 1/\sqrt{K}$ or $b_K = 1/K$.

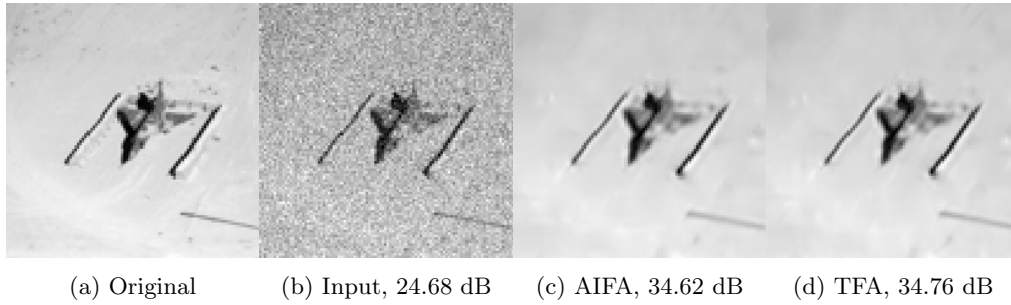


Fig L.1: Sample AIFA and TFA denoised images have comparable quality. **(a)** shows the noiseless image. **(b)** shows the corrupted image. **(c,d)** are sample denoised images from finite models with $K = 60$. PSNR (in dB) is computed with respect to the noiseless image.

L.3. Estimation of mass and concentration

Fig. L.6 shows that we can use an AIFA to estimate the underlying mass and concentration for a variety of ground-truth masses and concentrations. The experimental setup is from Appendix K.4. Since the error bars in the left and right panels are comparable, we conclude that the AIFA yields comparable inference to the full nonparametric process.

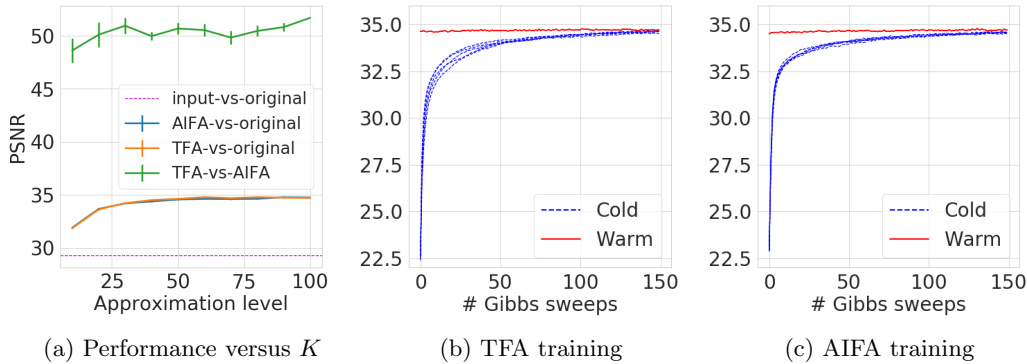


Fig L.2: **(a)** Peak signal-to-noise ratio (PNSR) as a function of approximation level K . The error bars reflect randomness in both initialization and simulation of the conditionals across 5 trials. AIFA denoising quality improves as K increases, and the performance is similar to TFA across approximation levels. Moreover, the TFA- and AIFA-denoised images are very similar: the PSNR ≈ 50 for TFA versus AIFA, whereas PSNR < 35 for TFA or AIFA versus the original image. **(b,c)** Show how PSNR evolves during inference. The “warm-start” lines in indicate that the AIFA-inferred (respectively, TFA-inferred) parameters are excellent initializations for TFA (respectively, AIFA) inference.

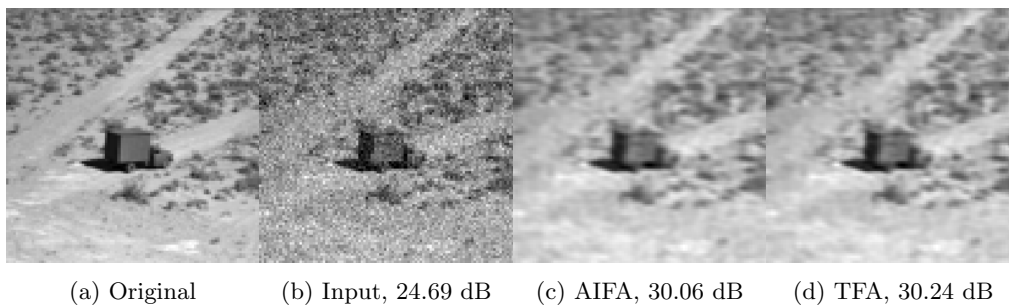


Fig L.3: Sample AIFA and TFA denoised images have comparable quality. **(a)** shows the noiseless image. **(b)** shows the corrupted image. **(c,d)** are sample denoised images from finite models with $K = 60$. PSNR (in dB) is computed with respect to the noiseless image.

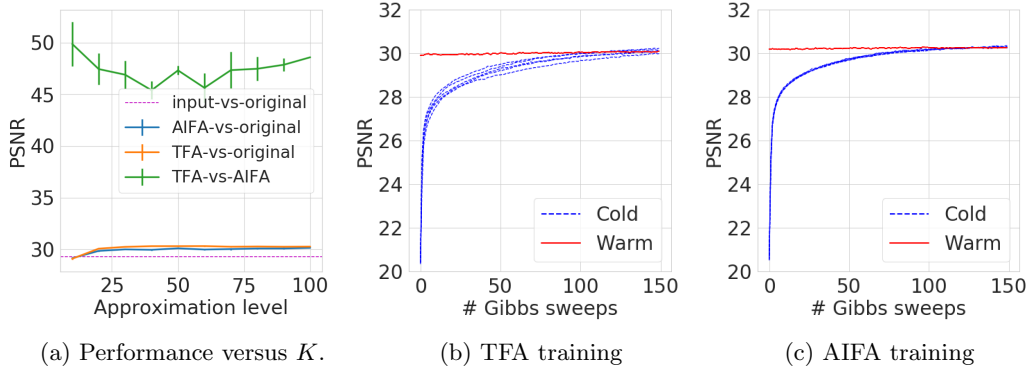


Fig L.4: **(a)** Peak signal-to-noise ratio (PSNR) as a function of approximation level K . The error bars reflect randomness in both initialization and simulation of the conditionals across 5 trials. AIFA denoising quality improves as K increases, and the performance is similar to TFA across approximation levels. Moreover, the TFA- and AIFA-denoised images are very similar: the PSNR ≈ 47 for TFA versus AIFA, whereas PSNR < 31 for TFA or AIFA versus the original image. **(b,c)** Show how PSNR evolves during inference. The “warm-start” lines in indicate that the AIFA-inferred (respectively, TFA-inferred) parameters are excellent initializations for TFA (respectively, AIFA) inference.

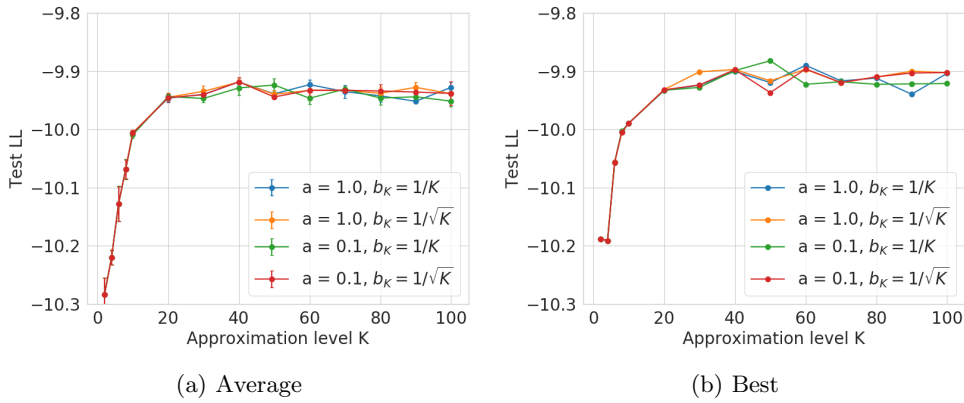
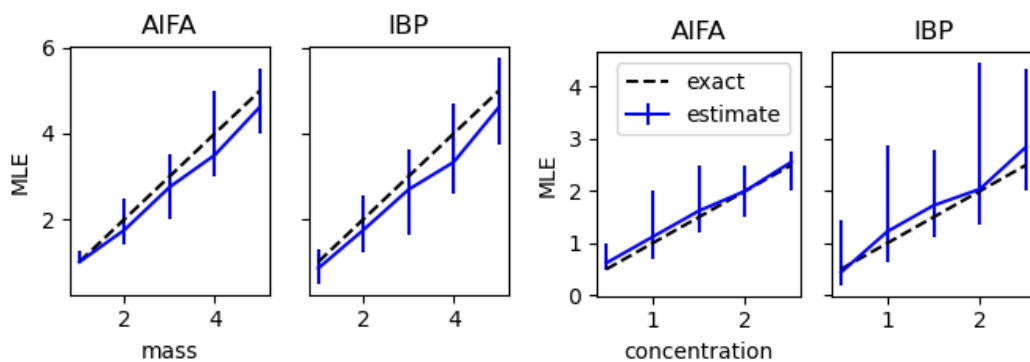


Fig L.5: The predictive log-likelihood of AIFA is not sensitive to different settings of a and b_K . Each color corresponds to a combination of a and b_K . **(a)** is the average across 5 trials with different random seeds for the stochastic optimizer, while **(b)** is the best across the same trials.



(a) Estimation of mass γ

(b) Estimation of concentration α

Fig L.6: In Fig. L.6a, we estimate the mass by maximizing the marginal likelihood of the AIFA (left panel) or the full process (right panel). The solid blue line is the median of the estimated masses, while the lower and upper bounds of the error bars are the 20% and 80% quantiles. The black dashed line is the ideal value of the estimated mass, equal to the ground-truth mass. The key for Fig. L.6b is the same, but for concentration instead of mass.